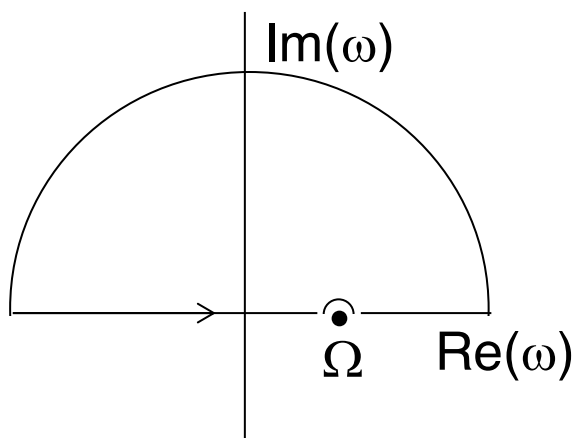


Crystallographic Compendium

Assorted derivations and “cool stuff” from the world of crystallography and related areas

Douglas C. Rees
California Institute of Technology



$$f'(\Omega) = \frac{2}{\pi} \int_0^{\infty} \frac{\omega f''(\omega)}{\Omega^2 - \omega^2} d\omega$$

$$f''(\Omega) = -\frac{2\Omega}{\pi} \int_0^{\infty} \frac{f'(\omega)}{\Omega^2 - \omega^2} d\omega$$

© Douglas C. Rees, 2024

Table of Contents

<i>Introduction and Overview</i>	4
<i>Section I: Fourier Transformations, Structure Factors and Electron Density</i>	5
Useful Properties of Fourier Transforms	5
Sampling Theory with Applications to Molecular Replacement and NCS Averaging.....	6
Electron Atomic Scattering Factors and the Relationship to X-ray Atomic Scattering Factors.....	9
Electron Density Calculation Using A and B Expressions from Old International Tables	15
Space group C2 Structure Factor and Electron Density Expressions	16
Integrated Electron Density about a Point	18
Relationship between B_{ave} and Resolution	19
<i>Section II: Random Walks and Crystallography</i>	23
<i>Section III: Coordinate and Reflection Transformations; Molecular Replacement</i>	27
Unit Cell Transformations	27
Changing the Hand of a Space Group	29
Equivalent Reflections and Phase Relationships.....	30
Phase Relationships of Friedel Pairs in the Presence of Anomalous Scattering	32
Orthogonalization Convention	33
Molecular Replacement - Practical Considerations.....	35
Coordinate Superposition Considerations: Overview	38
Superposition Relationships for Oligomeric Proteins.....	40
Generalization to N-mer Oligomeric Symmetry.....	44
Calculation of Screw (Helical) Parameters from a General Transformation.....	48
Transformation Matrix to a New Coordinate System	49
Transformation to a Skew Frame	50
Strain Calculations	52
<i>Section IV: Phasing and Phase Distributions</i>	54
Hendrickson-Lattman ABCD Coefficients.....	54
Probability Distributions for Heavy Atom Isomorphous Differences.....	56
Direct Methods Notes.....	58
<i>Section V: Minimization, Maximization and Refinement</i>	65
Lagrange Multipliers and Constrained Extrema	65
Least Squares in Crystallography.....	66
Variance - Covariance in Least Squares Refinements.....	69

Incorporation of Constraints in Least Squares Refinements	70
Modeling the Correlation between Z and B in an X-ray Crystal Structure Refinement	72
Section VI: Geometrical Calculations	75
Geometry Overview: Polyhedra, Lines, and Planes.....	75
Least Squares Plane	77
Close Packing of Spheres.....	78
Shortest Distance from a Point to a Line	83
Helix Packing Relationships.....	86
Angles between Planar Units in a Helix	92
Useful Properties of Gaussians.....	94
Ellipsoids, B factors and g-Tensors	96
The geometry of 2Fe2S and 4Fe4S clusters.....	105
Section VII: Lorentz and Polarization Factors.....	109
Lorentz Factor.....	109
Polarization Factor.....	113
Section VIII: Anomalous Scattering.....	115
Classical Description of Scattering: Anomalous Dispersion	115
Derivation of Kramers-Krönig (KK) Transform	117
Evaluation of f' from f'' by the KK transform	121
Bijvoet Difference (Anomalous Difference) Fourier Maps.....	122
Anisotropic Anomalous Scattering	124
Section IX: Non-crystalline Diffraction	130
Small Angle Scattering	130
Diffraction Pattern of Helical Structures.....	137
Computational Background to Fourier Transforms and Helical Diffraction	142

Introduction and Overview

These notes have been prepared (and revised, re-revised, etc.) over the past decades while working through various problems encountered in our crystallographic analyses. They are not intended as a complete and systematic development of crystallography, but rather they reflect topics or problems of interest to me or that were particularly challenging that I needed to work through to better understand. This effort reflects the “learn-by-doing” approach that I have found to be valuable when I am trying to master new material.

The inspiration for this compendium is Charles Kittel’s *Elementary Statistical Physics* (Dover, 2004, originally published in 1958) that is organized around 45 sections, each a few pages in length, that cover a set of important topics in this field. By comparison, the present effort makes no attempt (yet) to develop the material in a systematic way, either in the flow of topics, the depth of treatment, or even (alas) using a consistent set of symbols. I hope to be able to correct these defects at some time in the future. At the same time, there are always new topics to incorporate (as I learned from my time in Student Affairs “there is always more to learn”) and the evolution of this collection will undoubtedly reflect the tension between clarifying (and correcting) existing material and tackling new subjects.

I would like to take this opportunity to acknowledge the incredible effort of the graduate students, postdoctoral fellows, staff and visitors in my research group who have provided the inspiration and motivation for this work – it’s been a blast! Thank you.

Douglas C. Rees
26 November 2024
dcree@caltech.edu

NOTE: Since my proofreading and error correction skills are “imperfect”, be aware that mistakes remain. If a derivation or equation doesn’t make sense, don’t exclude the possibility that it is because of errors in the text or equations.

Section I: Fourier Transformations, Structure Factors and Electron Density
Useful Properties of Fourier Transforms
(see pp 50-51 of Titchmarsh)

Convolution Theorem

If the Fourier transforms of two functions $g(x)$ and $f(x)$ are given by $G(h)$ and $F(h)$, then:

$$\int g(x)f(x)e^{2\pi ihx} dx = \sum_k G(k)F(h-k)$$

ie the Fourier transform of the product of two functions is the convolution of the Fourier transforms of the two functions, and *vice-versa*. This result relates the Fourier transform of a crystal to the Fourier transforms of the molecule and the lattice, for example.

Parseval's Theorem:

$$\int |f(x)|^2 dx = \sum_h |F(h)|^2$$

This relationship is useful for calculating the mean square density over the entire unit cell from the structure factor amplitudes.

Generalizations to multiple functions are also possible; an extension to $\rho^3(x)$ is given by:

$$\begin{aligned} \int \rho^3(x) dx &= \int \sum_h \sum_p \sum_q F(h)F(p)F(q)e^{-2\pi i(h+p+q)x} dx \\ &= \sum_{hpq} F(h)F(p)F(q)\delta(h+p+q) \\ &= \sum_h F(-h) \sum_p F(p)F(h-p) \end{aligned}$$

To maximize this expression, the value of the second summation should be proportional to $F(h)$:

$$F(h) \approx \sum_p F(p)F(h-p)$$

since then the overall integral is given approximately by:

$$\int \rho^3(x) dx \approx \sum_h F(-h)F(h) = \sum_h I(h)$$

The relationship between Sayre's equation (*Acta Crystallogr.* **5**, 60-65 (1952)) and the maximization of ρ^3 has been noted by E. Stanley (*Acta Crystallogr.* **A35**, 966-970 (1979)). Another way in which maximization of ρ^3 may be accomplished is if all the structure factors have a phase angle of 0° ; this corresponds to the Patterson solution (superatom at the origin) which does satisfy all these relationships, but which is (almost always, anyways) not the desired solution.

Sampling Theory with Applications to Molecular Replacement and NCS Averaging

The molecular and crystal transforms of an object are given by:

$$F(S) = \int_{-1/2}^{1/2} \rho(x) e^{2\pi i S x} dx$$

$$F(h) = \int_{-1/2}^{1/2} \rho(x) e^{2\pi i h x} dx; h = \text{integer}$$

The crystal transform is given by the molecular transform sampled at reciprocal lattice points (convolution theorem).

By the inverse Fourier transform:

$$\rho(x) = \sum_h F(h) e^{-2\pi i h x} \quad (\text{neglecting the volume factor})$$

$$F(S) = \int_{-1/2}^{1/2} \sum_h F(h) e^{-2\pi i h x} e^{2\pi i S x} dx$$

$$= \sum_h F(h) \int_{-1/2}^{1/2} e^{2\pi i (S-h)x} dx$$

$$= \sum_h F(h) \frac{\sin \pi (S-h)}{\pi (S-h)}$$

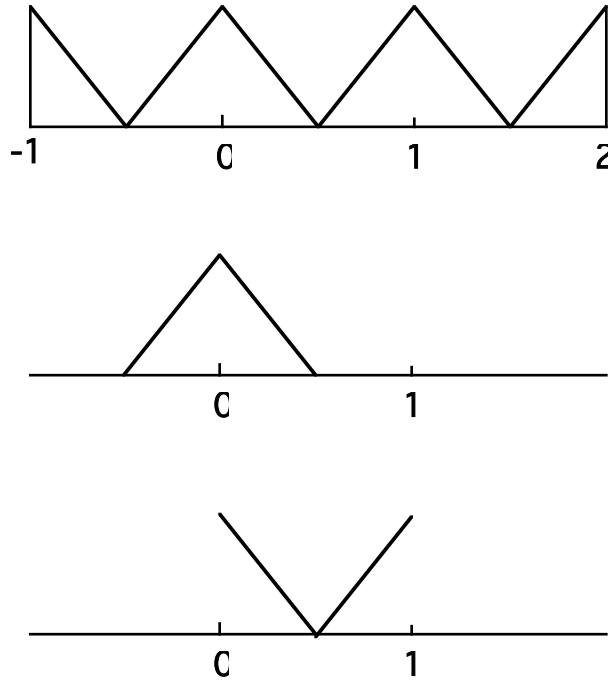
This sampling theorem permits reconstruction of the continuous molecular transform from the discrete, sampled crystal transform.

Now, for integer n , $\frac{\sin \pi n}{\pi n} = \delta(n)$, so that when S equals an integer h , $F(S) = F(h)$, and the value of this amplitude is independent of all other $F(h)$'s.

The exact form of the sampling theorem depends on the precise limits used in the integration. If instead of $-1/2 < x < 1/2$, the limits $0 < x < 1$ are used, then :

$$F(S) = \sum_h F(h) \frac{\sin \pi (S-h)}{\pi (S-h)} \left[e^{\pi i (S-h)} \right]$$

This reflects the different molecular transforms of the following objects, although they have the exact same crystal transform:



The term in brackets is related to the phase shift of the diffraction pattern associated with a real space translation.

Application of the Sampling Theorem to the Rotation Function:

The Patterson functions of two crystals (possibly corresponding to the same crystal) are given by the expressions:

$$P_1(x) = \sum_h |F_h|^2 e^{-2\pi i h x}$$

$$P_2(y) = \sum_p |F_p|^2 e^{-2\pi i p y}$$

if $y = Cx$, where C is a rotation matrix, then

$$P_2(Cx) = \sum_p |F_p|^2 e^{-2\pi i p C x}$$

define the rotation function R (Rossmann and Blow, *Acta Crystallogr.* **15**, 24 (1962))

$$\begin{aligned} R(C) &= \int_U P_1(x) P_2(Cx) dx \\ &= \sum_h \sum_p |F_h|^2 |F_p|^2 \int_U e^{-2\pi i (h+pC)x} dx \\ &\equiv \sum_h \sum_p |F_h|^2 |F_p|^2 G_{hp} \end{aligned}$$

G_{hp} is the sampling or interference function, and has a value near 0 unless $h \sim -Cp$. G_{hp} interpolates the value of the diffraction pattern corresponding to a non-integral $-pC$ point.

With $H \equiv pC+h$, G_{hp} may be derived for a sphere of radius R (using a coordinate system where H is along the unique axis, ϕ is the angle between r and H , and θ is the angle in the equatorial plane):

$$G_{hp} = \frac{1}{\frac{4}{3}\pi R^3} \int_0^{2\pi} \int_0^{\pi} \int_0^R e^{-2\pi i H r \cos \phi} r^2 \sin \phi dr d\phi d\vartheta$$

$$= \frac{3[\sin(2\pi HR) - (2\pi HR)\cos(2\pi HR)]}{(2\pi HR)^3}$$

And for a one dimensional box with $|x| < a/2$, G_{hp} is given by:

$$G_{hp} = \frac{1}{a} \int_{-a/2}^{a/2} e^{-2\pi i h x} dx$$

$$= \frac{\sin \pi H a}{\pi H a}$$

Applications to Noncrystallographic Symmetry and Solvent Flattening:

$$F(S) = \int_{-1/2}^{1/2} \rho(x) e^{2\pi i S x} dx$$

$$\text{if } \rho(x) = 0 \text{ when } \frac{a}{2} < |x| < \frac{1}{2}$$

$$= \int_{-a/2}^{a/2} \rho(x) e^{2\pi i S x} dx$$

$$F(S) = \sum_h F(h) \int_{-a/2}^{a/2} \rho(x) e^{2\pi i (S-h)x} dx$$

$$= \sum_h F(h) \frac{\sin \pi (S-h)a}{\pi (S-h)}$$

for integer $S \equiv p$

$$F(p) = \sum_h F(h) \frac{\sin \pi (p-h)a}{\pi (p-h)}$$

In this case, other $F(h)$'s contribute to $F(p)$ in addition to the term $p=h$. For example, when $a=1/2$, then for $|p-h| = 0, 1, 2, 3$, etc., the $\sin x/x$ term has the value 0.5, 0.319, 0, -0.106, etc., compared to the values 1, 0, 0, 0, ... when $a=1$. This interdependence of the structure factors permits the estimation and refinement of phase information, which is beautifully detailed in papers based on Crowther's thesis work (*Acta Crystallogr.* **22**, 758-764 (1967); *Acta Crystallogr.* **B25**, 2571-2580 (1969)), and by P. Main and M.G. Rossmann (*Acta Cryst.* **21**, 67-72 (1966))

Electron Atomic Scattering Factors and the Relationship to X-ray Atomic Scattering Factors

references

International Tables, vol III (1968) pp 217-227

International Tables, vol C (1992) pp 223-225 plus following tables

L.M. Peng Micron 30, 625-648 (1999)

The electron atomic scattering factor and the Mott equation

We will describe scattering in terms of the two related reciprocal space quantities S and s defined as

$$\begin{aligned} S &= \frac{1}{d} = \frac{2 \sin \vartheta}{\lambda} \\ s &= \frac{S}{2} = \frac{1}{2d} = \frac{\sin \vartheta}{\lambda} \end{aligned}$$

where ϑ is half the scattering angle. Some papers use $2\pi S$ or $4\pi s$ – so beware when comparing different formulas!

The electron atomic scattering factor describing the elastic scattering of a beam of electrons is given by the Fourier transform of the electrostatic Coulomb potential $V(r)$ of the atom

$$f_e(S) = \frac{2\pi m_0 e}{h^2} \int V(r) e^{2\pi i r \cdot S} dr$$

where m_0 is the rest mass of the electron and e is the magnitude of the electron charge.

For comparison, the X-ray atomic scattering factor describing the elastic scattering of a beam of X-rays is given by the Fourier transform of the electron density $\rho(r)$ of the atom:

$$f_x(S) = \int \rho(r) e^{2\pi i r \cdot S} dr$$

For an atom with an atomic number Z and an electron density distribution $\rho(r)$, the Coulomb electrostatic potential of an atom is given by

$$V(r) = \frac{1}{4\pi\epsilon_0} \left\{ \frac{Ze}{r} - \int \frac{e\rho(r')}{|r-r'|} dr' \right\}$$

where the two terms on the right-hand side reflect the electrostatic potential due to the positive nucleus (a point charge) and the negative electron distribution, respectively.

The Fourier transform of the Coulomb electrostatic potential (Eq. 4, see the Peng reference) gives the Mott equation relating the atomic scattering factors of electrons and X-rays:

$$f_e(s) = \frac{m_0 e^2}{8\pi\epsilon_0 h^2} \frac{[Z - f_x(s)]}{s^2}$$

Note that this expression is defined in terms of the scattering parameter s (not S).

Dimensional analysis

Analysis of the units for these equations is most straightforward using SI units.

The various parameters are

$$m = 9.1094 \times 10^{-31} \text{ kg}$$

$$h = 6.6261 \times 10^{-34} \text{ J s}$$

$$q = 1.6022 \times 10^{-19} \text{ C}$$

$$4\pi\epsilon_0 = 1.1126 \times 10^{-10} \text{ C V}^{-1} \text{ m}^{-1} \text{ (or C}^2 \text{ N}^{-1} \text{ m}^{-2}\text{)}$$

$$1 \text{ J} = 1 \text{ V} \times 1 \text{ C}$$

and the units of J and N are $\text{kg m}^2 \text{ s}^{-2}$ and kg m s^{-2} , respectively.

From equation 2, we have
$$f_e(S) = \frac{2\pi m_0 e}{h^2} \int V(r) e^{2\pi i r \cdot S} dr$$

Using the SI system, the units of the Fourier transform of $V(r)$ are V m^3 , while the constants can be shown to have units $\text{V}^{-1} \text{ m}^{-2}$, so that the electron atomic scattering factor has units of m. Instead of m, however, Å units are conventionally used; the Mott equation then has the numerical form:

Eq. 5b
$$f_e(s) = 0.023934 \frac{[Z - f_x(s)]}{s^2} \text{ Å}$$

where Z and $f_x(s)$ are in electrons, s in Å^{-1} and $f_e(s)$ in Å. Although the unit of the electron atomic scattering factor is distance, it should be possible to convert them to correspond directly to the Fourier transform of the electrostatic potential (V).

Limit as $s \rightarrow 0$

It may appear from the Mott equation that $f_e(s)$ has a singularity as $s \rightarrow 0$, but since $f_x(s) \rightarrow Z$, the convergence limit is not immediately obvious. If the X-ray atomic scattering factor is approximated as a Gaussian

Eq. 6a
$$f_x(s) = Z e^{-B_0 s^2}$$

then in the limit of $s \rightarrow 0$, Eq. 5b reduces to

Eq. 6b
$$f_e^{(0)}(s) \sim 0.024 B_0 Z$$

which predicts that the electron scattering factors are proportional to Z at low scattering angle, as are the X-ray scattering factors. Although the X-ray scattering factors are not generally approximated as single Gaussians, their parameterizations do utilize multiple Gaussians.

However, the 1968 International Tables states (pg 217) that the electron scattering factors are proportional to $Z^{1/2}$ (and “This is exact for the Thomas-Fermi statistical model”(no reference is given for this statement, however)). One consequence of a smaller dependence of the electron scattering factors on Z is that “other factors being equal, the detection of light atoms in the presence of heavy atoms is easier with electrons than X-rays” (Ibers, Acta Cryst. 14, 540 (1961); Ibers received his PhD in Chemistry at Caltech for his thesis “Studies in Electron and X-ray Diffraction” (1954))

Charged species (ions)

For neutral ions, the electron scattering factor is a well-defined function (ie. no singularity at $s = 0$), as captured by the Mott equation (Eq. 5). If the number of protons is not equal to the number of electrons, however, then there is a singularity (at least numerically), which has the consequence that in the limit as $s \rightarrow 0$, the values of the electron scattering factors at low scattering will be large and positive for cations, and large and negative for anions. These effects can be used to establish the atomic charge (see, for example, Wang et al Acta Cryst. D77, 534 (2021), where Mg^{2+} ions are identified next to nucleotides in cryo-EM maps).

As discussed in the Peng reference (Eq. 15), the effect of ionic charge on the electron scattering factor may be approximated within the framework of the Mott equation:

$$\text{Eq. 7} \quad f_e(s) = \frac{m_0 e^2}{8\pi\epsilon_0 h^2} \frac{[Z - f_x(s)]}{s^2} = f_e^{(0)}(s) + \frac{m_0 e^2}{8\pi\epsilon_0 h^2} \frac{\Delta Z}{s^2}$$

where ΔZ represents the ionic charge so that the first term on the right-hand side of Eq. 7 is the scattering factor of the neutral atom, while second term represents the contribution of the excess charge to the ionic scattering factor.

Example – the hydrogen atom

For a radially symmetric function, the Fourier transform of a function $\rho(r)$ and the inverse transform are given by the expressions:

$$\text{Eq. 8} \quad F(S) = \int_0^\infty \frac{2r}{S} \rho(r) \sin(2\pi Sr) dr$$
$$\rho(r) = \int_0^\infty \frac{2S}{r} F(S) \sin(2\pi Sr) dS$$

The electron density $\rho(r)$ is given by square of the wavefunction; for a hydrogen atom with an electron in the 1s orbital, the wavefunction has an exponential dependence on r . The Fourier transform of this distribution gives the X-ray scattering factor for hydrogen:

$$\text{Eq. 9} \quad \rho(r) = \frac{1}{\pi a^3} e^{-2r/a}$$
$$f_x(S) = \frac{1}{(1 + (\pi Sa)^2)^2}$$

Note: in Eq. 9, the X-ray atomic scattering factor is defined in terms of S (not s), and a = the Bohr radius of the hydrogen atom, with

$$\text{Eq. 10} \quad a = \frac{\epsilon_0 h^2}{\pi m_0 e^2} = 5.2918 \times 10^{-11} m = 0.52918 \text{ \AA}$$

The numerical values calculated from this expression agree with those in the International Tables for the hydrogen X-ray atomic scattering factor.

The electron atomic scattering factor is the Fourier transform (Eq. 2) of the electrostatic potential of the hydrogen atom (Eq. 4). We will not go through the math in detail, but will outline that the Fourier transform of Eq. 4 can be calculated as the sum of the Fourier transform of the proton term plus the Fourier transform of the electron distribution term (the latter has a minus sign, as in Eq. 4, since the electron has a negative charge). To do this, we utilize the important (but non-trivial) relationship of the Fourier transform of $1/r$ (see Electrostatics notes)

$$\text{Eq. 11} \quad FT\left(\frac{1}{r}\right) = \frac{1}{\pi S^2}$$

To calculate the Fourier transform of the electron distribution in Eq. 4, we recognize that term represents a convolution, and by the convolution theory, the Fourier transform of a convolution is the product of the Fourier transforms of the two functions (see “Useful properties of Fourier Transform” section of these notes). Hence, the Fourier transform of Eq. 4 becomes:

$$\text{Eq. 12} \quad f_e(S) = \frac{2\pi m_0 e}{h^2} FT(V(r)) = \frac{2\pi m_0 e}{h^2} \left[\frac{1}{4\pi\epsilon_0} \left(\frac{Ze}{\pi S^2} - \frac{e}{\pi S^2} \frac{1}{(1+(\pi Sa)^2)^2} \right) \right]$$

Rearranging gives

$$\text{Eq. 13} \quad f_e(S) = \frac{m_0 e^2}{2\pi\epsilon_0 h^2} \left[\frac{1}{S^2} \left(Z - \frac{1}{(1+(\pi Sa)^2)^2} \right) \right]$$

using $Z = 1$ and replacing S with $2s$, we have

$$\text{Eq. 14a} \quad f_e(s) = \frac{m_0 e^2}{8\pi\epsilon_0 h^2} \left[\frac{1}{s^2} \left(1 - \frac{1}{(1+(2\pi sa)^2)^2} \right) \right]$$

which is in the form of the Mott equation. The electron atomic scattering factors calculated with Eq. 14a agree with those tabulated in Table 3.3.3A of the 1968 International Tables. Using the definition of the Bohr radius, a (Eq. 10) and a bit more rearranging gives the equivalent expression

$$\text{Eq. 14b} \quad f_e(s) = \frac{a}{2} \left[\frac{2 + (2\pi sa)^2}{(1 + (2\pi sa)^2)^2} \right]$$

which explicitly highlights that the units of the electron atomic scattering factor are length.

Mott equation in terms of Bohr radius

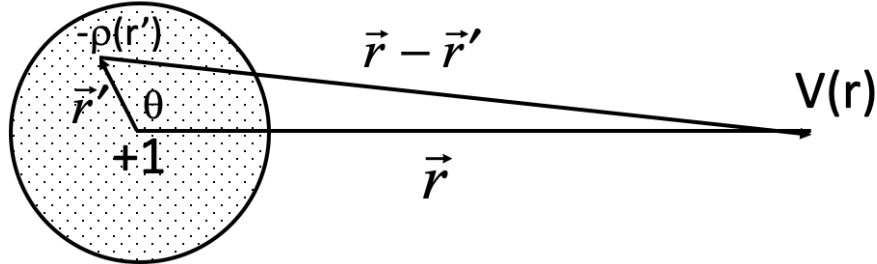
Using Eq. 10, the Mott equation can be expressed in terms of the Bohr radius of the hydrogen atom

$$\text{Eq. 5c} \quad f_e(s) = \frac{m_0 e^2}{8\pi\epsilon_0 h^2} \frac{[Z - f_x(s)]}{s^2} = \frac{1}{8\pi^2 a} \frac{[Z - f_x(s)]}{s^2}$$

which again emphasizes that the corresponding units are length ($a = \text{m}$, $s = \text{m}^{-1}$).

Alternative derivation of the atomic electron scattering factor for hydrogen by direct calculation of the Coulomb's law electrostatic potential

Define the following coordinate system for hydrogen with the origin at the proton:



The electrostatic potential, $V(r)$, at the point r may be expressed

$$\begin{aligned}
 \text{Eq. 15} \quad V(r) &= \frac{e}{4\pi\epsilon_0} \left[\frac{1}{r} - \int \frac{\rho(\vec{r}')}{|\vec{r} - \vec{r}'|} d\vec{r}' \right] \\
 &= \frac{e}{4\pi\epsilon_0} \left[\frac{1}{r} - \int_0^\infty r'^2 dr' \int_0^\pi \sin \vartheta d\vartheta \int_0^{2\pi} d\varphi \left[\frac{\rho(\vec{r}')}{(r^2 + r'^2 - 2rr' \cos \vartheta)^{3/2}} \right] \right]
 \end{aligned}$$

with

$$\text{Eq. 9} \quad \rho(r) = \frac{1}{\pi a^3} e^{-2r/a}$$

this expression may be integrated (I used Mathematica® – H_atom_electron_scattering_factors_calculations_Sept2021.nb) to give

$$\text{Eq. 16} \quad V(r) = \frac{e}{4\pi\epsilon_0} \left[\left(\frac{1}{r} + \frac{1}{a} \right) e^{-2r/a} \right]$$

Note that even though the hydrogen atom is electrically neutral, the potential $V(r)$ is always positive!

Combining Eqs. 2, 8 and 16 gives the following equation. Evaluating the integral with Mathematica® and introducing the Bohr radius gives the following expression for the electron atomic scattering factor:

$$\begin{aligned}
f_e(S) &= \frac{2\pi m_0 e}{h^2} \left[\int_0^\infty \frac{2r}{S} V(r) \sin(2\pi Sr) dr \right] \\
&= \left(\frac{2\pi m_0 e}{h^2} \right) \left(\frac{e}{4\pi\epsilon_0} \right) \left[\int_0^\infty \frac{2r}{S} \cdot \left\{ \left(\frac{1}{r} + \frac{1}{a} \right) e^{-2r/a} \right\} \cdot \sin(2\pi Sr) dr \right] \\
&= \left(\frac{2\pi m_0 e}{h^2} \right) \left(\frac{e}{4\pi\epsilon_0} \right) \left[\pi a^2 \frac{(2 + (\pi Sa)^2)}{(1 + (\pi Sa)^2)^2} \right] \\
&= \frac{a}{2} \left[\frac{2 + (\pi Sa)^2}{(1 + (\pi Sa)^2)^2} \right] \\
&= \frac{a}{2} \left[\frac{2 + (2\pi sa)^2}{(1 + (2\pi sa)^2)^2} \right]
\end{aligned}$$

Eq. 17

as derived previously.

Electron Density Calculation Using A and B Expressions from Old International Tables

General expression

$$\rho(x) = \frac{2}{V} \sum_{h,asu} (A(h,x)A_c(h) + B(h,x)B_c(h))$$

where $A(h,x)$ and $B(h,x)$ are the International Table expressions
and $A_c(h)$ and $B_c(h)$ are $|F(h)|\cos\alpha_h$ and $|F(h)|\sin\alpha_h$, respectively.

If the F's are on an absolute scale, with F_{000} included, then the electron density of the bulk solvent should be $\sim 0.4 \text{ e}/\text{\AA}^3$ (see Lang et al. PNAS 111, 237 (2014)).

Space group C2 Structure Factor and Electron Density Expressions
 (see old International Tables, vol I, page 376, space group 5, b as unique axis)

relationships between symmetry related amplitudes and phases:

$$\begin{aligned} |F(hkl)| &= |F(\bar{h}\bar{k}\bar{l})| = |F(\overline{hk\bar{l}})| = |F(h\bar{k}l)| \\ \alpha(hkl) &= \alpha(\bar{h}\bar{k}\bar{l}) = -\alpha(\overline{hk\bar{l}}) = -\alpha(h\bar{k}l) \\ F(hkl) &= |F(hkl)| e^{i\alpha(hkl)} = |F(hkl)| (\cos \alpha + i \sin \alpha) = A(hkl) + iB(hkl) \equiv A_h + iB_h \end{aligned}$$

Structure factor expression

equivalent positions in C2 $x, y, z; \bar{x}, \bar{y}, \bar{z}; x + \frac{1}{2}, y + \frac{1}{2}, z; \bar{x} + \frac{1}{2}, \bar{y} + \frac{1}{2}, \bar{z}.$

$$\begin{aligned} F(hkl) &= \sum_{\text{atoms } j} f_j e^{-B_j \sin^2 \vartheta / \lambda^2} \left(e^{2\pi i(hx+ky+lz)} + e^{2\pi i(-hx+ky-lz)} \right) \left(1 + e^{2\pi i((h+k)/2)} \right) \\ \left(1 + e^{2\pi i((h+k)/2)} \right) &= 0 \text{ when } h+k = 2n+1 \text{ and } = 2 \text{ when } h+k = 2n \\ &= 2 \sum_{\text{atoms } j} f_j e^{-B_j \sin^2 \vartheta / \lambda^2} \left(e^{2\pi i(hx+ky+lz)} + e^{2\pi i(-hx+ky-lz)} \right) \\ &= 2 \sum_{\text{atoms } j} f_j e^{-B_j \sin^2 \vartheta / \lambda^2} \left(\cos(2\pi(hx+ky+lz)) + \cos(2\pi(\bar{h}x+ky+\bar{l}z)) \right) \\ &\quad + i 2 \sum_{\text{atoms } j} f_j e^{-B_j \sin^2 \vartheta / \lambda^2} \left(\sin(2\pi(hx+ky+lz)) + \sin(2\pi(\bar{h}x+ky+\bar{l}z)) \right) \\ \cos A + \cos B &= 2 \cos\left(\frac{A+B}{2}\right) \cos\left(\frac{A-B}{2}\right) \text{ and } \sin A + \sin B = 2 \sin\left(\frac{A+B}{2}\right) \cos\left(\frac{A-B}{2}\right) \\ &= 4 \sum_{\text{atoms } j} f_j e^{-B_j \sin^2 \vartheta / \lambda^2} \cos 2\pi(hx+lz) \cos(2\pi ky) \\ &\quad + i 4 \sum_{\text{atoms } j} f_j e^{-B_j \sin^2 \vartheta / \lambda^2} \cos 2\pi(hx+lz) \sin(2\pi ky) \\ A_h &= \sum_{\text{atoms } j} f_j e^{-B_j \sin^2 \vartheta / \lambda^2} \left[4 \cos 2\pi(hx+lz) \cos(2\pi ky) \right] = \sum_{\text{atoms } j} f_j e^{-B_j \sin^2 \vartheta / \lambda^2} A(h, x) \\ B_h &= \sum_{\text{atoms } j} f_j e^{-B_j \sin^2 \vartheta / \lambda^2} \left[4 \cos 2\pi(hx+lz) \sin(2\pi ky) \right] = \sum_{\text{atoms } j} f_j e^{-B_j \sin^2 \vartheta / \lambda^2} B(h, x) \end{aligned}$$

where A(h,x) and B(h,x) correspond to the expressions for A and B in the International tables for h+k = even.

electron density expression

(modified slightly from IT expression at bottom of C2 listing)

$$\rho(xyz) = \frac{4}{V_c} \sum_{\text{all } h} \sum_{k=0} \sum_{l=0} |F(hkl)| \cos 2\pi(hx + lz) \cos(2\pi ky - \alpha(hkl)) \quad \text{for } h+k = 2n$$

$$\cos(A - B) = \cos A \cos B + \sin A \sin B$$

$$\sin(A - B) = \sin A \cos B - \cos A \sin B$$

$$= \frac{4}{V_c} \sum_{\text{all } h} \sum_{k=0} \sum_{l=0} |F(hkl)| \cos 2\pi(hx + lz) [\cos(2\pi ky) \cos \alpha + \sin(2\pi ky) \sin \alpha]$$

$$= \frac{4}{V_c} \sum_{\text{all } h} \sum_{k=0} \sum_{l=0} A_h \cos 2\pi(hx + lz) \cos(2\pi ky) + B_h \cos 2\pi(hx + lz) \sin(2\pi ky)$$

$$= \frac{1}{V_c} \sum_{\text{all } h} \sum_{k=0} \sum_{l=0} A_h 4 \cos 2\pi(hx + lz) \cos(2\pi ky) + B_h 4 \cos 2\pi(hx + lz) \sin(2\pi ky)$$

$$= \frac{1}{V_c} \sum_{\text{all } h} \sum_{k=0} \sum_{l=0} (A_h A(h,x) + B_h B(h,x))$$

where A(h,x) and B(h,x) correspond to the expressions for A and B in the International tables for h+k = even.

Integrated Electron Density about a Point

The integrated electron density, $I(R, x_0)$ contained within a sphere of radius R about a point x_0 may be calculated by evaluation of the following integral

$$I(R, x_0) = \int_{|r-x_0| < R} \rho(r) dr$$

One way to calculate $I(R, x_0)$ is to numerically evaluate this integral by calculating values of $\rho(r)$ on a fine grid within the specified volume, with the value of the volume element dr obtained from the details of the grid spacings along xyz . The Uppsala program MAPMAN works this way.

A computationally more efficient way of calculating this integral may be identified by noting that $I(R, x_0)$ can be equivalently written as the product of the electron density times a shape function $\sigma(r)$ that is 1 when $r \leq R$ and 0 for $r > R$.

$$I(R, x_0) = \int \rho(r) \sigma(r - x_0) dr$$

This expression is the convolution of the electron density with the shape function. By the properties of Fourier transforms, the Fourier transform of a convolution is the product of the Fourier transforms of the two functions:

$$\begin{aligned} FT[I] &= FT[\rho(r)] FT[\sigma(r)] \\ FT[\rho(r)] &= F(hkl) \\ FT[\sigma(r)] &= \int_0^R \sigma(r) \frac{2r}{S} \sin(2\pi Sr) dr = \frac{\sin(2\pi SR) - 2\pi SR \cos(2\pi SR)}{2\pi^2 S^3} \\ FT[I] &= \left[\frac{\sin(2\pi SR) - 2\pi SR \cos(2\pi SR)}{2\pi^2 S^3} \right] F(hkl) \end{aligned}$$

Hence, the integrated electron density within a radius R of a point x_0 may be obtained from the value of the inverse Fourier transform of $FT[I]$ at the point x_0 .

A beautiful example of the use of the convolution theorem to evaluate an equivalent type of integral may be found in Andrew Leslie's article *Acta Cryst.* A43, 134-136 (1987) which described a computationally efficient algorithm for the calculation of a Wang-type solvent envelope.

Relationship between B_{ave} and Resolution

The Wilson plot displays the resolution dependence of the average values of the diffracted intensities measured from a crystal. If normalized to the value of the lowest resolution bin, the Wilson plot would ideally have the following dependence on $\sin^2 \vartheta / \lambda^2$ or equivalently resolution (d):

$$(Eq. 1) \quad \ln \frac{\langle I(d) \rangle}{\langle I(0) \rangle} = -\frac{2B \sin^2 \vartheta}{\lambda^2} = -\frac{2B}{4d^2}$$

One could imagine that for structures diffracting to different resolutions, the value of $\ln[\langle I \rangle / \langle I(0) \rangle]$ at the high resolution limit for each structure might be approximately the same

(designated “ p ” in the schematic below), where $\ln \frac{\langle I(d_{max}) \rangle}{\langle I(0) \rangle} = -\frac{B}{2d_{max}^2} \equiv p$:

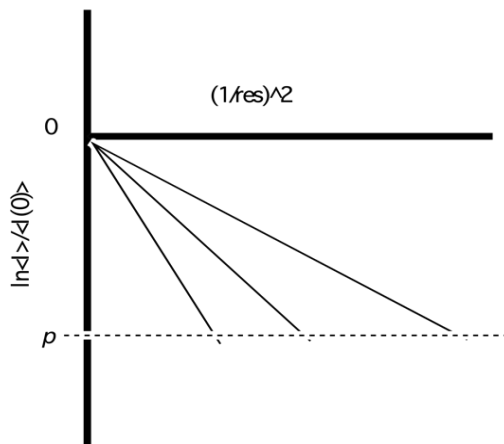


Fig. 1

For the collection of structures illustrated below, the value of p is ~ -3 to -4 . The Wilson plots shown below were calculated with the CCP4 program “Truncate” for a set of structures solved in our group (ie – this is not a systematic survey).

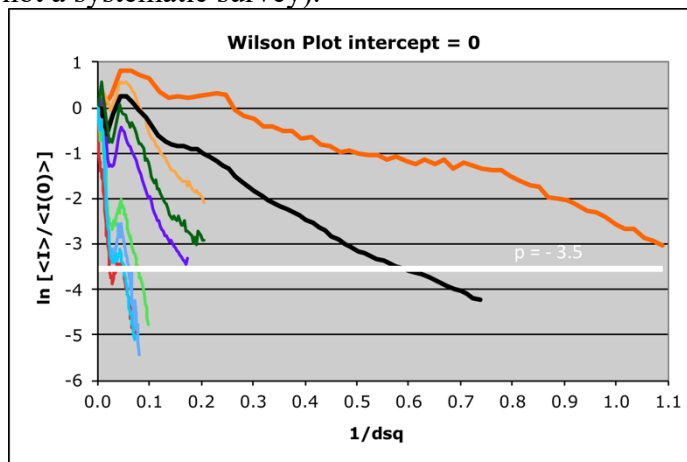


Fig. 2

The slope of the Wilson plot ($\ln\langle I \rangle$ vs $\sin^2 \vartheta / \lambda^2$) equals $-2B_{ave}$, so that the slope of $\ln\langle I \rangle$ vs $1/d^2$ will equal $-B_{ave}/2$. If a crystal diffracts to the high resolution limit, d_{max} , then if $\frac{B_{ave}}{2} \times \left(\frac{1}{d_{max}}\right)^2 = -p$, and if $p \sim$ constant for different structures, we would expect $B_{ave} \propto d_{max}^2$.

The relationship between B_{ave} and d_{max}^2 is plotted below for proteins in the PDB (cyan), based on an unpublished analysis of James Holton from ~ 2010 (but see *J. Sync. Rad.* 16, 133 (2009), *Acta Cryst.* D66, 393 (2010)). For this analysis, the B 's are averaged in resolution bins. While there does appear to be a reasonable linear dependence of B_{ave} on d_{max} , there is also a constant term so that the empirical fit may be approximated as

Eq. 2
$$B_{ave} \sim 4 d_{max}^2 + 12.$$

For comparison, a set of membrane proteins (from a non-comprehensive analysis we did in 2010) and low resolution complexes from an analysis by Brunger (*Acta Cryst.* D65, 128 (2009)) are shown that suggest for a given resolution, the B_{ave} for these classes of macromolecules are about 2x that observed relative to the set of proteins deposited in the PDB (dominated by soluble proteins).

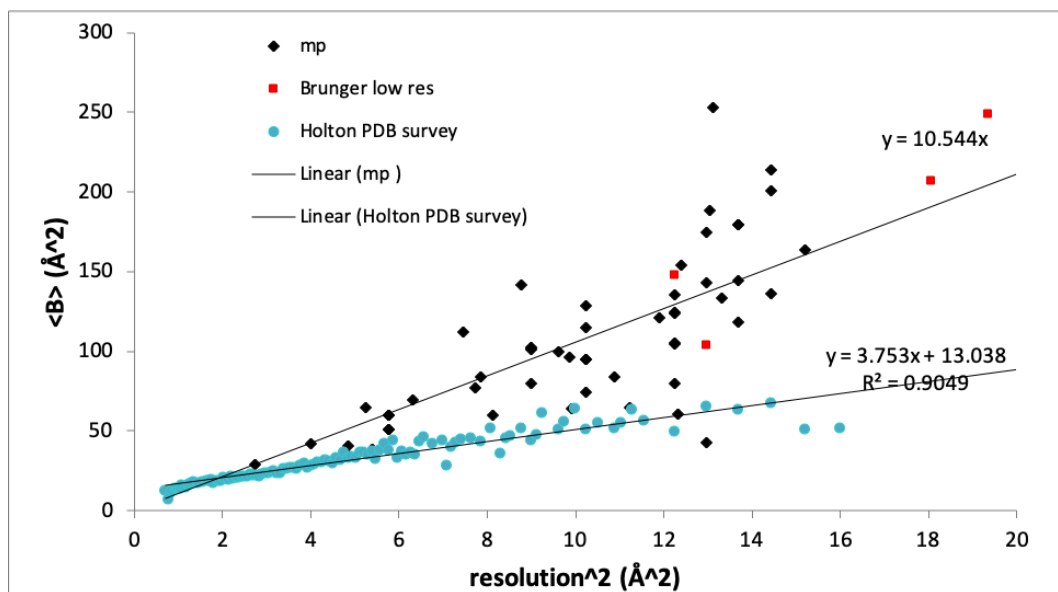


Fig. 3

At the resolution limit of a structure, the limiting point on the Wilson plot is given by

$$\ln \frac{\langle I(d_{\max}) \rangle}{\langle I(0) \rangle} = -\frac{B_{\text{ave}}}{2d_{\max}^2}$$

With $B_{\text{ave}} \sim 4d_{\max}^2 + 12$, the relationship between B_{ave} and d_{\max} may be rewritten as

$$\text{(Eq. 3)} \quad -\frac{B_{\text{ave}}}{2d_{\max}^2} = -\frac{4d_{\max}^2 + 12}{2d_{\max}^2} = -2 - \frac{6}{d_{\max}^2} = p$$

This indicates that p is not a constant, but increases as the resolution numerically decreases, as indicated in the following schematic:

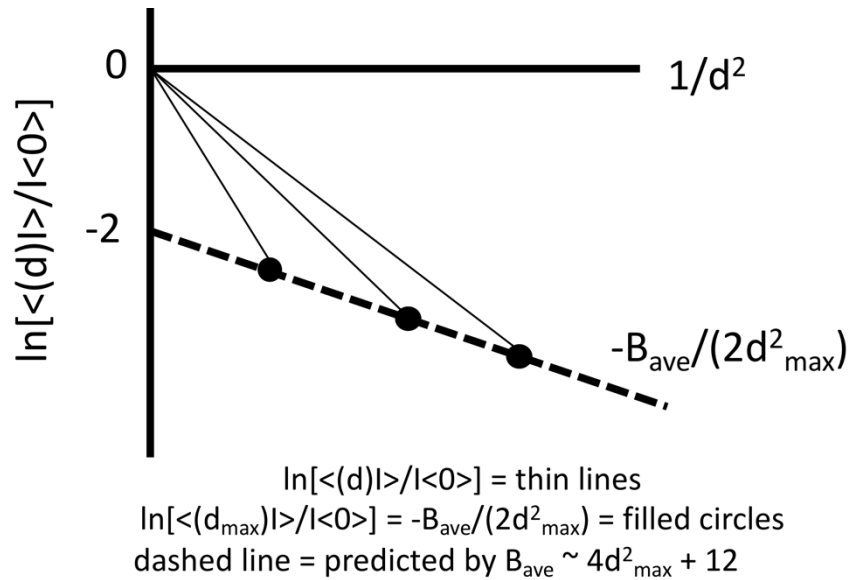


Fig. 4

Replotting the data in Figure 3 in the form of Figure 4 gives the following. For the proteins in James' survey, the "predicted" dependence of B_{ave} on d_{max} is observed (not surprisingly, because that data was used to derive the relationship in Eq. 2). Again, we see that the membrane proteins surveyed have a much higher B than anticipated based on Eq. 2, predominantly derived from water-soluble proteins.

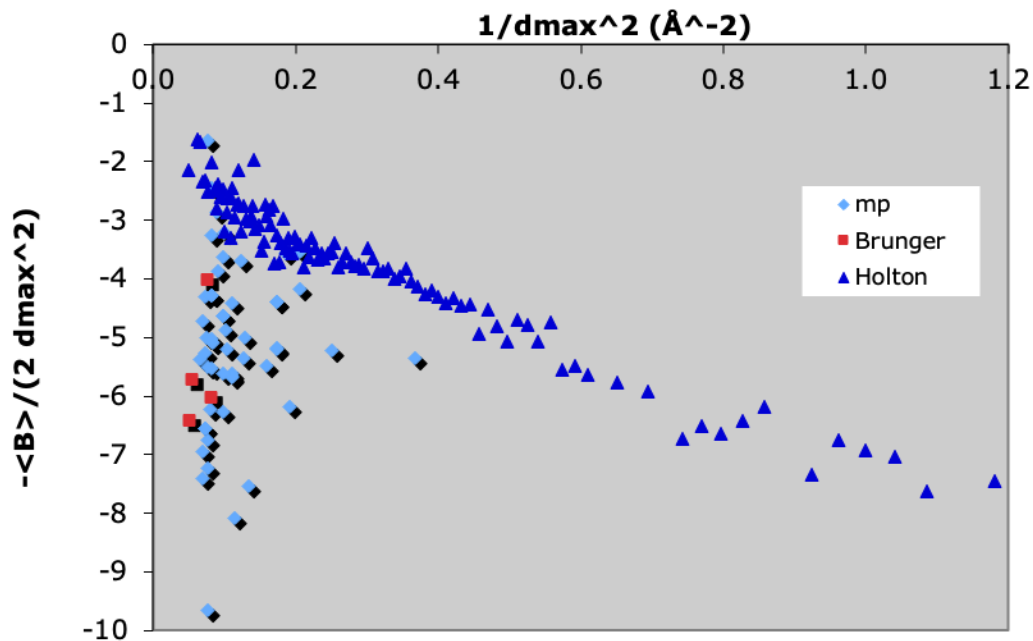


Fig. 5

The differences between Fig. 1 and Figs. 4/5 reflect the contribution of the constant term in equation 2 – could this be a reflection of lattice dynamics?

And, why do membrane proteins have such high B s for their resolution?

Section II: Random Walks and Crystallography

Useful references

R. Srinivasan and S. Parthasarathy (1976) *Some Statistical Applications in X-ray Crystallography*, Oxford: Pergamon

S. Chandrasekhar, *Rev. Mod. Physics* 15, 1 (1943) in N. Wax, ed. *Selected Papers on Noise and Stochastic Processes*, Dover (1954).

H.C. Berg (1993) *Random Walks in Biology*, Princeton, 2nd edition.

Background

A one dimensional random walk starting at the origin with step-length l and an equal probability of moving to the right or left may be described by a Gaussian in the limit of large step number:

$$P(x) = \frac{1}{\sqrt{2\pi\sigma^2}} e^{-x^2/2\sigma^2}$$

where $\sigma^2 = N l^2$ is the variance, or mean square distance from the origin, after N steps.

Consider the crystallographic structure factor expression for a centric reflection:

$$A = \sum_1^{N/2} 2f \cos(2\pi hx)$$

where f is the scattering factor for each atom (assumed equal). The mean square value of A is:

$$\begin{aligned} \langle A^2 \rangle &= (N/2) \langle (2f \cos(2\pi hx))^2 \rangle \\ &= (N/2) (4f^2) / 2 = Nf^2 = \langle F^2 \rangle = \langle I \rangle \equiv 1 \end{aligned}$$

so that the probability distribution becomes:

$$\begin{aligned} P(F) = P(A) &= \frac{1}{\sqrt{2\pi\langle I \rangle}} e^{-|F^2|/2\langle I \rangle} = \frac{1}{\sqrt{2\pi}} e^{-|F^2|/2} \\ P(|F|) &= P(|F|) + P(-|F|) = 2P(F) = \sqrt{\frac{2}{\pi}} e^{-|F^2|/2} \end{aligned}$$

The corresponding probability distribution on intensities is (with:

$$\begin{aligned} P_2(I) &= \frac{1}{2\sqrt{I}} P_1(\sqrt{I}) \quad (\text{S+P eqn. B.53}) \\ &= \frac{1}{\sqrt{2\pi I}} e^{-I/2} \end{aligned}$$

The noncentric distributions are slightly more complex to derive, because the contribution of the imaginary B component to the structure factors also needs to be included; ie in this case, one has a two dimensional random walk. Following the discussion in Chap. 1 of Srinivasan and Parthasarathy, one finds:

$$\begin{aligned} P(|F|) &= 2|F| e^{-|F|^2} \\ P(I) &= e^{-I} \end{aligned}$$

see also Wilson, *Acta Cryst.* **2**, 318 (1949)

Random R-values

Wilson *Acta Cryst.* **3**, 397 (1950)

The upper limit on R may be derived as follows. First, notice that R can be written as:

$$R = \frac{\langle \Delta F \rangle}{\langle F \rangle} \equiv \frac{\langle X \rangle}{\langle F \rangle}$$

Let the probability distribution of X be given by Q(X), where X is the difference of F and F+X for F>0, and F-X and F, for F>X. The probability that two reflections have values F and F+X is given by P(F)*P(F+X). The total probability distribution (Q(X)) is summed over all Fs:

$$\begin{aligned} Q(X) &= \int_0^{\infty} P(F)P(F+X)dF + \int_X^{\infty} P(F)P(F-X)dF \\ &\quad \text{change variables from F, F-X to F+X,F} \\ &= 2 \int_0^{\infty} P(F)P(F+X)dF \\ \langle X \rangle &= \int_0^{\infty} XQ(X)dX \end{aligned}$$

plugging in the above distribution functions gives the following values for random Rs, based on F and I, for centric and non-centric reflections:

R-factor	NC	C
F	0.586	0.828
I	1.000	1.273

Other important cases include having correct, but incomplete models, and complete models with coordinate errors. In this case, the R-factor is a function of resolution, and the dependence can be calculated by appropriate treatment of the variance in a random walk problem (Luzzati AC 5, 802 (1952)):

$$\sigma_A = \sigma_1 \langle \cos(2\pi h\Delta r) \rangle$$

Randy Read (*Acta Cryst.* **A42**, 140 (1986)) has also developed an analysis that estimates coordinate errors via sigma-A from the differences between Fo and Fc.

Random Walks and Intensity Statistics

From the properties of one and two-dimensional random walks, the intensity probability distributions for centrosymmetric and noncentrosymmetric crystals may be derived (Wilson, *Acta Cryst.* **2**, 318-321 (1949)):

$$P_{NC}(z) = e^{-z}$$

$$P_C(z) = \frac{1}{\sqrt{2\pi z}} e^{-z/2}$$

where z = the intensity value normalized as a function of resolution. From these and related distributions, various useful quantities, such as the R-factor expected for a random structure, may be derived. A powerful approach to the treatment of more complex situations, such as treatment of twinning, is provided by the general solution to one-dimensional random walk problems (Chandrasekhar, *Rev. Mod. Phys.* **15**, 1-89 (1943)). Let the observed length of an N step, one-dimensional random walk be denoted by p , where p is the result of N individual steps u_k , $k=1, \dots, N$:

$$p = \sum_{k=1}^N u_k$$

The probability distribution $P_N(p)$ may be determined by a two-step process:

(1) Calculation of λ_k , the characteristic function for the k^{th} step, which is given by the Fourier transform of the probability distribution function for the k^{th} step, $P(u_k)$: (note that Chandrasekhar uses a form of the Fourier transform without the 2π)

$$\lambda_k(\phi) = \int_{-\infty}^{\infty} e^{i\phi u_k} P(u_k) du_k$$

(2) The probability distribution function of p , $P_N(p)$ is then given by the inverse Fourier transform of the repeated product of all N characteristic functions:

$$P_N(p) = \frac{1}{2\pi} \int_{-\infty}^{\infty} e^{-i\phi p} \left\{ \prod_{k=1}^N \lambda_k(\phi) \right\} d\phi$$

Applications to twinning:

For the case of perfect twinning, the twinning fractions are given by $1/N$, where N is the total number of crystals in a twin. For structures obeying Wilson statistics:

$$\begin{aligned}
P_{NC}(u_k) &= Ne^{-Nu_k} \\
\lambda_{k,NC}(\phi) &= \frac{Ni}{\phi + Ni} \\
P_{N,NC}(p) &= \frac{N^N p^{N-1}}{(N-1)!} e^{-Np} \\
\\
P_C(u_k) &= \sqrt{\frac{N}{2\pi u_k}} e^{-Nu_k/2} \\
\lambda_{k,C}(\phi) &= \frac{\sqrt{Ni/2}}{\sqrt{\phi + Ni/2}} \\
P_{N,C}(p) &= \frac{(N/2)^{N/2} p^{(N-2)/2}}{\Gamma(N/2)} e^{-Np/2}
\end{aligned}$$

The $P_N(p)$ distributions were first derived by E. Stanley (*J. Appl. Cryst.* **5**, 191-194 (1972)).

The intensity distributions for noncentric, centric, twinned (N=2) noncentric and twinned centric reflections are given by $P(z) = \exp(-z)$, $(2\pi z)^{-1/2} \exp(-z/2)$, $4z \exp(-2z)$ and $\exp(-z)$ respectively. The ratio $\langle I^2 \rangle / \langle I \rangle^2$ calculated from these distributions are 2, 3, 1.5, and 2, respectively. Hence, this ratio provides a sensitive assay for the presence of twinning, provided the untwinned structure obeys Wilson statistics (M.R. Redinbo & T.O. Yeates, *Acta Crystallogr.* **D49**, 375-380 (1993); T.O. Yeates, *Meth. Enz.* **276**, 344-358 (1997)).

Section III: Coordinate and Reflection Transformations; Molecular Replacement Unit Cell Transformations

On occasion, it may be necessary to transform coordinates and reflection lists between different choices of unit cell. This may arise if the unit cell chosen by auto-indexing during data collection is not the cell that you would like, or if there is some relationship between different crystal forms that one wishes to emphasize. These transformations are easy to implement, and more details can be found on pages 70-72 of Volume A of the International Tables.

Let \mathbf{P} be the matrix that transforms the unit cell axes (\mathbf{a}_1) of crystal form 1 into the unit cell axes of crystal form 2 (\mathbf{a}_2):

$$\mathbf{a}_2^T = \mathbf{a}_1^T \mathbf{P}$$

where \mathbf{a}_1^T is the row vector (a b c), etc. The determinant of \mathbf{P} gives the unit cell volume of crystal 2 relative to crystal 1 (and will be positive if right-handed coordinate systems are used).

\mathbf{P} also transforms the reflection indices from crystal 1 (\mathbf{h}_1) to the indices of crystal 2 (\mathbf{h}_2):

$$\mathbf{h}_2^T = \mathbf{h}_1^T \mathbf{P}$$

where \mathbf{h}_1^T is the row vector (h k l). The inverse transform from crystal 2 to crystal 1 is given by the matrix $\mathbf{Q} = \mathbf{P}^{-1}$ (and usually, \mathbf{P}^{-1} is not the same as \mathbf{P}^T). \mathbf{Q} transforms the basis vectors:

$$\mathbf{a}_2^* = \mathbf{Q} \mathbf{a}_1^*$$

$$\mathbf{x}_2 = \mathbf{Q} \mathbf{x}_1$$

where \mathbf{a}_1^* is the column vector of the reciprocal space vectors, \mathbf{x}_1 is the column vector of the coordinates of a point in real space, etc. The eigenvectors of \mathbf{Q} with unit eigenvalues correspond to directions (\mathbf{x} vectors) that are unchanged by this transformation.

If the real space lattice is translated by a vector \mathbf{p} , then the inverse shift is given by $\mathbf{q} = -\mathbf{Q} \mathbf{p}$.

The real space metric tensor, $G_{ij} = \mathbf{a}_i \cdot \mathbf{a}_j$, transforms as

$$\mathbf{G}_2 = \mathbf{P}^T \mathbf{G}_1 \mathbf{P}$$

and the reciprocal space metric tensor transforms as

$$\mathbf{G}_2^* = \mathbf{Q} \mathbf{G}_1^* \mathbf{Q}^T$$

Example: Transformation from primitive rhombohedral cell to triply primitive hexagonal cell

The standard obverse setting is used for the hexagonal cell, with origins at (0,0,0), (2/3,1/3,1/3), (1/3,2/3,2/3), and the reflection condition $-h+k+l = 3n$ (see Table 5.1 and figure 5.7 of Vol A of the International Tables). For this transformation (see Table 5.1):

$$\begin{aligned}
 P &= \begin{bmatrix} 1 & 0 & 1 \\ \bar{1} & 1 & 1 \\ 0 & \bar{1} & 1 \end{bmatrix} & Q = P^{-1} &= \begin{bmatrix} 2/3 & -1/3 & -1/3 \\ 1/3 & 1/3 & -2/3 \\ 1/3 & 1/3 & 1/3 \end{bmatrix} \\
 G_R &= a_R^2 \begin{bmatrix} 1 & \cos\alpha_R & \cos\alpha_R \\ \cos\alpha_R & 1 & \cos\alpha_R \\ \cos\alpha_R & \cos\alpha_R & 1 \end{bmatrix} \\
 G_H &= \begin{bmatrix} a_H^2 & a_H^2 \cos\gamma_H & 0 \\ a_H^2 \cos\gamma_H & a_H^2 & 0 \\ 0 & 0 & c_H^2 \end{bmatrix} \\
 &= P^T G_R P \\
 &= a_R^2 \begin{bmatrix} 2-2\cos\alpha_R & \cos\alpha_R-1 & 0 \\ \cos\alpha_R-1 & 2-2\cos\alpha_R & 0 \\ 0 & 0 & 3+6\cos\alpha_R \end{bmatrix}
 \end{aligned}$$

equating the relevant matrix elements gives:

$$\begin{aligned}
 \cos\gamma_H &= -\frac{1}{2}; \quad \gamma_H = 120^\circ \\
 a_H &= a_R \sqrt{2(1-\cos\alpha_R)} \\
 c_H &= a_R \sqrt{3(1+2\cos\alpha_R)} \\
 \cos\alpha_R &= \frac{2-3(a_H/c_H)^2}{6(a_H/c_H)^2+2} \\
 a_R^2 &= \frac{c_H^2(6(a_H/c_H)^2+2)}{18}
 \end{aligned}$$

Changing the Hand of a Space Group

CCP4 Program Suite Documentation

file:///sw/share/xtal/ccp4-4.2.2/html/reindexing.html#changing_hand

Test to see if the other hand is the correct one:

Change x,y,z for $(cx-x, cy-y, cz-z)$

Usually $(cx,cy,cz) = (0,0,0)$.

Remember you need to change the twist on the screw-axis stairs for $P3_i$, $P4_i$, or $P6_i$!

$P2_1$ to $P2_1$; For the half step of 2_1 axis, the symmetry stays the same.

$P3_1$ to $P3_2$

$P3_2$ to $P3_1$

$P4_1$ to $P4_3$

($P4_2$ to $P4_2$: Half c axis step)

$P4_3$ to $P4_1$

$P6_1$ to $P6_5$

$P6_2$ to $P6_4$

($P6_3$ to $P6_3$)

etc.

In a few non-primitive spacegroups, you can change the hand and not change the spacegroup by a cunning shift of origin:

$I4_1$

(x,y,z) to $(-x, 1/2-y, -z)$

$I4_122$

(x,y,z) to $(-x, 1/2-y, 1/4-z)$

$F4_132$

(x,y,z) to $(3/4-x, 1/4-y, 3/4-z)$

Plus some centric ones:

$Fdd2$ (space group 43)

(x,y,z) to $(1/4-x, 1/4-y, -z)$

$I4_1md$ (space group 109)

(x,y,z) to $(1/4-x, 1/4-y, -z)$

$I4_1cd$ (space group 110)

(x,y,z) to $(1/4-x, 1/4-y, -z)$

$I4\bar{2}d$ (space group 122)

(x,y,z) to $(1/4-x, 1/4-y, -z)$

Equivalent Reflections and Phase Relationships

Let the j^{th} symmetry operation have a rotation matrix C_j and a translation vector t_j . Then

$$\mathbf{h}_j^T = \mathbf{h}^T C_j$$

$$\alpha(\mathbf{h}_j) = \alpha(\mathbf{h}) - 2\pi (\mathbf{h}^T \cdot \mathbf{t}_j)$$

For centric reflections where $\mathbf{h}^T C_j = -\mathbf{h}^T$

$$\alpha(\mathbf{h}_j) = \pi (\mathbf{h}^T \cdot \mathbf{t}_j)$$

Proof (see Bertaut *Acta Crystallogr.* **17**, 778 (1964))

$$\begin{aligned} F(\mathbf{h}) &= \sum_j f e^{2\pi i \mathbf{h} \cdot (\mathbf{C}_j \mathbf{x} + \mathbf{t}_j)} \\ F(\mathbf{h}_1) &= F(\mathbf{h} C_1) = \sum_j f e^{2\pi i \mathbf{h} C_1 (\mathbf{C}_j \mathbf{x} + \mathbf{t}_j)} \\ &= e^{-2\pi i \mathbf{h} \cdot \mathbf{t}_1} \left\{ \sum_j f e^{2\pi i \mathbf{h} C_1 (\mathbf{C}_j \mathbf{x} + \mathbf{t}_j) + \mathbf{t}_1} \right\} \end{aligned}$$

If C_j , t_j and C_1 , t_1 are crystallographic symmetry operators, then by definition, transformation of a point \mathbf{x} by any C_j, t_j generates an equivalent position. Hence, if $(C_j \mathbf{x} + t_j) = \mathbf{x}_j$, then $C_1 \mathbf{x}_j + t_1$ is another equivalent position. Therefore, the term in $\{ \} = F(\mathbf{h})$, and

$$F(\mathbf{h} C_1) = e^{-2\pi i \mathbf{h} \cdot \mathbf{t}_1} F(\mathbf{h})$$

If $\mathbf{h} C_1 = -\mathbf{h}$, then $F(\mathbf{h})$ and $F(\mathbf{h} C_1)$ are both Friedel mates and centric. Since $\alpha(-\mathbf{h}) = -\alpha(\mathbf{h})$ by Friedel's law, then for centric reflections:

$$\begin{aligned} \alpha(\bar{h}) &= \alpha(\mathbf{h}) - 2\pi \mathbf{h} \cdot \mathbf{t}_1 = -\alpha(\mathbf{h}), \text{ or} \\ \alpha(\mathbf{h}) &= \pi \mathbf{h} \cdot \mathbf{t}_1 \quad (\text{modulo } \pi) \end{aligned}$$

P2₁2₁2₁ phase relationships

Space group 19 equivalent positions:

$$\left| x, y, z; \quad \frac{1}{2} - x, \bar{y}, \frac{1}{2} + z; \quad \frac{1}{2} + x, \frac{1}{2} - y, \bar{z}; \quad \bar{x}, \frac{1}{2} + y, \frac{1}{2} - z \right|$$

from the section in the crystallographic appendices on equivalent reflections and phase relationships

$$h_j^T = h^T C_j$$

$$\alpha(h_j^T) = \alpha(h^T) - 2\pi(h^T \cdot t_j)$$

with $h^T = (hkl)$, and j corresponding to the equivalent positions listed above, one can derive:

$$\alpha(hkl) = -\alpha(\bar{h}\bar{k}\bar{l})$$

$$\alpha(\bar{h}\bar{k}\bar{l}) = \alpha(hkl) - 2\pi\left(\frac{h+l}{2}\right) = \alpha(hkl) + \pi(h+l) = -\alpha(hk\bar{l})$$

$$\alpha(hk\bar{l}) = \alpha(hkl) - 2\pi\left(\frac{h+k}{2}\right) = \alpha(hkl) + \pi(h+k) = -\alpha(\bar{h}kl)$$

$$\alpha(\bar{h}kl) = \alpha(hkl) - 2\pi\left(\frac{k+l}{2}\right) = \alpha(hkl) + \pi(k+l) = -\alpha(h\bar{k}\bar{l})$$

For comparison, the phase relationships can also be obtained from the structure factor tables in Volume I of the "old" International Tables

indices conditions	(hkl)	$(\bar{h}\bar{k}\bar{l})$	$(hk\bar{l})$	$(\bar{h}kl)$
$h+k=2n$ $k+l=2n$ $(h,k,l \text{ even})$	α	α	α	α
$h+k=2n$ $k+l=2n+1$ $(h+l=2n+1)$	α	$\pi+\alpha$	α	$\pi+\alpha$
$h+k=2n+1$ $k+l=2n$ $(h+l=2n+1)$	α	$\pi+\alpha$	$\pi+\alpha$	α
$h+k=2n+1$ $k+l=2n+1$ $(h+l=2n)$	α	α	$\pi+\alpha$	$\pi+\alpha$

addition of π to a phase is equivalent to the transformation $A + iB$ to $-A - iB$.

Phase Relationships of Friedel Pairs in the Presence of Anomalous Scattering

In the absence of X-ray absorption (anomalous scattering), the electron density values are real, so that $F(h) = F^*(\bar{h})$, which is equivalent to $|F(h)| = |F^*(\bar{h})|$ and $\alpha(h) = -\alpha(\bar{h})$ (Friedel's law).

For centrosymmetric reflections (either from a centrosymmetric crystal, or certain projections of a noncentrosymmetric crystal), an inversion center at the origin gives rise to the relationship $\alpha(h) = \alpha(\bar{h}) = -\alpha(\bar{h})$, so that $\alpha(h) = 0$ or π .

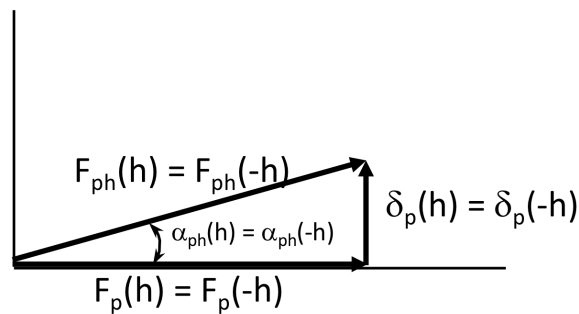
In the presence of X-ray absorption (anomalous scattering), due to absorption and the associated introduction of an imaginary component to the relevant atomic scattering factors, $F(h) \neq F^*(\bar{h})$ and Friedel's law no longer holds.

For noncentrosymmetric structures when the absorption effects due to the presence of a heavy atom (h) are small relative to the overall scattering from the rest of the structure (p), the difference between Friedel mates can be derived (see the Crystallography notes)

$$\Delta_{ano} = (|F_{ph}(h)| - |F_{ph}(\bar{h})|) = -2|\delta_h| \sin(\psi - \alpha_{ph})$$

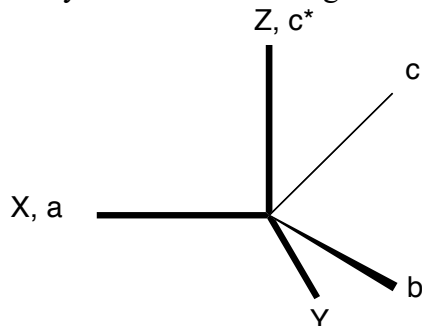
where α_{ph} = phase of the "normal" scatterers, ψ = phase of the absorbing atoms, and $|\delta|$ = magnitude of imaginary component of the scattering factor for absorbing atoms.

For centrosymmetric structures, Friedel's law is valid, with $|F(h)| = |F^*(\bar{h})|$ and $\alpha(h) = \alpha(\bar{h})$, but the phases are no longer restricted to 0 or π , as shown by the following construct.



Orthogonalization Convention

We use the convention adopted by Brookhaven, TOM/FRODO, O, X-PLOR and CCP4 (ncode = 1) - unit cells are orthogonalized onto a Cartesian coordinate system defined by **a**, **c*** **x** **a** and **c***. Beware: other programs may use different orthogonalization conventions.



With this convention, the matrix converting fractional to orthogonal coordinates is:

$$\begin{bmatrix} X \\ Y \\ Z \end{bmatrix}_{\text{orthogonal}} = \begin{bmatrix} \hat{X} \cdot a & \hat{X} \cdot b & \hat{X} \cdot c \\ \hat{Y} \cdot a & \hat{Y} \cdot b & \hat{Y} \cdot c \\ \hat{Z} \cdot a & \hat{Z} \cdot b & \hat{Z} \cdot c \end{bmatrix} \begin{bmatrix} x \\ y \\ z \end{bmatrix}_{\text{fractional}} = \begin{bmatrix} a & b \cos \gamma & c \cos \beta \\ 0 & b \sin \gamma & c \left\{ \frac{\cos \alpha - \cos \beta \cos \gamma}{\sin \gamma} \right\} \\ 0 & 0 & \frac{\text{Volume}}{ab \sin \gamma} \end{bmatrix} \begin{bmatrix} x \\ y \\ z \end{bmatrix}_{\text{fractional}}$$

where $\text{Vol} = abc (1 - \cos^2 \alpha - \cos^2 \beta - \cos^2 \gamma + 2 \cos \alpha \cos \beta \cos \gamma)^{1/2} = \text{sqrt}(\text{Det}(\mathbf{G}))$. This matrix can be calculated by **ORTMAT(SUB_2).FOR**.

Specific forms of this matrix for monoclinic and trigonal cells are given:

Monoclinic cells - orthogonal x and y superimpose with crystallographic a and b axes:

$$\begin{bmatrix} a & 0 & c \cos \beta \\ 0 & b & 0 \\ 0 & 0 & c \sin \beta \end{bmatrix}$$

Trigonal cells - orthogonal x and z superimpose with crystallographic a and c axes:

$$\begin{bmatrix} a & a \cos \gamma & 0 \\ 0 & a \sin \gamma & 0 \\ 0 & 0 & c \end{bmatrix}$$

Deorthogonalization:

Deorthogonalization matrices are the **inverse (not transpose)** of the orthogonalization matrix - these may also be obtained from ORTMAT(SUB_2). For monoclinic and trigonal cells, these matrices take the form:

Monoclinic:

$$\begin{bmatrix} \frac{1}{a} & 0 & -\frac{\cos\beta}{a\sin\beta} \\ 0 & \frac{1}{b} & 0 \\ 0 & 0 & \frac{1}{c\sin\beta} \end{bmatrix}$$

Trigonal:

$$\begin{bmatrix} \frac{1}{a} & -\frac{\cos\gamma}{a\sin\gamma} \sim \frac{0.57735}{a} & 0 \\ 0 & \frac{1}{a\sin\gamma} \sim \frac{1.15470}{a} & 0 \\ 0 & 0 & \frac{1}{c} \end{bmatrix}$$

Molecular Replacement - Practical Considerations

Situations often arise where it is necessary to create an output electron density map from one or more input electron density maps. Variations on this theme include non-crystallographic symmetry (NCS) averaging, skewing maps down a particular axis (such as a molecular twofold), or molecular replacement (MR) between different crystal forms. The algorithms we use for this purpose are loosely based on the double sort method introduced by Bricogne (*Acta Cryst.* **A32**, 832-847 (1976)); given the advances in computer memory, this is not needed in the 21st century.

NCS averaging and MR provide important methods for both obtaining and refining phases. If multiple images of a molecule are present in one or more different crystal forms, then it is possible to get an improved representation of the molecule by averaging these different images. We will specifically address implementation of this process in the case that no atomic models are available, so that we must work directly with electron density maps. This has the critical consequence that we are primarily concerned with grid points in electron density maps that are defined only at specific sites in the unit cell (given by integer multiples of the sampling number along each cell axis), rather than atomic coordinates that may be located at any position in the unit cell.

An essential step in averaging is determination of the orientational and translational relationships between different molecules. These relationships may be established by some combination of:

(1) rotation functions (Rossmann and Blow *Acta Cryst.* 15, 24-31 (1962)). - self and cross; these usually are calculated with intensity data only, but can be performed with two Patterson maps (X-PLOR, REALRF). Contiguous regions in electron density maps (molecules?) can also be masked off and inverted to simplify the rotation function. Crowther's Fast Rotation Function (Crowther, in "The Molecular Replacement Method" MG Rossmann, ed., pp 173-178, Gordon & Breach (1972)), MERLOT, X-PLOR, AMORE, and CCP4 programs can be used for these calculations.

(2) native Patterson functions - useful for identifying even fold NCS rotations that are parallel to even fold crystallographic rotation axes, or for molecules that are related by a translation. If the NCS relationships are approximate, characteristic peaks should be stronger at low resolution (8Å or so) than at higher resolutions.

Native Patterson maps and self rotation functions should always be calculated if NCS is suspected.

(3) translation functions - various flavors, depending on what sort of phase or model information is available for the various crystal forms. We have programs for either Crowther-Blow translation functions (*Acta Cryst.* 23, 544-548 (1967); problem specific); GENTF (more general), or phased translation programs (when a source of phase information is available for an unknown model).

(4) native anomalous Patterson functions - can establish equivalent positions in different crystal forms.

(5) heavy atom coordinates - can be used to derive NCS relationships, if they can be assigned to appropriate groups.

(6) brute force search - if all else fails, one can systematically search rotation and translation space for NCS relationships in either electron density maps or with models (really desperation time). We don't have an official program to do this, but Pamela has implemented this for MHC and FcRn; Mitch and Geoff also have genetic algorithm programs to do this.

(7) refinement methods based on Patterson functions (TNT, X-PLOR or INTREF (T. Yeates)) or electron density maps (RHOPRP) can be used to improve initial NCS parameters. The RHOPRP programs (PNTGEN, RHOREF) need to be rewritten into a single, modern package.

We will assume that the NCS relationships have been established, and are represented in the form:

$$(I) \quad x_2 = C x_1 + d$$

where x_1 and x_2 are coordinates of equivalent positions in two molecules related by NCS. C is the rotation matrix, and d is the translation vector. Rotation matrices are specified by 3 rotation angles. At least three different conventions are in use in our group:

(a) Euler angles: $\theta_1, \theta_2, \theta_3$

(b) Crowther's Euler angles: $\alpha = \theta_1 - 90, \beta = \theta_2, \gamma = \theta_3 + 90$

(c) spherical polar angles: ϕ, ψ, κ

The FRF rotation function convention is that C obtained from a rotation function calculation rotates crystal 1 into crystal 2. A handy property of rotation matrices is that the inverse rotation (from molecule 2 to molecule 1) is given by the transpose matrix, C^T . Whenever possible, we are trying to use spherical polar angles, since they are easier to visualize. In this case, the inverse rotation to ϕ, ψ, κ is given by $\phi, \psi, -\kappa$. Routines for generating rotation matrices from Euler and spherical polar angles, and vice versa, are in [rees.math]matsub.for. Four subroutines are of particular utility:

ROTMATS(phi,psi,fkappa,C)	generates C from spherical polar angles
SPHANG(C,phi,psi,fkappa)	generates spherical polar angles from C

ROTMATE(the1,the2,the3,C)	generates C from Euler angles
EULERANG(C,the1,the2,the3)	generates Euler angles from C

Equation (I) is valid only for orthogonal coordinate systems, which means that the crystallographic coordinates must first be transformed by an orthogonalization matrix. Our official orthogonalization conventions (as of 11/28/92) are described in a separate section of this document.

Unlike crystallographic symmetry operators, C and d only relate specific sets of molecules. It is therefore essential that the molecular boundaries be defined in order to assign electron density grid points to a specific molecule. This is accomplished by specifying a molecular envelope; points inside the envelope belong to a particular molecule, whereas points outside belong to either solvent or another molecule. Depending on the status of the structure determination, the envelope may be defined in several ways. At early stages of a structure analysis, simple shapes like spheres or cubes may suffice for an envelope. At later stages, a more detailed envelope is required. This may be determined by some variant of B.C. Wang's algorithm (*Meth. Enzym.* 115, 90 (1985)) using either unaveraged maps (original Wang) or averaged maps, or from atomic models using either the muffin-tin option of EDCALCD or MAPMAN/O to both create and edit envelopes.

Once the NCS relationships and the envelope are defined, averaging may begin. This process may be envisioned as constructing a map in crystal 1 from electron density values in crystal 2. Crystal 1 and 2 may be the same in the case of NCS averaging, or they may be different for skewing and MR problems. In general, grid points in crystal 1 will not correspond to grid points in crystal 2; consequently, the required density values in crystal 2 must be obtained by interpolation from the nearest-neighbor grid points. Satisfactory linear interpolation in crystal 2 requires that this map (the "fine grid" map) be sampled at grid spacings of about 1/5 to 1/6 of the maximum resolution. Coarser grids can be used with quadratic interpolation, as in RAVE/MAVE. The crystal 1 map (the "coarse grid" map) need only be sampled at about 1/3 the resolution for satisfactory structure factor calculations by the inverse FFT.

Schematically, the averaging calculation proceeds as follows:

1. Test to see if grid point i in crystal 1 is inside the envelope;
if NO, go to the next grid point and repeat.
if YES, calculate coordinate of equivalent point x_2 in crystal 2
3. Interpolate the density value at x_2 in crystal 2.
3. Place this density value at x_1 in crystal 1 ("reconstruction").

Go to the next grid point in crystal 1, and repeat until all necessary points in crystal 1 have been tested. The reconstructed crystal 1 map may then be FFT inverted to give calculated structure factor amplitudes and phases. These calculated structure factors may be either combined or transferred to the observed structure factors. If this is an MR calculation, then the process stops here. If NCS averaging is being performed, then the process continues until convergence (4 or more cycles) is achieved.

Coordinate Superposition Considerations: Overview

originally prepared for ABC transporter review in *Nat. Rev. Mol. Cell Biol.* **10**, 218 (2009) – summarized in Supplementary Information S3 (box)

When structures are available for more than one homologous protein, an inevitable consideration concerns the conformational relationships between them. Although conceptually this comparison should be a straightforward process, a number of subjective decisions are involved that can influence the final conclusions. At the heart of these comparisons is the rigid body superposition between the coordinate sets for the two conformations, x and x' , which may be described in terms of a rotation matrix R and a translation vector d by the equation: $x' = Cx + d$. The calculation of this transformation is incorporated into a number of superposition programs and is unambiguous for a pair of truly rigid body structures. With real coordinate sets, the key operation is to identify structural elements that are essentially unchanged in the two conformational states, ie that behave as rigid bodies. A sensitive way to identify approximately rigid elements is with difference distance plots to find regions with conserved intramolecular distances. In practice, an iterative algorithm is used to find equivalent residues that superimpose within a certain limit. For the ABC subunits of ABC transporters, the secondary structure elements of the catalytic domain represent a commonly maintained rigid element. The TMDs are more variable, but conserved cores have been identified for the TMDs of both type I and type II ABC importers that can serve as a basic rigid scaffold.

Another aspect to characterizing conformational transformations is the choice of reference frame to compare the structures. For ABC transporters exhibiting two-fold molecular symmetry (which is approximately the case for all transporters solved to date), two principal reference frames are typically employed: the use of the entire transporter (all four domains of each transporter) in the superposition so that the symmetry axes coincide (the “symmetric frame”), or the use of only an individual domain (or part of a domain) in the superposition (the “single domain frame”). This problem has counterparts in the analysis of conformational transitions in any system, particularly symmetric, oligomeric assemblages (Perutz “Mechanisms of Cooperativity and Allosteric Regulation in Proteins”, Cambridge Univ. Press (1990)). Unless the two transporter structures are identical at the quaternary structural level, these comparisons are unlikely to yield equivalent results.

These considerations may be illustrated by the following analysis. Consider a molecular assemblage, a transporter for concreteness, that has two structurally equivalent subunits A and A' related by a two-fold operator T_A . Consider further a second conformation of the transporter with subunits B and B' related by a two-fold operator T_B . When the entire molecular assemblages are superimposed (the symmetric frame), the two-fold axes will coincide, corresponding to a single operator, T, and the arrangement depicted in (Fig 1a) is observed. With this choice of reference frame, the individual subunits do not coincide optimally, however. Let R be the rotation matrix that transforms B to the orientation observed in A, ie $A = RB$. By the properties of matrix algebra, $A' = TRT B'$ (for the purposes of this discussion, the translation component will be ignored). This transformation defines a new reference frame, the single domain frame (Fig 1b), in which one set of subunits are superimposed, B onto A, by the rotation R. The position of B' in this frame is given by $B'' = RB'$, and by the transformation that

converts B'' to A' becomes $A' = TRTR^{-1} B''$. If the two-fold operator T is taken along the z axis, and the rotation matrix R corresponds to a rotation angle κ about an axis with direction cosines $\left\{ \begin{matrix} 0 & m & \sqrt{1-m^2} \end{matrix} \right\}$, then with the help of Mathematica[®] (<http://www.wolfram.com>), the transformation converting B'' to A' is equivalent to a rotation about an axis with direction cosines $\left\{ \begin{matrix} p & q & 0 \end{matrix} \right\}$, with $p/q = -\sqrt{1-m^2} \tan[\kappa/2]$. This rotation axis is perpendicular to the reference two-fold axis oriented along z . The rotation angle φ is given by $\cos\varphi = 1 - 4m^2 + 3m^4 - 4m^2(m^2 - 1)\cos\kappa + m^4\cos 2\kappa$. The important point is that if the transformation interconverting subunits in the symmetric frame is predominantly along the two-fold axis (as observed for BtuCD and HI1470/1), then the equivalent transformation in the single domain frame corresponds to a nearly perpendicular axis in the plane normal to the two-fold. As discussed for BtuCD and HI1470/1, if the transformation in the symmetric frame is parallel to the two-fold axis, then the relative orientation of subunits is unchanged by this operation, but a translational displacement is generated. Furthermore, if the rotation axis is distant from a point, the distinction between a rotation about this axis and a perpendicular translation is blurred. Hence, without specification of the reference frame, terms such as hinge angle, twist axis, displacement vector, etc. in defining the relationship between subunits are ambiguous.

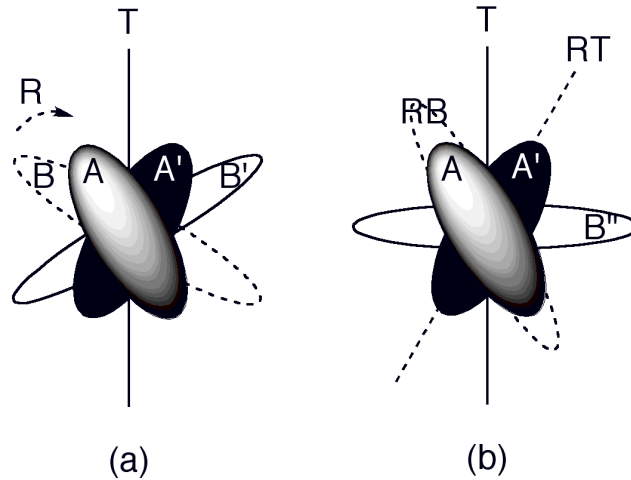


Figure 1 Illustration of the (a) symmetric and (b) single domain reference frames for the comparison of multidomain assemblies. Two conformations of a dimeric assembly, AA' and BB' are depicted. In the symmetric frame, the two-fold axes relating the pairs of subunits in the two assemblies are superimposed and correspond to the axis T oriented vertically. In (b), subunit B is superimposed onto A through a rotation R that also rotates B' to B'' and T to RT .

Superposition Relationships for Oligomeric Proteins

Two subunits related by a twofold rotation axis

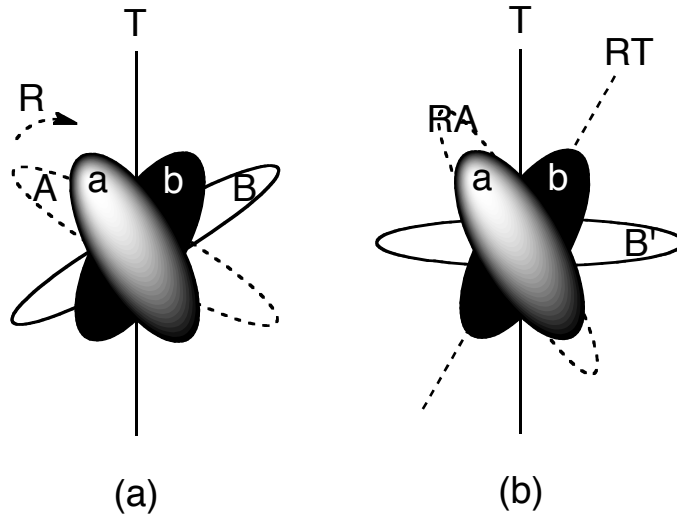


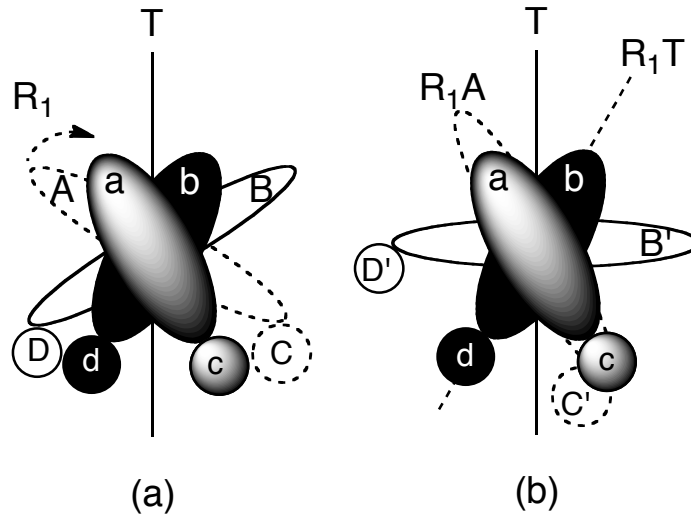
Illustration of the (a) symmetric and (b) single domain references frames for the comparison of multidomain assemblies. Two conformations of a dimeric assembly, **ab** and **AB** are depicted. In the symmetric frame, the two-fold axes relating the pairs of subunits in the two assemblies are superimposed and correspond to the axis **T** oriented vertically. In (b), subunit **A** is superimposed onto **a** through a rotation **R** that also rotates **B** to **B'** and **T** to **RT**.

R and **d** transform **A** to **a** and **B** to **B'**; the transformation between **b** and **B'** when **A** and **a** are superimposed becomes:

$$\begin{aligned}
 x_a &= Rx_A + d \\
 x_b &= Tx_a = TRx_A + Td \\
 &= TRTx_B + Td \\
 &\text{and} \\
 x_{B'} &= Rx_B + d \\
 Rx_B &= x_{B'} - d \\
 x_B &= R^{-1}(x_{B'} - d) \\
 x_b &= TRTx_B + Td = TRTR^{-1}x_{B'} + T(I - RTR^{-1})d \\
 &\equiv R_{B'}x_{B'} + d_{B'}
 \end{aligned}$$

Two subunits with two domains related by a twofold

R_1, d_1 superimpose A onto a

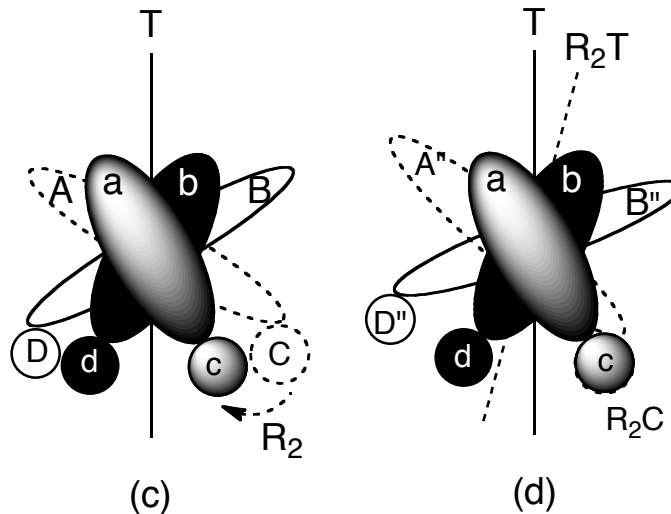


R_B, d_B transform B' to b when A is superimposed onto a.

$$x_b = R_B x_{B'} + d_B$$

$$R_B = TR_1TR_1^{-1} \text{ and } d_B = T(I - R_1TR_1^{-1})d_1$$

R_2, d_2 superimpose C onto c



R_D, d_D transform D'' to d when C is superimposed onto c.

$$x_d = R_D x_{D''} + d_D$$

$$R_D = TR_2TR_2^{-1} \text{ and } d_D = T(I - R_2TR_2^{-1})d_2$$

R_C, d_C transform C' to c when A is superimposed onto a

$$x_c = R_2 x_{C'} + d_2 = R_C (R_1 x_{C'} + d_1) + d_C \quad (= R_C x_{C'} + d_C)$$

$$R_C = R_2 R_1^{-1} \text{ and } d_C = d_2 - R_2 R_1^{-1} d_1$$

additional relationships

$$TR_B = R_1 TR_1^{-1}$$

$$TR_D = R_2 \cdot T \cdot R_2^{-1} = R_C R_1 \cdot T \cdot R_1^{-1} R_C^{-1} = R_C \cdot R_1 TR_1^{-1} \cdot R_C^{-1} = R_C \cdot TR_B \cdot R_C^{-1}$$

$$R_D = TR_C TR_B R_C^{-1}$$

$$d_B = (T - R_B) d_1$$

$$d_C = d_2 - R_C d_1$$

$$d_D = (T - R_D) d_2$$

properties of rotation axes

if the rotation axis corresponding to R_1 and/or R_2 is $\left\{ \begin{matrix} 0 & m & \sqrt{1-m^2} \end{matrix} \right\}$ with angle κ , then

$R_B = TR_1 TR_1^{-1}$ or $R_D = TR_2 TR_2^{-1}$ is about the axis with direction cosines $\left\{ \begin{matrix} p & q & 0 \end{matrix} \right\}$, with

$p/q = -\sqrt{1-m^2} \tan[\kappa/2]$, which is perpendicular to the original molecular twofold along z (but is not perpendicular to the R_1 or R_2 rotation axis; for molecular symmetry greater than 2, the equivalent to R_B is also not perpendicular to the original molecular symmetry axes, but rather it is perpendicular to the bisector of the original and rotated molecular symmetry axes. The rotation angle corresponding to R_B is given by $\cos\phi = 1 - 4m^2 + 3m^4 - 4m^2(m^2 - 1)\cos\kappa + m^4 \cos 2\kappa$.

If $m = 0$, $\cos\phi = 1$, and $RTR^{-1} = T$ so

$$T - TRTR^{-1} = T - I = \begin{bmatrix} -2 & 0 & 0 \\ 0 & -2 & 0 \\ 0 & 0 & 0 \end{bmatrix}$$
$$d_B = (T - TRTR^{-1})d_1 = \begin{bmatrix} -2x_0 \\ -2y_0 \\ 0 \end{bmatrix}$$

the net result is a relative translation of the two subunits perpendicular to the twofold.

if $m = 1$ (rotation axis along y (ie, perpendicular to molecular twofold), then $\phi = 2\kappa$.

if R_B and R_C are both along y , with rotation angles κ_1 and κ_2 , then R_D is also along y , with rotation angle $\kappa_1 - 2\kappa_2$.

If a y translational component is present in d_B and d_C of y_0 and y_1 , the translational component of R_D along $y = y_0 - 2y_1$ (this statement needs to be confirmed).

tests of relationships with methionine/maltose transporter

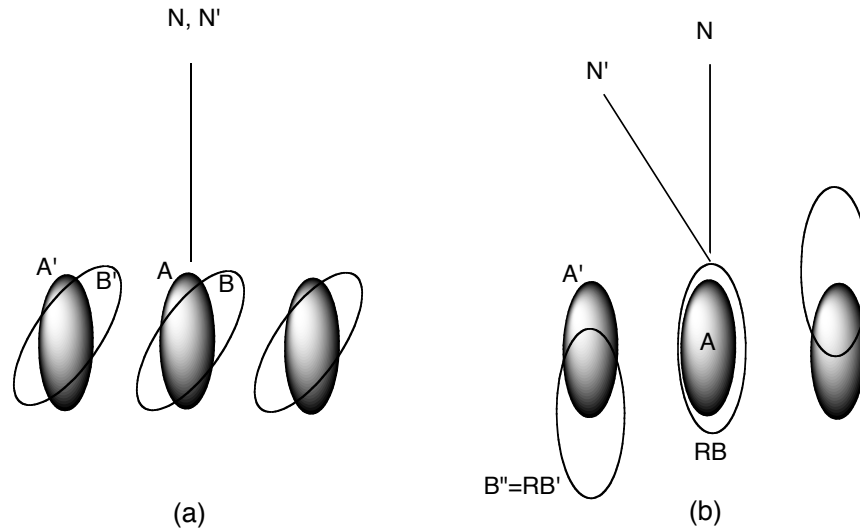
MetNI (Cy5) = AC/BD

Mal (2R6G) = FA/GB = ac/bd

R1,d1 superimposes A onto a

operator	ϕ	ψ	κ	dx	dy	dz
R ₁ A → F	340.26	29.60	340.33	-5.69	4.19	-4.33
R _B B → G	186.91	148.81	324.45	11.56	-9.49	-3.78
R _C C → B	134.21	149.43	331.27	-3.50	-0.19	6.26
R _D D → A	229.39	8.55	340.99	21.51	-3.84	4.13
R ₂ C → B	104.65	132.50	349.48	-11.01	3.23	5.23
TmalFG	269.33	89.32	180	-0.30	0.30	-0.01
TmetAB	90	90	180	0	0	0

Generalization to N-mer Oligomeric Symmetry



One conformation of the oligomer has subunit coordinates A, A', \dots , with the N -fold rotation axis N , while another has coordinates B, B', \dots , with rotation axis N' . The rotation matrix R rotates B to A (and B' to B'').

$$\begin{aligned}
 B'' &= RB' = N'RB \\
 B' &= \underbrace{R^{-1}N'R}_N B = NB \quad (= R^{-1}B''; B = N^T B') \\
 &\Rightarrow N = R^{-1}N'R \text{ and } N' = RNR^{-1} \\
 A' &= NA = NRB \\
 &= NRN^T B' \\
 &= NRN^T R^{-1} B'' = N \cdot RN^T R^{-1} \cdot B'' \\
 &= N(N')^T B''
 \end{aligned}$$

(for a two-fold, $A' = TRTB' = TRTR^{-1}B''$, as derived previously)

points on the B'' to A' rotation axis are consequently on an eigenvector of $N(N')^T$.

Only for twofold molecular symmetry is the B'' to A' rotation axis perpendicular to the molecular symmetry axis. In general, it is perpendicular to a bisector of N and N' , as derived in the following.

As above, let the rotation axis be in the yz plane $\left\{ \begin{matrix} 0 & m & \sqrt{1-m^2} \end{matrix} \right\}$ with angle κ . The z axis (the direction of N) then rotates to

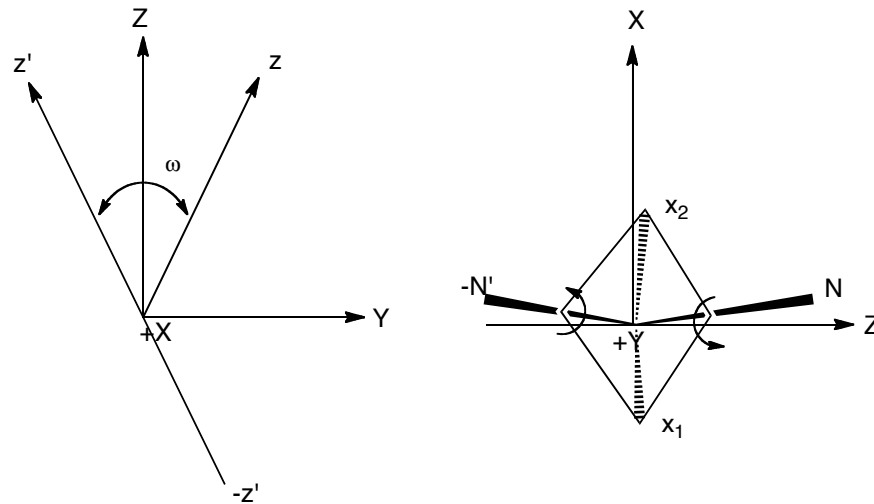
$$\hat{z}' = \left\{ \begin{matrix} m \sin \kappa, & m \sqrt{1-m^2} (1 - \cos \kappa), & 1 - m^2 + m^2 \cos \kappa \end{matrix} \right\}$$

and the angle between the old and new z axes is given by

$$\hat{z} \cdot \hat{z}' = 1 - m^2 + m^2 \cos \kappa \equiv \cos \omega$$

A general solution for the eigenvector of $N(N')^T$ corresponding to this B'' to A' rotation axis has been too complicated for me to find by explicitly calculating the eigenvectors in Mathematica[®]. A solution can be derived by noting that if x_1 is an eigenvector of $N(N')^T$, then if $(N')^T$ takes x_1 to x_2 , N must take x_2 back to x_1 .

For this calculation, transform to new coordinate system with Z axis bisecting z and z', and z x z' = X; hence N and N' are in the new ZY frame



For the N' transpose, either need a (+) rotation around $-N'$, or a (-) rotation around $+N'$ direction. x_1, x_2 go from one N-mer rotation axis (N or N') to points in the XY plane and are perpendicular to both N and N' .

$$(-N')x_1 = (+N')^T x_1 = x_2$$

$$Nx_2 = x_1$$

$$\therefore N(N')^T x_1 = x_1$$

To solve for x_1, x_2 in the XY plane - first find coordinates of point on unit circle in XY plane that is closest to N (or equivalently, N') axis.

$$\text{XY circle } x_2 = \begin{pmatrix} x & \sqrt{1-x^2} & 0 \end{pmatrix}, \quad x_1 = \begin{pmatrix} -x & \sqrt{1-x^2} & 0 \end{pmatrix}$$

$$\text{N-fold axis } \begin{pmatrix} 0 & \alpha \sin \frac{\omega}{2} & \alpha \cos \frac{\omega}{2} \end{pmatrix}$$

where α is a parameter that defines all the points on that line

The point on N-fold axis closest to a point on the unit XY circle minimizes the following quantity with respect to α

$$x^2 + \left(\sqrt{1-x^2} - \alpha \sin \frac{\omega}{2} \right)^2 + \left(\alpha \cos \frac{\omega}{2} \right)^2$$

giving for α and for the point \hat{n} on the N-fold axis

$$\alpha = \sqrt{1-x^2} \sin \frac{\omega}{2}$$

$$\hat{n} = \left(0 \quad \sqrt{1-x^2} \sin^2 \frac{\omega}{2} \quad \sqrt{1-x^2} \sin \frac{\omega}{2} \cos \frac{\omega}{2} \right) = \left(0 \quad \sqrt{1-x^2} \sin^2 \frac{\omega}{2} \quad \frac{\sqrt{1-x^2}}{2} \sin \omega \right)$$

Now, the vectors $x_1 - \hat{n}$ and $x_2 - \hat{n}$ are related by a $360/N$ degree rotation about N, giving:

$$\frac{(x_1 - \hat{n}) \cdot (x_2 - \hat{n})}{\|x_1 - \hat{n}\| \|x_2 - \hat{n}\|} = \frac{1 - 3x^2 + (1-x^2)\cos\omega}{1 + x^2 + (1-x^2)\cos\omega} = \cos \frac{2\pi}{N}$$

Which can be solved for x to give

$$x = \pm \sqrt{\frac{1 + \cos\omega - \cos \frac{2\pi}{N} - \cos\omega \cos \frac{2\pi}{N}}{3 + \cos\omega + \cos \frac{2\pi}{N} - \cos\omega \cos \frac{2\pi}{N}}} = \sqrt{\frac{(\cos\omega - 1) \left(\cos \frac{2\pi}{N} - 1 \right)}{3 + \cos \frac{2\pi}{N} + 2 \cos\omega \sin^2 \frac{\pi}{N}}}$$

as $\omega \rightarrow 0$, $x \sim \sin(\pi/N)$ and $y \sim \cos(\pi/N)$

this derivation was originally worked out in rotmat_frames_yahoo!.nb

summary

the B'' to A' rotation axis is an eigenvector of $N(N')^T$ and perpendicular to the bisector of the N and N' rotation axes.

For a twofold axis, it is also perpendicular to the T and T' rotation axes:

$$\begin{aligned} R_{axis} &= \left\{ \begin{array}{ccc} 0 & m & \sqrt{1-m^2} \end{array} \right\}, \text{ rotation angle } \kappa \\ z &= \left\{ \begin{array}{ccc} 0 & 0 & 1 \end{array} \right\} \\ \hat{z}' &= \left\{ \begin{array}{ccc} m \sin \kappa, & m \sqrt{1-m^2} (1 - \cos \kappa), & 1 - m^2 + m^2 \cos \kappa \end{array} \right\} \\ \rho &= \left\{ \begin{array}{ccc} -\sqrt{1-m^2} \tan[\kappa/2] & 1 & 0 \end{array} \right\} = \text{eigenvector of } TRTR^{-1} \\ \rho \cdot (z + \hat{z}') &= \rho \cdot z + \rho \cdot \hat{z}' = 0 + 0 = 0 \end{aligned}$$

For N-fold symmetry, the rotation axis relating B'' to A' is the eigenvector of $N(N')^T$ with unit eigenvalue.

Calculation of Screw (Helical) Parameters from a General Transformation

Reference: J.M. Cox, *J. Mol. Biol.* **28**, 151-156 (1967)

Let a general transformation be described by:

$$x' = Cx + d$$

where C and d are the rotation matrix and translation vector, respectively. The vector, r , describing the direction of the rotation (screw) axis is given by the eigenvector of C with unit eigenvalue, while the screw rotation, δ , about this axis may be calculated from the trace of C :

$$\delta = \cos^{-1} \left[\frac{\text{Tr}(C) - 1}{2} \right]$$

The translation component, s , along the screw axis given by:

$$s = r \cdot d$$

Example (from Mathematica[®] for heparin polymer model):

MatrixForm[C]

```
-0.57538    0.81146    -0.10232           rotation matrix elements
-0.81757    -0.57413     0.04427
-0.02282    0.10913     0.99377
```

d={14.72189,3.82232,8.85950} translation vector (Å)

{vals, vects} = Eigensystem[C]

```
{{-0.5779 + 0.8161 I, -0.5779 - 0.8161 I, 1.}, eigenvalues
```

```
{{-0.9896 - 0.1382 I, 0.1363 - 0.9895 I, -0.04605 + 0.04279 I},
{-0.9896 + 0.1382 I, 0.1363 + 0.9895 I, -0.04605 - 0.04279 I},
{-0.0397337, 0.0487046, 0.998023}} three sets of eigenvectors
```

r=vects[[3]]

```
{-0.0397337, 0.0487046, 0.998023} eigenvector with eigenvalue=1.
```

s = r.d

```
8.44319Å
```

δ = (180./3.14159)*ArcCos[((Sum[mat[[i,i]],{i,3}]-1.)/2.)]

```
125.301°
```

repeat = s*360/δ

```
24.258Å
```

Transformation Matrix to a New Coordinate System

The matrix that premultiplies a coordinate vector to transform the corresponding point to a new coordinate frame that lets one project down an axis with normalized components (xyz) in the original coordinate system, so that this axis becomes y in the new coordinate frame is given by:

$$\begin{bmatrix} \frac{y}{\sqrt{1-z^2}} & \frac{-x}{\sqrt{1-z^2}} & 0 \\ x & y & z \\ \frac{-xz}{\sqrt{1-z^2}} & \frac{-yz}{\sqrt{1-z^2}} & \frac{x^2+y^2}{\sqrt{1-z^2}} \end{bmatrix}$$

this system is created by taking (xyz) to be the new y; the new x is given by the cross product of (xyz) with the vector along the old z axis (001); and the new z axis is the cross product of the new x and y axes.

With (xyz) defined as the new "z" axis; the new x is given by the cross product of the old y axis (010) and (xyz); and the new y axis as the cross product of the new z and new x axes, the transformation matrix becomes:

$$\begin{bmatrix} \frac{z}{\sqrt{1-y^2}} & 0 & \frac{-x}{\sqrt{1-y^2}} \\ \frac{-xy}{\sqrt{1-y^2}} & \frac{x^2+z^2}{\sqrt{1-y^2}} & \frac{-yz}{\sqrt{1-y^2}} \\ x & y & z \end{bmatrix}$$

And with (xyz) defined as the new "x" axis, the new "y" axis as the cross product of the old z axis (001) and (xyz) ; and the new "z" axis as the cross product of the new x and y axes, the transformation matrix becomes:

$$\begin{bmatrix} x & y & z \\ \frac{-y}{\sqrt{1-z^2}} & \frac{x}{\sqrt{1-z^2}} & 0 \\ \frac{-xz}{\sqrt{1-z^2}} & \frac{-yz}{\sqrt{1-z^2}} & \frac{x^2+y^2}{\sqrt{1-z^2}} \end{bmatrix}$$

Transformation to a Skew Frame

If a rotation operation is specified by the spherical polar angles ϕ, ψ, κ , then the transformation to the skew frame with the rotation axis along y is given by the spherical polar angles $\phi-90^\circ, 90^\circ, \psi$. [If $\kappa=180^\circ$, then a second rotational transformation is given by the spherical polar angles $\phi, 180+\psi/2, 180^\circ = \phi, \psi/2, 180^\circ$, which corresponds to a rotation of 180° about an axis half way between the rotation axis and the original y axis.]

In terms of the transformation matrices defined in the preceding section, for a rotation axis with spherical polar angles ϕ, ψ (and equivalent direction cosines (l, m, n)), the transformation matrix corresponding to the spherical polar angles $\phi-90^\circ, 90^\circ, \psi$ (and equivalent direction cosines

$\left(-n/\sqrt{1-m^2} \quad 0 \quad l/\sqrt{1-m^2} \right)$) is (see relevant section of the Math Overview):

$$\begin{bmatrix} \frac{n^2 + l^2 m}{1 - m^2} & -l & \frac{-nl}{1 + m} \\ l & m & n \\ \frac{-nl}{1 + m} & -n & \frac{l^2 + n^2 m}{1 - m^2} \end{bmatrix}$$

Since the second row has elements l, m, n , the original rotation axis has become the new y axis, but the new x and z axes are different than the various conventions described in the preceding section. The trace of this rotation matrix $= 1 + 2m = 1 + 2\cos\kappa$, so that $\kappa = \psi$, as indicated.

For the case of $\kappa = 180^\circ$, the second transformation can be obtained by premultiplying the above transformation by a two-fold rotation about y :

$$\begin{bmatrix} -\frac{n^2 + l^2 m}{1 - m^2} & l & \frac{nl}{1 + m} \\ l & m & n \\ \frac{nl}{1 + m} & n & -\frac{l^2 + n^2 m}{1 - m^2} \end{bmatrix} = \begin{bmatrix} -1 & 0 & 0 \\ 0 & 1 & 0 \\ 0 & 0 & -1 \end{bmatrix} \begin{bmatrix} \frac{n^2 + l^2 m}{1 - m^2} & -l & \frac{-nl}{1 + m} \\ l & m & n \\ \frac{-nl}{1 + m} & -n & \frac{l^2 + n^2 m}{1 - m^2} \end{bmatrix}$$

This is a symmetric matrix (it equals its transpose) so it corresponds to a rotation of 180° (as can be seen from the trace $= -1 = \cos\kappa$. From the general definition of the rotation matrix in terms of the direction cosines (λ, μ, ν) and κ (Math Overview), then the diagonal elements of the rotation matrix equal $2\lambda^2 - 1, 2\mu^2 - 1, 2\nu^2 - 1$. Equating these terms gives

$$2\mu^2 - 1 = m = \cos\psi$$

$$\mu = \cos\psi' = \sqrt{(m+1)/2} = \cos(\psi/2)$$

$$\tan\phi' = \frac{-\nu}{\lambda} = -\sqrt{\left(1 - \frac{n^2 + l^2 m}{1 - m^2}\right) / \left(1 - \frac{l^2 + n^2 m}{1 - m^2}\right)} = \frac{-n}{l} = \tan\phi$$

giving $\phi' = \phi; \psi' = \psi/2$, as stated above.

If x_0 is a point on the rotation axis defined by rotation matrix C and translation vector d :

$$\begin{aligned}x_0 &= Cx_0 + d \\d &= (I-C)x_0\end{aligned}$$

If there is a screw component to the transformation, it needs to be taken into account in the transformations.

Strain Calculations

See Diamond *Acta Cryst.* **A32**, 1-10 (1976); Yeates, T. O. & Rees, D. C. *J. Appl. Cryst.* **21**, 925-928 (1988).

The rigid body transformation relating two sets of points, x_1 and x_2 , may be written:

$$\bar{x}_2 = R\bar{x}_1 + d \quad (1)$$

Where R is the rotation matrix (orthogonal) and d is the translation vector. Although R and d have a total of 12 elements, there are only 6 independent variables; the three rotation angles and the three components of the translation vector. A more general transformation can be written in the following form:

$$\bar{x}_2^T = \bar{x}_1^T A' \quad (2)$$

$$\begin{bmatrix} x_{2,1} & y_{2,1} & z_{2,1} \\ \dots & \dots & \dots \\ x_{2,N} & x_{2,N} & x_{2,N} \end{bmatrix} = \begin{bmatrix} x_{1,1} & y_{1,1} & z_{1,1} & 1 \\ \dots & \dots & \dots & \dots \\ x_{1,N} & x_{1,N} & x_{1,N} & 1 \end{bmatrix} A'$$

where A' is a 4x3 matrix with 12 elements. Although a bit odd, the particular form of this expression facilitates comparison to least squares problems discussed elsewhere in this document, where the solution of $b = Ax$ is found to be $x = (A^T A)^{-1} A^T b$. In the present case, the solution for A' becomes

$$A' = [x_1^T x_1]^{-1} x_1^T x_2$$

$$[x_1^T x_1]_{ij} = \sum_{k=1}^N x_{1,k,i} x_{1,k,j}$$

$$[x_1^T x_2]_{ij} = \sum_{k=1}^N x_{1,k,i} x_{2,k,j}$$

where $x_{n,1,i} = x_{n,i}$
 $x_{n,2,i} = y_{n,i}$
 $x_{n,3,i} = z_{n,i}$

The first three rows of A' approximately correspond to R^T , while the fourth row corresponds to the translation vector in the first expression.

Since A' has 12 independent elements, while R and d only have 6 elements, A' contains additional information about the superposition of two objects. In particular, A' contains information not only on the rigid-body orientational relationship between two objects, but also on how one object must be distorted (strained) to optimize the superposition. This could occur, for

example, if two objects are protein molecules collected at different temperatures, so that some contraction (or expansion) has occurred; if the two objects are protein molecules in different crystal forms where some of the cell constants are incorrect; or if there has been some change in conformation between the two objects that may be represented as application of strain.

The Diamond reference describes how to extract information on both the rigid body rotation and strain matrices from A' . In the terminology of that paper, the 3x3 matrix D is defined that contains the first three columns of $[A']^T$. The transpose is needed because of the differing forms of the two transformation expressions utilized above in equations (1) and (2). Following Diamond, D may be factorized as

$$D = RT \quad (3)$$

where "R is an orthogonal matrix expressing a pure rotation having three independent elements, and T is symmetric having six independent elements, thus providing for nine degrees of freedom in D." In terms of the first transformation expression, this convention "provides for application of strain direct to the unrotated reference set"; ie, D represents "the application of a pure strain followed by the application of a pure rotation".

Now,

$$D^T D = T^T R^T R T = T^T T \text{ since } R^T R = 1$$

however, $T^T = T$ since T is symmetric

$$\therefore T = [D^T D]^{1/2}$$

$$R = D [D^T D]^{-1/2}$$

"The conventional strain tensor, S, is then given by

$$S = T - I "$$

" $[D^T D]^{1/2}$ is a matrix having the same eigenvectors as $D^T D$ and with eigenvalues equal to the square roots of those of $D^T D$ ", ie if E and Λ are the eigenvectors and eigenvalues, respectively of $D^T D$, then

$$[D^T D]^{1/2} = E^T \Lambda^{1/2} E$$

The eigenvectors and eigenvalues of S describe both the direction and the magnitude of the application of homogeneous strain to the entire object set. Diamond proceeds to analyze how "variations of T from place to place are also of interest, and may be regarded as the causes of changes in orientation" in comparing different forms of an object such as a molecule.

Section IV: Phasing and Phase Distributions Hendrickson-Lattman ABCD Coefficients

Hendrickson and Lattman (*Acta Crystallogr.* **B26**, 136 (1970)) recognized that phase probability curves with two or fewer maxima could be encoded in terms of 4 coefficients, A, B, C and D, where, in un-normalized form:

$$P(\alpha) = \exp(A \cos\alpha + B \sin\alpha + C \cos 2\alpha + D \sin 2\alpha)$$

The ABCD coefficients can be determined explicitly from the parameters of the particular source of phase information, or by numerical fitting of the phase probability curve. From $P(\alpha)$, the best phase and figure of merit can be determined by numerical evaluation of the expressions:

$$m \cos \alpha_{best} = \frac{\int \cos \alpha P(\alpha) d\alpha}{\int P(\alpha) d\alpha}$$

$$m \sin \alpha_{best} = \frac{\int \sin \alpha P(\alpha) d\alpha}{\int P(\alpha) d\alpha}$$

$$\alpha_{best} = \tan^{-1} \left[\frac{m \sin \alpha_{best}}{m \cos \alpha_{best}} \right]$$

$$m = \left[(m \cos \alpha_{best})^2 + (m \sin \alpha_{best})^2 \right]$$

Sometimes, it is necessary to extract ABCD coefficients from m and α_{best} . The simplest way to do this is by analogy to the treatment of molecular replacement phase information in terms of only two coefficients, A and B:

$$A = X \cos \alpha_{known}$$

$$B = X \sin \alpha_{known}$$

where X is given by the Sim's (*AC* **12**, 813-15 (1959)) expression:

$$X = \frac{2F_{known} F_{obs}}{\langle F_{unknown}^2 \rangle}$$

following Bricogne *AC* **A32**, 832 (1976), esp pp 838-839:

$$\langle F_{unknown}^2 \rangle = \langle |I_{obs} - \vartheta I_{known}| \rangle$$

where ϑ is the "known" fraction of the total structure

the Sim's weight (figure of merit) is defined:

$$m = \frac{I_1(X)}{I_0(X)}$$

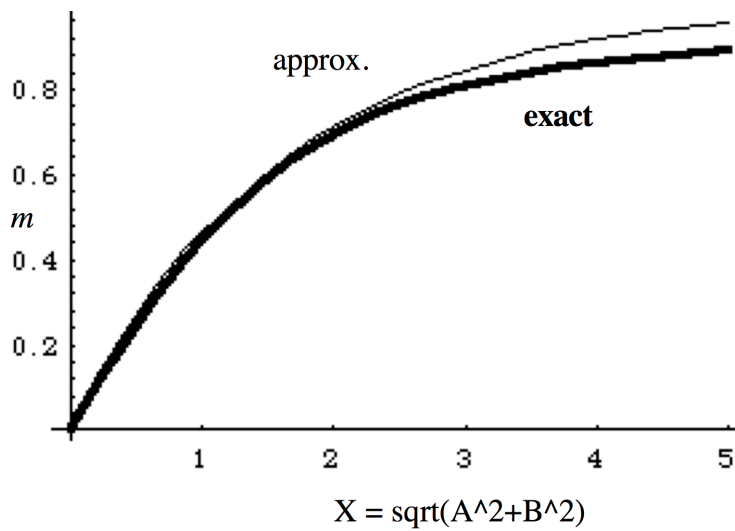
to a reasonable approximation

$$m \sim 1 - e^{-X/1.6}$$

or

$$X \sim -1.6 \ln(1 - m)$$

The relationships between these quantities are illustrated below, courtesy of Mathematica®.



Probability Distributions for Heavy Atom Isomorphous Differences

If $y = Yx$, then the probability distributions $P_2(y)$, $P_1(Y)$ and $P(x)$ are related by (equation references from Srinivasan and Parthasarathy (1976) *Some Statistical Applications in X-ray Crystallography*, Oxford:Pergamon):

$$P_2(y) = \int_y^{\text{upper limit } Y} P_1(Y)P(x = y/Y) \frac{dY}{Y} \quad (\text{B.55})$$

For the probability distribution of heavy atom isomorphous differences:

$$\Delta F = f_h \cos(\Delta\phi)$$

with $\Delta F = y$, $f_h = Y$, and $x = \cos(\Delta\phi)$, where $\Delta\phi \sim$ the phase difference between the protein and heavy atom. $P(x)$ is given by (eqn. B56):

$$P(x) = \frac{2}{\pi} \frac{1}{\sqrt{1-x^2}}$$

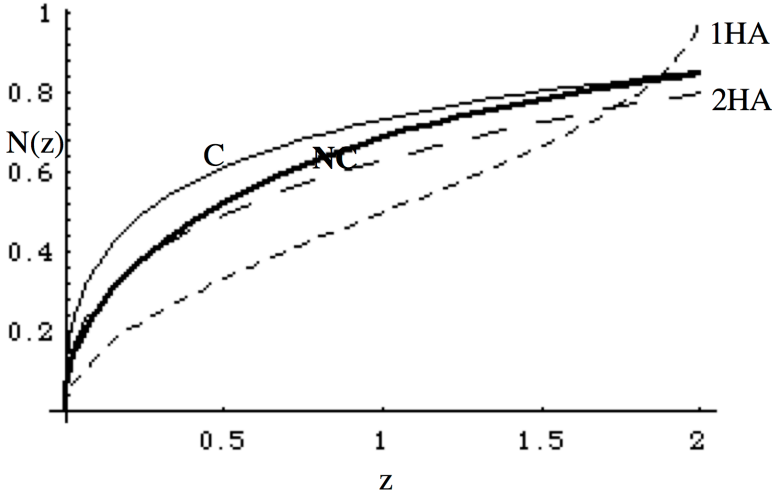
The probability distributions for the one heavy atom (1HA), two heavy atoms (2HA), many centric heavy atoms (C) and many noncentric heavy atoms (NC) per unit cell cases are given by:

case	$P_1(Y=f_h)$	eqn.	$P_2(y=\Delta F)$
1HA	$\delta(Y-1)$	3.1	$\frac{2}{\pi} \frac{1}{\sqrt{1-y^2}}$
2HA	$\frac{2}{\pi} \frac{1}{\sqrt{2-Y^2}}$	3.3	$\frac{4}{\pi^2} \frac{1}{\sqrt{2}} F\left(\frac{\pi}{2}, \sqrt{\frac{2-y^2}{2}}\right)$
C	$\sqrt{\frac{2}{\pi}} e^{-y^2/2}$	1.38	$\sqrt{\frac{2}{\pi^3}} e^{-y^2/4} K_0\left(\frac{y^2}{4}\right)$
NC	$2Ye^{-Y^2}$	1.39	$\frac{2}{\sqrt{\pi}} e^{-y^2}$

F is the complete elliptic integral of the first kind. The $P_1(Y)$ are normalized such that $\langle Y^2 \rangle = 1$, while the $P_2(y)$ are such that $\langle y^2 \rangle = 1/2$, since $\langle \cos^2 x \rangle = 1/2$. Tabulations of the cumulative $N(z)$ function, where N gives the fraction of reflections with $y^2 \leq z$ (with $\langle z \rangle = \langle y^2 \rangle = 1$) may be obtained from the expression:

$$N(z) = \int_0^{\sqrt{z/2}} P_2(y) dy$$

where the factor of 1/2 in the upper limit ensures that $\langle z \rangle = 1$:



Due to the presence of the $\cos \Delta\phi$ term, there are relatively more weak ΔF terms compared to the component structure factor amplitude distribution. Of particular interest, the NC ΔF distribution is described by exactly the same expression as for the C structure factor amplitude distribution.

Mathematica® expressions:

```
nnc[z_] := NIntegrate[(2/Sqrt[Pi]) Exp[-y^2], {y,0,Sqrt[z/2]}]
nc[z_] := NIntegrate[(Sqrt[2/Pi^3])* Exp[-(y^2)/4] BesselK[0,((y^2)/4)] , {y,0,Sqrt[z/2]}]
n2ha[z_] := NIntegrate[(2/Pi^2) (1/Sqrt[1-m]) EllipticK[m] , {m,(1-(z/4)),1}]
n1ha[z_] := NIntegrate [(2/Pi) (1-y^2)^(-(1/2)), {y,0,Sqrt[z/2]}]
```

```
Table[nnc[z],{z,0,2,.1}]
{0, 0.24817, 0.345279, 0.416118, 0.472911, 0.5205, 0.561422, 0.597216, 0.628907, 0.657218,
0.682689, 0.705734, 0.726678, 0.745787, 0.763276, 0.779329, 0.794097, 0.807712, 0.820288,
0.831922, 0.842701}
```

```
Table[nc[z],{z,0,2,.1}]
{0, 0.367807, 0.463248, 0.526186, 0.573595, 0.611637, 0.64333, 0.670402, 0.693946, 0.7147,
0.73319, 0.749803, 0.764835, 0.778516, 0.791029, 0.802525, 0.813124, 0.822929, 0.832026,
0.840489, 0.848379}
```

```
Table[n2ha[z],{z,0,2,.1}]
{0, 0.271455, 0.35285, 0.410037, 0.455443, 0.493637, 0.526878, 0.556472, 0.583247, 0.607768,
0.630437, 0.651554, 0.671348, 0.689999, 0.707649, 0.724417, 0.740398, 0.755674, 0.770313,
0.784374, 0.797906}
```

```
Table[n1ha[z],{z,0,2,.1}]
{0, 0.143566, 0.204833, 0.253183, 0.295167, 0.333333, 0.36901, 0.403013, 0.435906, 0.468116,
0.5, 0.531884, 0.564094, 0.596987, 0.63099, 0.666667, 0.704833, 0.746817, 0.795167, 0.856434}
```

```
Plot[{nnc[z],nc[z],n2ha[z],n1ha[z]}, {z,0,2},PlotStyle->{{Thickness[0.006]},
{Thickness[0.003]}, {Thickness[0.004],Dashing[{0.05,0.05]}}, {Thickness[0.004],
Dashing[{0.02,0.02]}}}]
```

Direct Methods Notes

Basic crystallographic relationships:

$$\begin{aligned}
 F_h &= |F_h| e^{i\phi_h} \\
 \rho(x) &= \frac{1}{V} \sum_h F_h e^{-2\pi i h x} \\
 &= \frac{1}{V} \sum_h |F_h| e^{i\phi_h} e^{-2\pi i h x} \\
 &= \frac{2}{V} \sum_{h>0} |F_h| \cos(2\pi h x - \phi_h) + \frac{F_{000}}{V}
 \end{aligned}$$

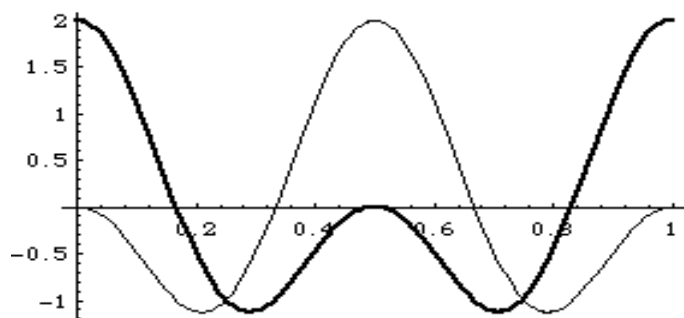
An infinite number of "structures" or electron density maps are consistent with a given set of diffraction amplitudes.

How is the correct phase set established?

1. Trial and Error - guess structure Bragg, etc. [Pauling "Stochastic method"]
2. Patterson methods (F^2 synthesis)
3. Heavy atom method - Hodgkin (cholesteryl iodide; vitamin B₁₂)
4. Isomorphous replacement-Hodgkin (K/Rb benzyl penicillin); Perutz (hemoglobin)
5. Anomalous dispersion - absolute configuration (Bijvoet)
6. Molecular replacement - Hodgkin (K, Na benzyl penicillin)
7. Noncrystallographic symmetry averaging (Rossmann & Blow)
8. Density modification (solvent flattening, histogram matching, skeletonization)
9. Direct methods

Direct methods utilize features of the electron density to derive relationships between the amplitudes and phases of the diffraction pattern:

Positivity of electron density: $\rho \geq 0$. For a centric structure, if both $|F_h|$ and $|F_{2h}|$ are strong, F_{2h} is likely to be positive, irrespective of the sign of F_h (Harker-Kasper inequalities: AC 1, 70 (1948)). (aside – this doesn't look so convincing to me, unless both reflections are really strong)



$$\begin{aligned}
 \cos(2\pi hx) + \cos(2\pi 2hx) &\quad \text{bold} \\
 -\cos(2\pi hx) + \cos(2\pi 2hx) &\quad \text{thin}
 \end{aligned}$$

positivity and atomicity: ρ map looks like ρ^2 map, which leads to Sayre's equation (AC 5, 60 (1952)):

$$\begin{aligned}
FT[\rho^2(x)] &= \int_0^1 \rho^2(x) e^{2\pi i h x} dx \\
&= \frac{1}{V^2} \int_0^1 \left[\sum_k F_k e^{-2\pi i k x} \right] \left[\sum_l F_l e^{-2\pi i l x} \right] e^{2\pi i h x} dx \\
&\propto \sum_k \sum_l F_k F_l \int_0^1 e^{2\pi i (h-k-l)x} dx \\
&= \sum_k \sum_l F_k F_l \delta(h-k-l) \\
&= \sum_k F_k F_{h-k} \\
&\propto F_h = \text{Fourier Transform of } \rho
\end{aligned}$$

This is an example of the convolution theorem (FT of the product of two functions is the convolution of the two Fourier transforms).

Another, related, example of atomicity and positivity is the maximization of ρ^3 integrated over the unit cell to help assign phases (Stanley *AC* **A35**, 966 (1979)). In this application, phases of reflections are chosen so that the integral of ρ^3 over the cell is maximized:

$$\begin{aligned}
\int \rho^3(x) dx &= \int \sum_h \sum_p \sum_q F(h) F(p) F(q) e^{-2\pi i (h+p+q)x} dx \\
&= \sum_{hpq} F(h) F(p) F(q) \delta(h+p+q) \\
&= \sum_h F(-h) \sum_p F(p) F(h-p)
\end{aligned}$$

To maximize this expression, the value of the second summation should be proportional to $F(h)$:

$$F(h) \approx \sum_p F(p) F(h-p)$$

since then the overall integral is given approximately by:

$$\int \rho^3(x) dx \approx \sum_h F(-h) F(h) = \sum_h I(h)$$

Unfortunately, as the size of the structure increases, the number of very strong reflections required to make these summations practically doable decreases to the point that these methods don't work. At this point, it is necessary to introduce other types of constraints.

Envelopes: A macromolecular crystal may be divided into two mutually exclusive, contiguous regions; the volume containing the molecule, and the solvent region of about equal volumes. The molecular envelope separates the two regions. To a first approximation, the solvent may be

modeled with uniform density. The existence of the solvent region places influences the diffraction pattern in ways which can potentially be used for phasing, as seen below.

First, the "sampling theory" is introduced. The molecular and crystal transforms of an object are given by:

$$F(S) = \int_{-1/2}^{1/2} \rho(x) e^{2\pi i S x} dx$$

$$F(h) = \int_{-1/2}^{1/2} \rho(x) e^{2\pi i h x} dx; h = \text{integer}$$

The crystal transform is given by the molecular transform sampled at reciprocal lattice points (convolution theorem).

By the inverse Fourier transform:

$$\rho(x) = \sum_h F(h) e^{-2\pi i h x} \quad (\text{neglecting the volume factor})$$

$$F(S) = \int_{-1/2}^{1/2} \sum_h F(h) e^{-2\pi i h x} e^{2\pi i S x} dx$$

$$= \sum_h F(h) \int_{-1/2}^{1/2} e^{2\pi i (S-h)x} dx$$

$$= \sum_h F(h) \frac{\sin \pi (S-h)}{\pi (S-h)}$$

This sampling theorem permits reconstruction of the continuous molecular transform from the discrete, sampled crystal transform.

Now, for integer n , $\frac{\sin \pi n}{\pi n} = \delta(n)$, so that when S equals an integer h , $F(S) = F(h)$, and the value of this amplitude is independent of all other $F(h)$'s.

Applications to Noncrystallographic Symmetry and Solvent Flattening:

$$\begin{aligned}
 F(S) &= \int_{-1/2}^{1/2} \rho(x) e^{2\pi i S x} dx \\
 \text{if } \rho(x) &= 0 \text{ when } \frac{a}{2} < |x| < \frac{1}{2} \\
 &= \int_{-a/2}^{a/2} \rho(x) e^{2\pi i S x} dx \\
 F(S) &= \sum_h F(h) \int_{-a/2}^{a/2} \rho(x) e^{2\pi i (S-h)x} dx \\
 &= \sum_h F(h) \frac{\sin \pi (S-h)a}{\pi (S-h)} \\
 \text{for integer } S &\equiv p \\
 F(p) &= \sum_h F(h) \frac{\sin \pi (p-h)a}{\pi (p-h)}
 \end{aligned}$$

In this case, other $F(h)$'s contribute to $F(p)$ in addition to the term $p=h$. For example, when $a=1/2$, then for $|p-h| = 0, 1, 2, 3$, etc., the $\sin x/x$ term has the value 0.5, 0.319, 0, -0.106, etc., compared to the values 1, 0, 0, 0, ... when $a = 1$. This interdependence of the structure factors permits the estimation and refinement of phase information, which is beautifully detailed in papers based on Crowther's thesis work (*Acta Crystallogr.* **22**, 758-764 (1967); *Acta Crystallogr.* **B25**, 2571-2580 (1969)), and by P. Main and M.G. Rossmann (*Acta Cryst.* **21**, 67-72 (1966)). Another example of the use of envelopes to derive *ab initio* phase information from an eigenvector formulation is given in Rees, *AC* **46**, 915 (1990).

Topography of the diffraction pattern: The sampling theory connects the crystal transform (sampled and reciprocal lattice points) and the molecular transform (continuous). Knowledge of the molecular transform should help phase determination; for example, in a centric space group the nodes of the transform would separate regions with either + or - phases. Even less information, such as the amplitude at half integral lattice points apparently can also provide the same information (Sayre *AC* **5**, 843 (1952)). Perhaps some relationships in the topography (peaks, pits, nodes and saddle points) are present? Or relationships between phases of neighboring reflections (a complication in this analysis is posed by the origin ambiguity).

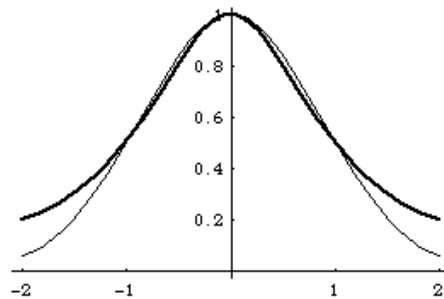
Maximum Entropy. I don't understand these; I guess maximum entropy methods should find the smoothest map consistent with the diffraction amplitudes. References G. Bricogne *AC* **A46**, 284, 97 (1990); AK Livesey, J. Skilling *AC* **A41**, 113 (1985).

Other constraints: Any properties of the electron density, such as the histogram distribution (Zhang & Main, *AC A46*, 41, 507 (1990)) or skeletonization (Baker et al, *AC D49*, 429 (1993)), should impose phases constraints (if they can be applied). An example follows:

Suppose the electron density may be modeled by a Lorentzian curve, with the one-dimensional form:

$$\rho(x) = \frac{1}{1+x^2}$$

This form approximates a Gaussian-type curve often used for electron density:

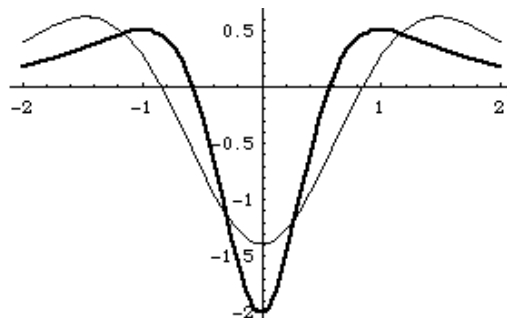


where the Lorentzian curve is dark, and the Gaussian curve (adjusted to equal 0.5 at $x=\pm 1$) is light.

The curvature of the electron density is given by:

$$\begin{aligned} \frac{\partial^2 \rho}{\partial x^2} &= \frac{8x^2}{(1+x^2)^3} - \frac{2}{(1+x^2)^2} \\ &= 6\rho^2 - 8\rho^3 \end{aligned}$$

The curvature of the Lorentzian and Gaussian curves are illustrated below:



The relationship between the curvature, ρ^2 and ρ^3 is true for Lorentzians in 1 to 3 dimensions:

$$\frac{\partial^2 \rho}{\partial x^2} = \alpha \rho^2 - \beta \rho^3$$

n	α	β
1	6a	8a
2	4a	8a
3	2a	8a

$$\text{for } \rho(r) = \frac{1}{1 + ar^2}.$$

The utility of this relationship can be seen from taking the Fourier transform of the density curvature:

$$\begin{aligned} FT\left(\frac{\partial^2 \rho}{\partial x^2}\right) &= \int_0^1 \frac{\partial^2 \rho}{\partial x^2} e^{2\pi i h x} dx \\ &= \frac{1}{V} \int_0^1 \frac{\partial^2}{\partial x^2} \left[\sum_k F_k e^{-2\pi i k x} \right] e^{2\pi i h x} dx \\ &= \frac{1}{V} \int_0^1 \left[-4\pi^2 \sum_k k^2 F_k e^{-2\pi i k x} \right] e^{2\pi i h x} dx \\ &= \frac{-4\pi^2}{V} \sum_k k^2 F_k \int_0^1 e^{-2\pi i k x} e^{2\pi i h x} dx \\ &= -4\pi^2 h^2 F_h \end{aligned}$$

so that the Fourier transform of the curvature is directly related to F_h . It is also related to the Fourier transforms of ρ^2 and ρ^3 , which connects with Sayre's equation, and the use of triplets and quartets in direct methods:

$$\begin{aligned}
FT(\rho) &= F_h = \pi e^{-2\pi h} \\
FT\left(\frac{\partial^2 \rho}{\partial x^2}\right) &= -4\pi^2 h^2 F_h = -4\pi^3 h^2 e^{-2\pi h} \\
FT(\rho^2) &\propto \sum_k F_k F_{h-k} = \frac{\pi}{2} [1 + 2\pi h] e^{-2\pi h} \\
FT(\rho^3) &\propto \sum_{k,l} F_k F_l F_{h-k-l} = \frac{\pi}{8} [3 + 6\pi h + 4\pi^2 h^2] e^{-2\pi h} \\
F_h &= -\frac{1}{4\pi^2 h^2} \left[\alpha \sum_k F_k F_{h-k} - \beta \sum_{k,l} F_k F_l F_{h-k-l} \right]
\end{aligned}$$

The right hand side of the top equations give the expression for the Fourier transform of a simple one-dimensional Lorentzian.

The final expression should hold for a structure composed of isolated Lorentzian scatterers. What about proteins?

Section V: Minimization, Maximization and Refinement Lagrange Multipliers and Constrained Extrema

If A is an $n \times n$ symmetric matrix, and x is an n element vector, then $x^T A x$ is a symmetric quadratic expression. It is often desired to find the x vectors that correspond to extrema (such as the maximum) of this quadratic; to obtain meaningful solutions, it is necessary to impose constraints on the magnitudes of the elements of x , such as the normalization relationship $x^T x = 1$ (otherwise, the value of the quadratic expression can be adjusted simply by multiplying the elements of x by a scale factor). The constraining relationship may be incorporated into the maximization equation by the use of Lagrange multipliers, so that the resulting function to be maximized is:

$$x^T A x - \lambda(x^T x - 1)$$

At the extrema, the derivative of this equation with respect to x vanishes. Since A is symmetric, the x values defining these points satisfy the eigenvalue equation:

$$A x = \lambda x$$

Optimization problems of this type can often arise in crystallography, since diffraction intensities and Patterson functions are symmetric quadratic functions of the electron density values.

Constraining equations of the type $x^T B x = 1$ may be solved analogously to the generalized eigenvalue problem (G. Strang, *Linear Algebra and Its Applications*, Academic Press (1976) pp. 248-251). If B is positive definite, then $B = W^T W$. Consequently:

$$A x = \lambda B x$$

$$= \lambda W^T W x$$

Let $y = W x$, then

$$A W^{-1} y = \lambda W^T y$$

With $C = W^{-1}$, and $(W^T)^{-1} = C^T$

$$C^T A C y = \lambda y$$

The eigenvalues λ of $C^T A C$ are the same as for the original problem $A x = \lambda B x$, and the eigenvectors are related by $y_j = W x_j$. If the columns of a matrix S are given by the x_j , then the matrices A and B are simultaneously diagonalized by the congruence transformation S , ie. $S^T B S = I$ and $S^T A S = \Lambda$.

Least Squares in Crystallography

Linear Least Squares

n observations f_i , which depend on

m unknowns x_j .

$$f_1 = a_{11}x_1 + a_{12}x_2 + \dots + a_{1m}x_m$$

.

.

$$f_n = a_{n1}x_1 + a_{n2}x_2 + \dots + a_{nm}x_m$$

the a_{ij} are known coefficients

In matrix notation, these equations can be written

$$F = AX$$

$$F = \begin{pmatrix} f_1 \\ \dots \\ f_n \end{pmatrix} \quad A = \begin{pmatrix} a_{11} & \dots & a_{1m} \\ \dots & & \dots \\ a_{n1} & & a_{nm} \end{pmatrix} \quad X = \begin{pmatrix} x_1 \\ \dots \\ x_m \end{pmatrix}$$

Let V = error vector $\equiv (F)_{\text{obs}} - (F)_{\text{calc}}$

$$V = F - AX$$

The best least squares solution for X minimizes $V^T V$

$$\Phi = V^T V = (F - AX)^T (F - AX)$$

when Φ is a minimum, $\frac{\partial \Phi}{\partial X} = 0$

$$\frac{\partial \Phi}{\partial X} = \frac{\partial}{\partial X} [X^T A^T AX - X^T A^T F - F^T AX - F^T F]$$

$$= A^T AX - A^T F = 0$$

$$\Rightarrow X = (A^T A)^{-1} A^T F \quad \text{linear least squares solution}$$

Example: least squares scaling of two data sets

Given two sets of structure factor amplitudes F_i and G_i .

What is the best scale factor α that multiplies G_i ?

Guess $\alpha = \frac{\sum F_i}{\sum G_i}$? The least squares solution is given by:

$$\Phi = \sum_i (F_i - \alpha G_i)^2$$

$$\frac{\partial \Phi}{\partial \alpha} = -2 \sum_i (F_i - \alpha G_i) G_i = 0$$

$$\alpha = \frac{\sum_i F_i G_i}{\sum_i G_i^2}$$

Linear problems are nice, but most situations are non-linear. To treat these problems, the problem is linearized by expanding the function f in a Taylor series, and truncating to first order.

$$f_i^{obs}(x_1^0, x_2^0, \dots) = f_i^{calc}(x_1, x_2, \dots) + \frac{\partial f_i}{\partial x_1}(x_1^0 - x_1) + \frac{\partial f_i}{\partial x_2}(x_2^0 - x_2) + \dots$$

$x_1^0, \dots = x$ values at the minimum of f

$x_1, \dots =$ current x values

$$f_i^{obs} - f_i^{calc} = \sum_j \frac{\partial f_i}{\partial x_j}(x_j^0 - x_j)$$

$$\Delta f_i = \sum_j \frac{\partial f_i}{\partial x_j} \Delta x_j \Rightarrow \text{this expression is linear in the shifts to } x$$

$$F = AX \quad \text{matrix notation - equivalent to linear LSQ}$$

The application to crystallographic refinement problems is as follows:

F = vector with $|F_o(h)| - |F_c(h)|$

A = matrix of derivatives $\frac{\partial |F_c(h)|}{\partial x_i}$

X = vector with shifts = $(A^T A)^{-1} A^T F$

where

$$(A^T A)_{ij} = \sum_h \frac{\partial |F_c(h)|}{\partial x_i} \frac{\partial |F_c(h)|}{\partial x_j}$$

$$(A^T F)_i = \sum_h \frac{\partial |F_c(h)|}{\partial x_i} (|F_o(h)| - |F_c(h)|)$$

The calculations of the necessary derivatives are performed as follows:

need $\frac{\partial |F_c(h)|}{\partial x_i}$

$$\begin{aligned} F_c(h) &= |F_c(h)| e^{i\alpha_h} \\ &= |F_c(h)| \cos \alpha_h + i |F_c(h)| \sin \alpha_h \\ &= A + iB \end{aligned}$$

$$\text{Intensity } I = |F_c(h)|^2$$

$$dI = 2|F_c(h)| d|F_c(h)|$$

$$\frac{dI}{2|F_c(h)|} = d|F_c(h)|$$

$$\text{now: } I = A^2 + B^2$$

$$dI = 2AdA + 2BdB$$

$$\begin{aligned} d|F_c(h)| &= \frac{dI}{2|F_c(h)|} = \frac{A}{|F_c(h)|} dA + \frac{B}{|F_c(h)|} dB \\ &= \cos \alpha_h \frac{dA}{dx_i} + \sin \alpha_h \frac{dB}{dx_i} \end{aligned}$$

Space group specific expressions for A and B are found in volume I of the International Tables. Generally, the parameters x_i to be refined include coordinates, temperature factors, scale factor, and occasionally, occupancy.

Variance - Covariance in Least Squares Refinements

(W.C. Hamilton Statistics in Physical Science (1964), chapter 4)

Consider the system of linear equations

$$F = Ax$$

where F is the vector of n observations, A is the $n \times m$ matrix of known coefficients and x is the vector of m unknown parameters to be determined. Ignoring weights (this is equivalent to assuming constant weights for each observational equation), the least squares solution is given by:

$$x = (A^T A)^{-1} A^T F$$

An unbiased estimate of the variance-covariance matrix M is:

$$M = \frac{V^T V}{n - m} (A^T A)^{-1} \quad (\text{with } V = F - Ax = \text{vector of residuals})$$

$$M = \begin{pmatrix} \sigma_1^2 & \sigma_1 \sigma_2 \rho_{12} & \dots \\ \sigma_1 \sigma_2 \rho_{12} & \sigma_2^2 & \dots \\ \dots & \dots & \dots \end{pmatrix}$$

$V^T V$ is the sum of the squared differences between observed and calculated values of F (which is the quantity minimized in the least squares refinement); the i^{th} diagonal element of M is the variance in the estimated value for the i^{th} parameter; and the off-diagonal element ij will be proportional to the covariance ρ_{ij} between the i^{th} and j^{th} parameters:

$$\rho_{ij} = \frac{(A^T A)^{-1}_{ij}}{\sqrt{(A^T A)^{-1}_{ii} \times (A^T A)^{-1}_{jj}}}$$

If the observations are all uncorrelated (this should be a good approximation for diffraction data), then the weight matrix is diagonal with elements equal to the inverse of the variance for each observation, and the variance-covariance matrix becomes:

$$P = \begin{pmatrix} \frac{1}{\sigma_{h1}^2} & 0 & 0 \\ 0 & \frac{1}{\sigma_{h2}^2} & 0 \\ 0 & 0 & \dots \end{pmatrix}$$

$$M = \frac{V^T P V}{n - m} (A^T P A)^{-1}$$

Incorporation of Constraints in Least Squares Refinements

See K.N. Raymond lectures notes from the Least Squares Tutorial held at the Spring, 1974 ACA meeting, and W.C. Hamilton's *Statistics in Physical Science*, Ronald Press (1964) for additional details.

The least squares solution to a set of linear (or linearized) equations $Ax = b$ is given by:

$$x = (A^T A)^{-1} A^T b$$

where x represents either the solution vector (linear least squares) or the shift vector (non-linear least squares). For a crystallographic refinement, the elements of the normal matrix are given by:

$$A^T A_{ij} = \sum_h \frac{\partial F(h)}{\partial x_i} \frac{\partial F(h)}{\partial x_j}$$

Assume that the n elements of x are related by a set of m constraints:

$$f_1(x) = c_1; \quad f_2(x) = c_2; \quad \dots; \quad f_m(x) = c_m$$

$$df_i = \sum_{j=1}^n \left(\frac{\partial f_i(x)}{\partial x_j} \right) dx_j = 0$$

or, in matrix notation

$$C dx = 0$$

The $m \times n$ matrix C summarizes all constraints imposed on the problem.

As a result of the constraints, there are $k = n - m$ linearly independent variables which may be designated as the k element vector v . These are related to the n elements of x by the $k \times n$ matrix B :

$$Bx = v$$

$$B dx = dv$$

B can be defined such that v represents the first k elements of x , but any other linearly independent set of new variables is also acceptable.

The two sets of matrix equations can be combined to give:

$$\begin{pmatrix} B \\ C \end{pmatrix} dx = \begin{pmatrix} dv \\ 0 \end{pmatrix} \equiv Q dx$$

where $Q_{ij}=B_{ij}$, $i \leq k$ and $Q_{ij}=C_{ij}$, $i > k$. The $n \times n$ Q matrix will be nonsingular if both the constraints and new variables are linearly independent. The reverse transformation then may be obtained:

$$dx = Q^{-1} \begin{pmatrix} dv \\ 0 \end{pmatrix}$$

$$dx = Jdv$$

where J is the $n \times k$ matrix that gives the linear relationship between dx and dv , and is composed of the first k columns of Q^{-1} ; $J_{ij}=Q^{-1}_{ij}$, $j \leq k$.

The relationship between the derivatives dF/dv and dF/dx may be obtained via the J matrix:

$$\left(\frac{\partial F}{\partial v} \right) = J^T \left(\frac{\partial F}{\partial x} \right)$$

which can then be used to generate the derivatives needed to construct the normal matrix for the constrained least squares calculation.

For non-linear constraints, the same procedure is followed with the C_{ij} elements being given by the appropriate derivative of the constraint equations.

Linear constraints of the form $Cx=0$ can also be incorporated into the Lagrange multiplier formalism described in the preceding section to find extrema of the symmetric quadratic $x^T A x$. With the B matrix described above, a reduced set of variables, v may be derived from x :

$$\begin{pmatrix} B \\ C \end{pmatrix} x = \begin{pmatrix} v \\ 0 \end{pmatrix}$$

$$x = Jv$$

where J is equivalent to the $n \times k$ matrix described above that is composed of the first k columns of Q^{-1} . Incorporating this relationship into the optimization calculation gives:

$$x^T A x - \lambda x^T x$$

$$v^T J^T A J v - \lambda v^T J^T J v$$

$$v^T A' v - \lambda v^T B' v$$

which can be optimized by the eigenvalue methods described earlier. The solution vector x is then calculated from Jv .

Modeling the Correlation between Z and B in an X-ray Crystal Structure Refinement

TM Buscagan and DC Rees bioRxiv 2023.07.04.547724

To model the relationship between Z and B , we represent a scatterer by a single Gaussian with atomic number Z and overall temperature factor B (Ten Eyck, *Acta cryst.* **A33**, 486 (1977)). The electron density $\rho(r)$ is then described:

$$\text{Eq. 1} \quad \rho(r) = Z \left(\frac{4\pi}{B} \right)^{3/2} e^{-4\pi^2 r^2/B}$$

with

$$\text{Eq. 2} \quad \rho(0) = Z \left(\frac{4\pi}{B} \right)^{3/2}$$

It is important to recognize that the B in Eq. 1 and Eq. 2 includes contributions from both the atomic scattering factor B_0 and the isothermal temperature factor B_{iso} , with $B = B_0 + B_{\text{iso}}$. From Eq. 2 and calculated with the Cromers and Mann atomic scattering factors *Acta cryst.* **A34**, 321 (1968) and $B_{\text{iso}} = 16 \text{ \AA}^2$, B_0 is found to be approximately 8 \AA^2 and 6 \AA^2 for N and S, respectively. If the true Z/B for a given atom are Z_1 and B_1 , but the refinement is conducted with Z_2 , the corresponding B_2 will be shifted from the true value to compensate for the incorrect occupancy. We developed two simple models to capture the possible relationship between Z_2 and B_2 :

Model 1: B_2 is calculated for a given Z_2 such that the density at the atomic position, $\rho(0)$, has the same value as for Z_1, B_1 . For a single Gaussian, this is equivalent to equating $\rho(0)$ in Eq. 2 calculated for either Z_1, B_1 or Z_2, B_2 , which gives

$$\text{Eq. 3} \quad \frac{Z_1}{B_1^{3/2}} = \frac{Z_2}{B_2^{3/2}} \Rightarrow B_2 = B_1 \left(\frac{Z_2}{Z_1} \right)^{2/3}$$

$$\text{Eq. 4} \quad B_{2,\text{iso}} = (B_{1,\text{iso}} + B_0) \left(\frac{Z_2}{Z_1} \right)^{2/3} - B_0$$

The ratio Z_2/Z_1 corresponds to the occupancy of the Z_1 scatterer at the site (to within the approximation that the shape of the atomic scattering factor is independent of Z).

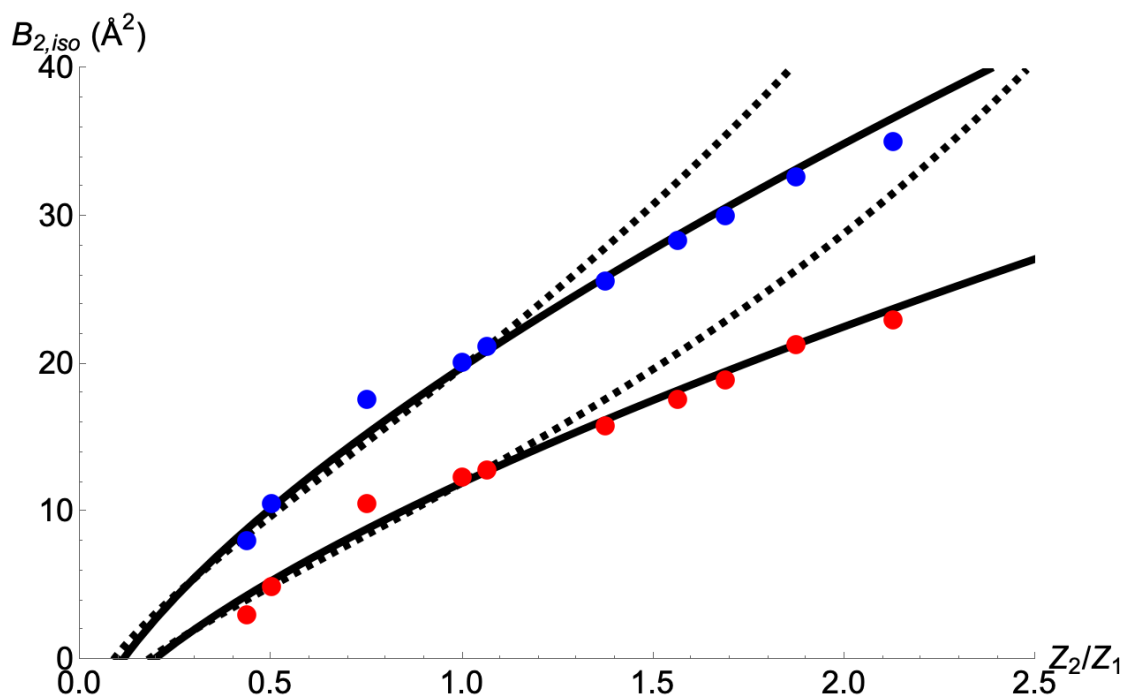
Model 2: In this case, B_2 is calculated for a given Z_2 to minimize the square of the difference density over the atomic volume:

$$\begin{aligned} \text{Eq. 5} \quad \Delta\rho^2 &= \int_0^\infty (\rho_1(r) - \rho_2(r))^2 4\pi r^2 dr \\ &= \int_0^\infty \left(\left[Z_1 \left(\frac{4\pi}{B_1} \right)^{3/2} e^{-4\pi^2 r^2/B_1} \right] - \left[Z_2 \left(\frac{4\pi}{B_2} \right)^{3/2} e^{-4\pi^2 r^2/B_2} \right] \right)^2 4\pi r^2 dr \end{aligned}$$

From the condition that $\frac{\partial \Delta\rho^2}{\partial B_2} = 0$ at the minimum, one can derive (see notes at the end of this section)

$$\text{Eq. 6} \quad B_2 = B_1 \frac{\left(\frac{Z_2}{Z_1}\right)^{2/5}}{2 - \left(\frac{Z_2}{Z_1}\right)^{2/5}} \Rightarrow B_{2,iso} = (B_{1,iso} + B_0) \frac{\left(\frac{Z_2}{Z_1}\right)^{2/5}}{2 - \left(\frac{Z_2}{Z_1}\right)^{2/5}} - B_0$$

The variations in $B_{2,iso}$ as a function of Z_2/Z_1 were evaluated from Eq. 4 and Eq. 6 (Figure 1). For these calculations, $Z_1 = 16 e^-$ and $B_0 = 6 \text{ \AA}^2$, with $B_{1,iso} = 12.0 \text{ \AA}^2$ and 19.8 \AA^2 for the 7TPW and 7TPY structures, respectively. (These $B_{1,iso}$ values correspond to the average B -factor for the two Fe sites in each structure; Appendix A.) As illustrated in Figure 1, while both Eq. 4 and Eq. 6 fit the refined B values reasonably well for $Z_2/Z_1 < 1$, the fit of Eq. 4 is superior over the entire range tested. This was a surprising result to us, as we anticipated that the $\Delta\rho^2$ model would better capture the structure refinement process; instead, the isolated atom approximation (reflected in the upper limit of $r = \infty$ in Eq. 5) for a macromolecular structure refinement is evidently less accurate relative to the localized treatment implicit in the derivation of Eq. 4.



Refined $B_{2,iso}$ values as a function of Z_2/Z_1 , the ratio of the atomic number of the scatterer refined in the chalcogenide site (Z_2) relative to $Z_1 = 16$ (the true scatterer, sulfur), in the $[4\text{Fe}:4\text{S}]$ cluster of the nitrogenase Fe protein (PDB data sets 7TPW (red circles) and 7TPY (blue circles)). The solid and dashed lines represent the fits to Eq. 4 and Eq. 6, respectively, with $Z_1 = 16 e^-$ and $B_0 = 6 \text{ \AA}^2$ for both structures, and $B_{1,iso} = 12.0 \text{ \AA}^2$ and 19.8 \AA^2 for the 7TPW and 7TPY structures, respectively.

Derivation of Equation 6

Eq. 6 can be derived from Eq. 5 as follows. The integral and derivative were evaluated with Mathematica[®].

$$\begin{aligned}
 \Delta\rho^2 &= \int_0^{\infty} (\rho_1(r) - \rho_2(r))^2 4\pi r^2 dr \\
 &= \int_0^{\infty} \left(\left[Z_1 \left(\frac{4\pi}{B_1} \right)^{3/2} e^{-4\pi^2 r^2 / B_1} \right] - \left[Z_2 \left(\frac{4\pi}{B_2} \right)^{3/2} e^{-4\pi^2 r^2 / B_2} \right] \right)^2 4\pi r^2 dr \\
 &= 2\pi^{3/2} \left[\frac{\sqrt{2}Z_1^2}{B_1^{3/2}} - \frac{8Z_1Z_2}{(B_1 + B_2)^{3/2}} + \frac{\sqrt{2}Z_2^2}{B_2^{3/2}} \right] \\
 \frac{\partial \Delta\rho^2}{\partial B_2} &= 2\pi^{3/2} Z_2 \left(\frac{12Z_1}{(B_1 + B_2)^{5/2}} - \frac{3Z_2}{\sqrt{2}B_2^{5/2}} \right) = 0 \\
 \frac{B_2^{5/2}}{(B_1 + B_2)^{5/2}} &= \frac{3Z_2}{12\sqrt{2}Z_1} = \frac{1}{(\sqrt{2})^{5/2}} \frac{Z_2}{Z_1} \\
 \frac{(\sqrt{2})^{5/2} B_2^{5/2}}{(B_1 + B_2)^{5/2}} &= \frac{Z_2}{Z_1} \\
 \frac{2B_2}{(B_1 + B_2)} &= \left(\frac{Z_2}{Z_1} \right)^{2/5} \\
 2B_2 &= \left(\frac{Z_2}{Z_1} \right)^{2/5} (B_1 + B_2) \\
 B_2 \left(2 - \left(\frac{Z_2}{Z_1} \right)^{2/5} \right) &= B_1 \left(\frac{Z_2}{Z_1} \right)^{2/5} \\
 B_2 &= B_1 \frac{\left(\frac{Z_2}{Z_1} \right)^{2/5}}{\left(2 - \left(\frac{Z_2}{Z_1} \right)^{2/5} \right)}
 \end{aligned}$$

Section VI: Geometrical Calculations

Geometry Overview: Polyhedra, Lines, and Planes

More complete discussions of this topic are presented in Chapter 2 of Volume II of the International Tables, and in Chapter 2 of D.E. Sands, *Vectors and Tensors in Crystallography*, Addison Wesley (1982).

Polyhedra: Euler's relation for convex polyhedra: $V - E + F = 2$, where V = number of vertices, E = number of edges and F = number of faces; the numerical constant is also known as the Eulerian characteristic χ . The value of χ depends on the surface topology; for example, any triangulation of a surface on a torus has $\chi = 0$ [see C.C. Adams, *The Knot Book*, W.H. Freeman (1994)]. This may also be generalized to "the mountaineer's equation" [H.B. Griffiths, *Surfaces*, Cambridge (1981)], with the identification V = number of peaks, E = number of passes (saddle points) and F = number of pits (valleys).

Peaks, saddle points and valleys in electron density maps may be identified from the signs of the eigenvalues of the Hessian matrix defined as:

$$\begin{bmatrix} \frac{\partial^2 \rho}{\partial x^2} & \frac{\partial^2 \rho}{\partial x \partial y} & \frac{\partial^2 \rho}{\partial x \partial z} \\ \frac{\partial^2 \rho}{\partial x \partial y} & \frac{\partial^2 \rho}{\partial y^2} & \frac{\partial^2 \rho}{\partial y \partial z} \\ \frac{\partial^2 \rho}{\partial x \partial z} & \frac{\partial^2 \rho}{\partial y \partial z} & \frac{\partial^2 \rho}{\partial z^2} \end{bmatrix}$$

When the rank of the Hessian is 3 (meaning there are three non-zero eigenvalues), peaks (maxima) are identified by three negative eigenvalues, while valleys (minima) have three positive eigenvalues. Saddle points with two negative eigenvalues are "passes", while those with only one negative eigenvalue are "pales" [L. Leherte, S. Fortier, J. Glasgow, F.H. Allen, *Acta Cryst.* **D50**, 155-166 (1994)]

Volumes/Areas: The volume of a prism (unit cell) defined by the three non-coplanar vectors **a**, **b** and **c** is given by the triple product $\mathbf{a} \times \mathbf{b} \cdot \mathbf{c}$. The volume of a pyramid may be calculated as (1/3) (base area) (altitude).

The area A of a triangle with vertices $x_i y_i$ is given by:

$$A = \pm \frac{1}{2} \begin{vmatrix} x_1 & y_1 & 1 \\ x_2 & y_2 & 1 \\ x_3 & y_3 & 1 \end{vmatrix}$$

The volume V of a tetrahedron with vertices $x_i y_i z_i$ is given by:

$$V = \pm \frac{1}{6} \begin{vmatrix} x_1 & y_1 & z_1 & 1 \\ x_2 & y_2 & z_2 & 1 \\ x_3 & y_3 & z_3 & 1 \\ x_4 & y_4 & z_4 & 1 \end{vmatrix}$$

Lines: The general equation for a straight line is:

$$Ax + By + C = 0$$

which can be reduced to the equivalent forms:

$$\frac{x}{a} + \frac{y}{b} = 1$$

where a and b are the intercepts of the line on the x and y axes, respectively, or:

$$lx + my - p = 0; \quad l^2 + m^2 = 1$$

where l and m are the vector components of the normal to the line, and p is the perpendicular distance from the line to the origin. Conventions for the correct signs of these terms are discussed in the International Tables.

The shortest (perpendicular) distance, P , from a line to a point (x_l, y_l) is given by:

$$P = lx_l + my_l - p$$

Where P is positive if x_l, y_l is on the side of the line opposite to that containing the origin.

Planes: The general equation for a plane is:

$$Ax + By + Cz + D = 0$$

which can be reduced to the equivalent forms:

$$\frac{x}{a} + \frac{y}{b} + \frac{z}{c} = 1$$

where a , b , and c are the intercepts of the plane of the x, y , and z axes, respectively, or:

$$lx + my + nz - p = 0; \quad l^2 + m^2 + n^2 = 1$$

where l , m , n are the vector components of the normal to the plane, and p is the perpendicular distance from the plane to the origin.

The shortest distance, P , from a point to the plane is given by:

$$P = lx_l + my_l + nz_l - p$$

The equation of a plane passing through three points is given by the determinant:

$$\begin{vmatrix} x & y & z & 1 \\ x_1 & y_1 & z_1 & 1 \\ x_2 & y_2 & z_2 & 1 \\ x_3 & y_3 & z_3 & 1 \end{vmatrix} = 0$$

Least Squares Plane

References

V. Schomaker, J. Waser, R.E. Marsh and G. Bergman, "To Fit a Plane or a Line to a Set of Points by Least Squares" *Acta Cryst.* 12, 600 (1959)

C.M. Shakarji "Least-Squares Fitting Algorithms of the NIST Algorithm Testing System" *J. Res. NIST* 103, 633-641 (1998)

Consider a set of N points with coordinates $\vec{x} = (x_i, y_i, z_i)$, with the origin defined as the centroid of these points (ie – so that the average value of these coordinates is (0,0,0)). To calculate the (unweighted) least squares plane, set up the matrix M, where the (x_i, y_i, z_i) correspond to the rows of M. The eigenvector of the matrix $M^T M$ corresponding to the smallest eigenvalue defines the normal to the least squares plane. The value of the eigenvalue equals the sum of the squares of the distances of each point from that plane. (The eigenvector corresponding to the largest eigenvalue is the normal to the "greatest squares plane").

To transform coordinates from the initial coordinate system to the new frame, with the z axis corresponding to the normal to the least squares plane, the matrix R is defined as follows.

1. let Z = the components of the eigenvector corresponding to the smallest eigenvalue
2. define X' – this vector may not be perpendicular to Z, but will define the X-Z plane.
3. calculate $Y' = Z \times X'$
4. Y = normalized Y'
5. calculate $X = Y \times Z$

so that R is defined as

$$R = \begin{bmatrix} X_1 & X_2 & X_3 \\ Y_1 & Y_2 & Y_3 \\ Z_1 & Z_2 & Z_3 \end{bmatrix}$$

and the transformed coordinates are given by $\vec{x}' = R\vec{x}$

Close Packing of Spheres

Packing densities are evaluated for different types of close packed arrangements of spheres, with applications to protein crystals - bacterioferritin, light harvesting complex, Tomato Bushy Stunt Virus (TBSV) - as well as Membrane Protein Polyhedra (MPP).

Definitions (see old Intl. Tables section 7.1, vol II)

V_s = volume of sphere

V_c = unit cell volume

N = number of spheres per unit cell

$D = N/V_c$ = density in spheres per unit volume

$C = N \cdot V_s / V_c$ = packing density (fractional coverage of space by spheres)

Z = number of contacts per sphere

Calculations are based on spheres of diameter = 1, with volume

$$V_s = \frac{4}{3} \pi \left(\frac{1}{2} \right)^3 = \frac{\pi}{6} \doteq 0.523599$$

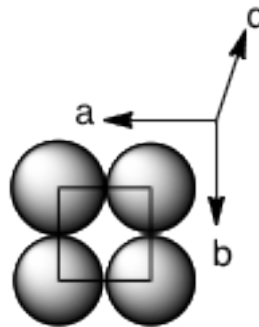
Simple cubic packing

all sides (a, b, c) have unit length

$V_c = 1$

$C = 0.523599$

$Z = 6$



Body center cubic

the body diagonal has length 2, or

$$3a^2 = 2^2 \Rightarrow a = \sqrt{4/3} \doteq 1.15$$

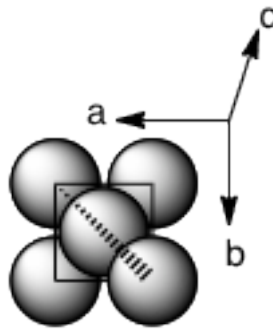
$$V_c = a^3 = \left(\sqrt{4/3}\right)^3 \doteq 1.0472$$

$$N = 2$$

$$C = NV_s/V_c \doteq 0.680175$$

$$Z = 8$$

diameter of sphere = $a / \sqrt{4/3} \sim a/1.15$



Face centered cubic, or cubic close packing

the face diagonal has length 2, or

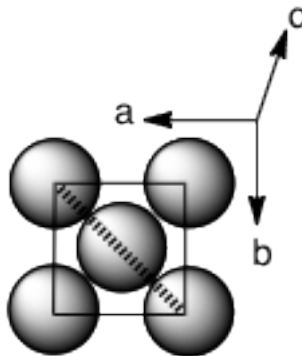
$$2a^2 = 2^2 \Rightarrow a = \sqrt{2} \doteq 1.414$$

$$V_c = a^3 = \left(\sqrt{2}\right)^3 \doteq 2.82843$$

$$N = 4$$

$$C = NV_s/V_c \doteq 0.74048$$

$$Z = 12$$



simple hexagonal

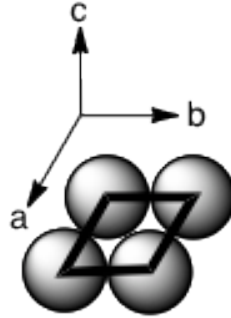
$a = b = c = 1$

$V_c = a^3 \sin 120 = 0.866025$

$N = 1$

$C = NV_s/V_c \doteq 0.6046$

$Z = 8$



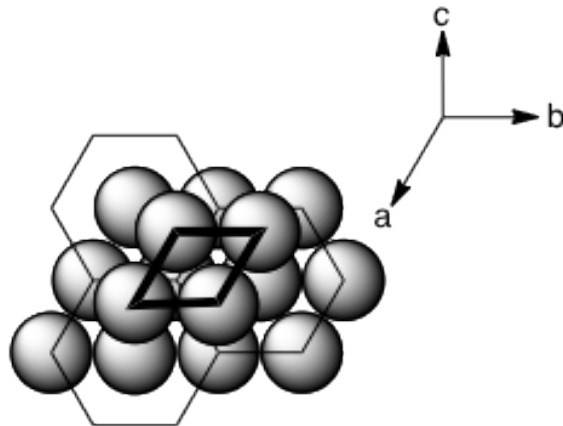
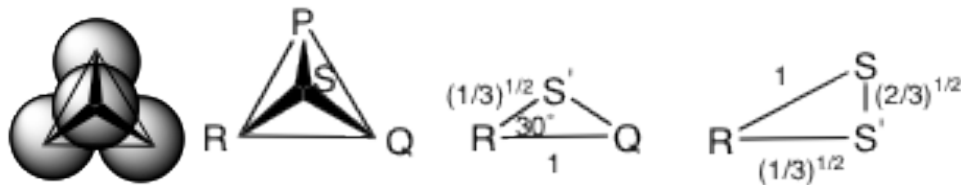
hexagonal close packing (= cubic close packing)

$a = b = 1$; the spacing along c can be calculated as follows; R-Q-S' are in the ab plane, and RSS' is normal to the ab plane, with $S-S' = (2/3)^{1/2}$ representing the vertical displacement between sphere centers projected onto the c axis.

$V_c = abc \sin 120 = \left(2 \left(\frac{2}{3} \right)^{1/2} \right) \sin 120 = 1.41421$

$N = 2$

$C = NV_s/V_c \doteq 0.74048$



tetragonal packing - two flavors:

short c and long a (body-centered tetragonal)

long c and short a (cubic-closest packing)

the diagonal = 2

$$2a^2 + c^2 = 2^2 \Rightarrow c = \sqrt{4 - 2a^2} \text{ and } a^2 = 2 - \frac{c^2}{2}$$

$$V_c = a^2 c = a^2 \sqrt{4 - 2a^2} = 2c - \frac{c^3}{2}$$

$$N = 2$$

the solutions must have c and a both > 1 (otherwise spheres interpenetrate)

c = 1 (a = (3/2)^{1/2}) - body centered tetragonal

$$c = 1 \Rightarrow a^2 = 2 - \frac{c^2}{2} = \frac{3}{2}; \quad a = \sqrt{\frac{3}{2}}$$

$$C = NV_s/V_c \doteq 0.698132$$

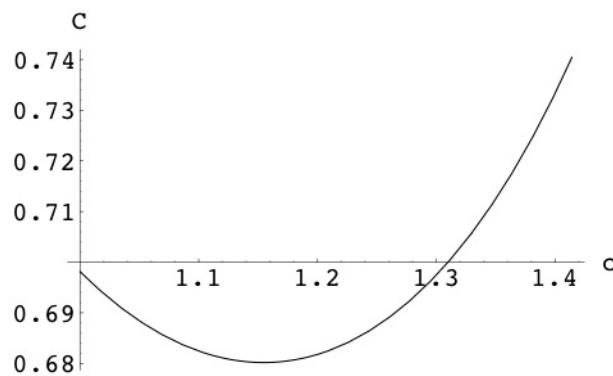
$$Z = 10$$

a = 1 (c = 2^{1/2}) - cubic close packing

$$a = 1 \Rightarrow c = \sqrt{2}$$

$$C = NV_s/V_c \doteq 0.74048$$

the packing density as a function of c is illustrated below:



Circumscribed Radii for Polyhedra

from <http://dmccooley.com/polyhedra/Lsncube.html>

in this analysis, the edge length is set to 1

tetrahedra (4 vertices):	$\sqrt{6}/4$	~ 0.612
cube (8 vertices):	$\sqrt{3}/2$	~ 0.866
octahedra (6 vertices):	$\sqrt{2}/2$	~ 0.707
icosahedra (20 vertices)::	$\sqrt{10+2\sqrt{5}}/4$	~ 0.951

snub cube (laevo)

$$\frac{\sqrt{3*(10+\text{cbrt}(199+3*\sqrt{33})) + \text{cbrt}(199-3*\sqrt{33}))}{6} \approx 1.3437133737446017013$$

(cbrt = cube root)

MscS - cytoplasmic domain ~ 13 nm MPP diameter $\sim 2 \times 1.34 \times 13 = 35$ nm

Protein crystal examples

Light Harvesting Complex

PDB 1RWT, space group R32 $a = 261.8 \text{ \AA}$, $c = 660.30 \text{ \AA}$

diameter = $a = 262 \text{ \AA}$

for hexagonal close packing, packing along c axis = $c/3 = \text{diameter} \times \sqrt{2/3} = 213 \text{ \AA}$

$213 \times 3 = 641 \text{ \AA}$ (vs 660)

$[(660/3) \times \sqrt{3/2}] = 269 \text{ \AA}$

Kouyama (ACD 60, 803 (2004)) diameter $\sim 250 \text{ \AA}$

PDB 1VCR, space group F23 $a = 360.65 \text{ \AA}$

diameter = $a/\sqrt{2} = 255 \text{ \AA}$

Bacterioferritin

space group I422, $a = 142.2 \text{ \AA}$, $c = 141.0 \text{ \AA}$

approximate as body centered cube, cell edge = diameter $\times \sqrt{4/3}$

diameter = $141 \times \sqrt{3/4} \sim 122 \text{ \AA}$

space group P6₃22, $a = 126.1 \text{ \AA}$, $c = 188.2 \text{ \AA}$

$a \sim \text{diameter} = 126 \text{ \AA}$

for hexagonal close packing, packing along c axis = $c/2 = \text{diameter} \times \sqrt{2/3}$

diameter = $(188/2) \times \sqrt{3/2} \sim 115 \text{ \AA}$

TBSV

space group I23, $a = 383.2 \text{ \AA}$

diameter = $383 \times \sqrt{3/4} \sim 332 \text{ \AA}$

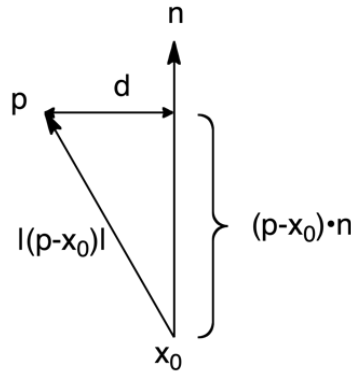
(early Bernal Nature paper has a cell constant of 394 \AA and diameter = 340 \AA)

Shortest Distance from a Point to a Line

A straight line in 3D may be described by the equation $\vec{x} = \vec{x}_0 + \alpha \hat{n}$, where \hat{n} gives the direction along the line and \vec{x}_0 is a point on the line. The minimum distance d to a point \vec{p} may be calculated by minimizing the expression $(\vec{x}_0 + \alpha \hat{n} - \vec{p})^2$ with respect to α . If the components of $(\vec{p}, \vec{x}_0, \hat{n})$ are given by (p, q, r) , (x_0, y_0, z_0) and (l, m, n) , then

$$\alpha = (\vec{p} - \vec{x}_0) \cdot \hat{n}$$

$$d^2 = |\vec{p} - \vec{x}_0|^2 - \alpha^2$$



Closest distance between two lines – derivation 1

Let the two lines be described by the equations: $\vec{y}_0 = \vec{x}_0 + \alpha \hat{n}_0$ and $\vec{y}_1 = \vec{x}_1 + \beta \hat{n}_1$

The closest distance between these two lines may be found by minimizing $d^2 = |(\vec{y}_0 - \vec{y}_1)|^2$ with respect to α and β .

$$\frac{\partial |(\vec{y}_0 - \vec{y}_1)|^2}{\partial \alpha} = 2\hat{n}_0 \cdot (\vec{x}_0 + \alpha \hat{n}_0 - \vec{x}_1 - \beta \hat{n}_1) = 0$$

$$\frac{\partial |(\vec{y}_0 - \vec{y}_1)|^2}{\partial \beta} = -2\hat{n}_1 \cdot (\vec{x}_0 + \alpha \hat{n}_0 - \vec{x}_1 - \beta \hat{n}_1) = 0$$

$$\begin{pmatrix} 1 & -\hat{n}_0 \cdot \hat{n}_1 \\ -\hat{n}_0 \cdot \hat{n}_1 & 1 \end{pmatrix} \begin{pmatrix} \alpha \\ \beta \end{pmatrix} = \begin{pmatrix} \hat{n}_0 \cdot (\vec{x}_1 - \vec{x}_0) \\ -\hat{n}_1 \cdot (\vec{x}_1 - \vec{x}_0) \end{pmatrix}$$

$$\begin{pmatrix} \alpha \\ \beta \end{pmatrix} = \frac{1}{1 - (\hat{n}_0 \cdot \hat{n}_1)^2} \begin{pmatrix} 1 & +\hat{n}_0 \cdot \hat{n}_1 \\ +\hat{n}_0 \cdot \hat{n}_1 & 1 \end{pmatrix} \begin{pmatrix} \hat{n}_0 \cdot (\vec{x}_1 - \vec{x}_0) \\ -\hat{n}_1 \cdot (\vec{x}_1 - \vec{x}_0) \end{pmatrix}$$

$$d^2 = (\vec{x}_0 + \alpha \hat{n}_0 - \vec{x}_1 - \beta \hat{n}_1)^2$$

Closest distance between two lines

At the distance of closest approach between two lines, the connecting segment is perpendicular to both lines:

$$\begin{aligned}\bar{x}_0 + \alpha \hat{n}_0 + d \frac{\hat{n}_0 \times \hat{n}_1}{|\hat{n}_0 \times \hat{n}_1|} &= \bar{x}_1 + \beta \hat{n}_1 \\ \alpha \hat{n}_0 - \beta \hat{n}_1 + d \frac{\hat{n}_0 \times \hat{n}_1}{|\hat{n}_0 \times \hat{n}_1|} &= \bar{x}_1 - \bar{x}_0\end{aligned}$$

$$\begin{pmatrix} (\hat{n}_0)_x & -(\hat{n}_1)_x & (\text{cross})_x \\ (\hat{n}_0)_y & -(\hat{n}_1)_y & (\text{cross})_y \\ (\hat{n}_0)_z & -(\hat{n}_1)_z & (\text{cross})_z \end{pmatrix} \begin{pmatrix} \alpha \\ \beta \\ d \end{pmatrix} = \begin{pmatrix} (\bar{x}_1 - \bar{x}_0)_x \\ (\bar{x}_1 - \bar{x}_0)_y \\ (\bar{x}_1 - \bar{x}_0)_z \end{pmatrix}$$

Least squares solution for point closest to a set of lines

Let the direction of, and a point on, the i^{th} line be denoted \hat{n}_i and \bar{x}_i , respectively, and the desired point be denoted \bar{p} . \bar{p} is defined such that it has the minimum sum of the squared distances to all the specified lines, where i indicates the specific line, and j and k are vector components, with $1,2,3 = x,y,z$.

$$\Phi(\bar{p}) = \sum_i d_i^2 = \sum_i \left[(\bar{p} - \bar{x}_i) \cdot (\bar{p} - \bar{x}_i) - ((\bar{p} - \bar{x}_i) \cdot \hat{n}_i)^2 \right]$$

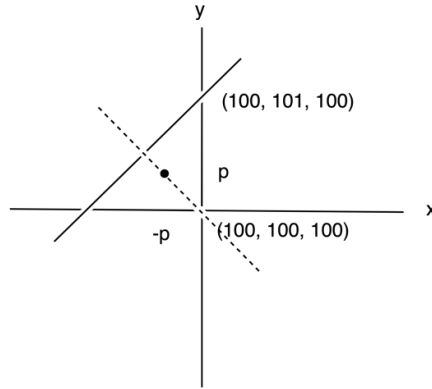
$$\frac{\partial \Phi(\bar{p})}{\partial p_j} = \sum_i \left[2p_j - 2x_{i,j} - 2n_{i,j} \sum_k (p_k - x_{i,k}) n_{i,k} \right]$$

$$\begin{pmatrix} \sum_i (1 - n_{i,1}^2) & -\sum_i n_{i,1} n_{i,2} & -\sum_i n_{i,1} n_{i,3} \\ -\sum_i n_{i,1} n_{i,2} & \sum_i (1 - n_{i,2}^2) & -\sum_i n_{i,2} n_{i,3} \\ -\sum_i n_{i,1} n_{i,3} & -\sum_i n_{i,2} n_{i,3} & \sum_i (1 - n_{i,3}^2) \end{pmatrix} \begin{pmatrix} p_1 \\ p_2 \\ p_3 \end{pmatrix} = \begin{pmatrix} \sum_i [(1 - n_{i,1}^2)x_{i,1} - n_{i,1}n_{i,2}x_{i,2} - n_{i,1}n_{i,3}x_{i,3}] \\ \sum_i [-n_{i,1}n_{i,2}x_{i,1} + (1 - n_{i,2}^2)x_{i,2} - n_{i,2}n_{i,3}x_{i,3}] \\ \sum_i [-n_{i,1}n_{i,3}x_{i,1} - n_{i,2}n_{i,3}x_{i,2} + (1 - n_{i,3}^2)x_{i,3}] \end{pmatrix}$$

This is implemented in polyhedra.com, to find the origin by calculating the least squares point closest to the symmetry axes of different MscS molecules modeled into mpp tomograms. (note: the notation is slightly different, so the subscripts should be carefully checked). To test this algorithm, the following model was analyzed in the program poly_test.f using 4 lines that intersect at (100, 100, 100) with $\Phi=0$:

$$\begin{aligned}
n_1 &= \begin{pmatrix} 1 & 0 & 0 \end{pmatrix}, x_1 = \begin{pmatrix} 110 & 100 & 100 \end{pmatrix} \\
n_2 &= \begin{pmatrix} 0 & 1 & 0 \end{pmatrix}, x_2 = \begin{pmatrix} 100 & 110 & 100 \end{pmatrix} \\
n_3 &= \begin{pmatrix} 0 & 0 & 1 \end{pmatrix}, x_3 = \begin{pmatrix} 100 & 100 & 110 \end{pmatrix} \\
n_4 &= \begin{pmatrix} \sqrt{2}/2 & \sqrt{2}/2 & 0 \end{pmatrix}, x_4 = \begin{pmatrix} 110 & 110 & 100 \end{pmatrix}
\end{aligned}$$

shifting x_4 to $(110, 111, 100)$ leads to the following result; the first three points still intersect at $100, 100, 100$, but line 4 now intersects the “ideal origin” at $(100, 101, 100)$, and the shifted origin will now be along the line oriented along $(1, -1, 0)$, shifted from the ideal origin by an amount p :



The mean squared deviations from n_1, n_2, n_3 and n_4 are $p^2, p^2, 2p^2$ and $2(1/2-p)^2$, respectively,

$$\Phi(p) = 6p^2 - 2p + 1/2$$

$$\frac{\partial \Phi(p)}{\partial p} = 12p - 2 = 0 \Rightarrow p = 1/6$$

$$\Phi(1/6) = 1/3; \text{ rms } \langle d^2 \rangle = \sqrt{\Phi(1/6)/4} = 0.289$$

$$\Phi(0) = 1/2; \text{ rms } \langle d^2 \rangle = \sqrt{\Phi(0)/4} = 0.354$$

and the point of intersection is found to be $(99.833, 100.167, 100.)$

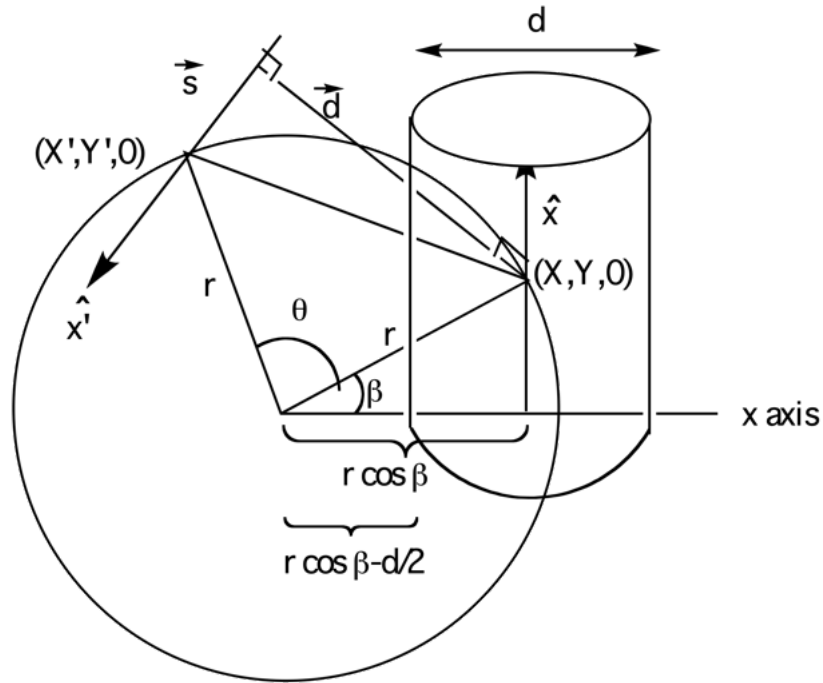
Helix Packing Relationships

see A.K. Dunker and D.J. Zaleske *Biochem. J.* **163**, 45-57 (1977)

R.H. Spencer and D.C. Rees, *Ann. Rev Biophys. Biomol. Struct.* **31**, 207 (2002)

Symbols

- z direction of rotation axis (that passes through xy origin) = membrane normal
- N number of equivalent subunits
- θ molecular symmetry rotation angle = $360^\circ/N$
- η tilt angle between helix axis and membrane normal
- α angle between axes of adjacent helices
- d shortest distance between axes of adjacent helices = helix diameter
- D distance between helix axes in $z=0$ plane (defined below)
- r radial distance to rotation axis from helix axis point $(X,Y,0)$ closest to adj. helix axis
- s vector along helix axis x' between intersection with d vector and $Z=0$ plane



the xy coordinate plane is oriented such that the \vec{x} vector has components $\{0 \ y \ z\}$, and it need not be perpendicular to the radial vector, \vec{r} , extending to the rotation axis

When the tilt angle between the membrane normal and the helix axis is η , then the components of \hat{x} are equal to $\{0, \sin \eta, \cos \eta\}$.

x and x' are related by a rotation of θ around the z axis, or:

$$\hat{x}' = \begin{bmatrix} \cos \vartheta & -\sin \vartheta & 0 \\ \sin \vartheta & \cos \vartheta & 0 \\ 0 & 0 & 1 \end{bmatrix} \hat{x} = \begin{bmatrix} -y \sin \vartheta \\ y \cos \vartheta \\ z \end{bmatrix}$$

$$\hat{x}' \cdot \hat{x} = y^2 \cos \vartheta + z^2 = \cos \alpha \quad \text{with } y^2 + z^2 = 1; \quad z = \cos \eta; \quad y = \sin \eta$$

$$\cos \alpha = \cos^2 \eta + \sin^2 \eta \cos \vartheta = \cos^2 \eta (1 - \cos \vartheta) + \cos \vartheta$$

(Note: $\hat{x}' \cdot \hat{x}$ will give the packing angle α since it corresponds to the torsion angle defined by the two helix axes at the distance of closest approach, when x and x' are both perpendicular to the vector between them).

At the distance of closest approach between x and x' , the points are separated by a distance d in the direction given by the cross product of these two vectors, $x \times x'$ that is perpendicular to both x and x' (and, by this definition, the vector points from x' towards x).

$$\hat{x} \times \hat{x}' = \begin{vmatrix} \hat{x} & \hat{y} & \hat{z} \\ 0 & \sin \eta & \cos \eta \\ -\sin \eta \sin \vartheta & \sin \eta \cos \vartheta & \cos \eta \end{vmatrix} = \begin{bmatrix} \cos \eta \sin \eta (1 - \cos \vartheta) \\ -\cos \eta \sin \eta \sin \vartheta \\ \sin^2 \eta \sin \vartheta \end{bmatrix}$$

The length of this vector is $\sin \alpha$, as shown below (this is unnecessary for the proof, since the magnitude of the cross product is by product of the lengths of the vector (each 1) times the sine of the angle between the two vectors, α):

$$|\hat{x} \times \hat{x}'|^2 = \text{length}^2$$

$$= \sin^2 \eta \left[\cos^2 \eta (1 - \cos \vartheta)^2 + \sin^2 \vartheta \right]$$

$$\text{Now } \sin^2 \eta = \frac{1 - \cos \alpha}{1 - \cos \vartheta} \quad \text{and} \quad \cos^2 \eta = \frac{\cos \alpha - \cos \vartheta}{1 - \cos \vartheta}$$

$$\text{so } |\hat{x} \times \hat{x}'|^2 = \frac{1 - \cos \alpha}{1 - \cos \vartheta} \left\{ (\cos \alpha - \cos \vartheta)(1 - \cos \vartheta) + (1 - \cos \vartheta)(1 + \cos \vartheta) \right\}$$

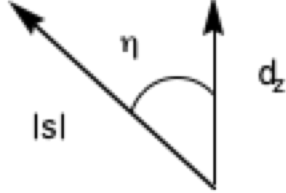
$$= (1 - \cos \alpha) \{1 + \cos \alpha\}$$

$$= 1 - \cos^2 \alpha$$

$$= \sin^2 \alpha$$

$$\text{and } \vec{d} = |\vec{d}| \frac{(\hat{x} \times \hat{x}')}{\sin \alpha} \equiv d \frac{(\hat{x} \times \hat{x}')}{\sin \alpha}$$

The vector s runs along x' from the point of intersection of x x x' to the plane $z=0$. The length of s , $|s|$, gives the offset along the helix axis between the two helix-helix interfaces and may be calculated from the following relationships:



$$\cos \eta = \frac{d_z}{|s|}$$

$$|s| = \frac{1}{\cos \eta} \frac{d \sin^2 \eta \sin \vartheta}{\sin \alpha}$$

(note: this gives the offset along the helix axes; in terms of the offset between the two $C\alpha$ positions at the helix-helix interfaces, this will be reduced from $|s|$ by twice the radius of the $C\alpha$'s from the helix axis divided by d , or $2 \cdot 2.3/d$)

From the magnitudes of s and d , the values of D and r can be calculated from the following relationships:

$$D^2 = d^2 + s^2$$

$$r = \frac{(D/2)}{\sin(\vartheta/2)}$$

The distance of closest approach of the helix axis to the rotation axis occurs when the helix axis is perpendicular to the radial vector from the rotation axis, which is when r is along the x axis, so that the minimum distance is given by $r \cos \beta$. This distance may be calculated by relating the x and y components of the x and x' vector through the appropriate components of the d and x vector. The negative sign of the d components is required by the cross-product definition of the d vector:

$$r \cos(\vartheta + \beta) \equiv r \cos \beta \cos \vartheta - r \sin \beta \sin \vartheta = r \cos \beta - d_x + s_x$$

$$r \sin(\vartheta + \beta) \equiv r \cos \beta \sin \vartheta + r \sin \beta \cos \vartheta = r \sin \beta - d_y + s_y$$

with:

$$\vec{d} = \left\{ \begin{matrix} d_x & d_y & d_z \end{matrix} \right\} = \frac{d}{\sin \alpha} \left\{ \begin{matrix} \cos \eta \sin \eta (1 - \cos \vartheta) & -\cos \eta \sin \eta \sin \vartheta & \sin^2 \eta \sin \vartheta \end{matrix} \right\}$$

$$\vec{s} = \left\{ \begin{matrix} s_x & s_y & s_z \end{matrix} \right\} = \frac{d \sin^2 \eta \sin \vartheta}{\sin \alpha \cos \eta} \left\{ \begin{matrix} -\sin \eta \sin \vartheta & \sin \eta \cos \vartheta & \cos \eta \end{matrix} \right\}$$

(since s is parallel to x')

r and β may be determined from solving the following equation, where all the terms on the right hand side are known:

$$\begin{pmatrix} r \cos \beta \\ r \sin \beta \end{pmatrix} = \begin{pmatrix} \cos \vartheta - 1 & -\sin \vartheta \\ \sin \vartheta & \cos \vartheta - 1 \end{pmatrix}^{-1} \begin{pmatrix} -d_x + s_x \\ -d_y + s_y \end{pmatrix}$$

After suitable manipulations, the minimum distance of the surface of a helix from the rotation axis (given by $r \cos \beta - d/2$ (the helix radius)) can be shown to be:

$$r \cos \beta - \frac{d}{2} = \frac{d}{2} \left(\left(\tan \eta \cot \frac{\alpha}{2} \right) - 1 \right)$$

The angle ω formed between the two vectors d between a given helix and its two nearest neighbors may be calculated from the following expression where R is the molecular symmetry operator:

$$\begin{aligned} \cos \omega &= -\hat{d} \cdot R \cdot \hat{d} \\ R &= \begin{bmatrix} \cos \vartheta & -\sin \vartheta & 0 \\ \sin \vartheta & \cos \vartheta & 0 \\ 0 & 0 & 1 \end{bmatrix} \\ \hat{d} &= \frac{1}{\sin \alpha} \begin{pmatrix} \cos \eta \sin \eta (1 - \cos \vartheta) & -\cos \eta \sin \eta \sin \vartheta & \sin^2 \eta \sin \vartheta \end{pmatrix} \end{aligned}$$

after simplification in Mathematica[®] (helix_tilt_offset.nb), this reduces to:

$$\cos \omega = 1 - \frac{8 \cos^2(\vartheta/2)}{3 + \cos \vartheta + 2 \cos 2\eta \sin^2(\vartheta/2)}$$

when the tilt angle $h=0$, this further reduces to

$$\cos \omega = -\cos \vartheta$$

as it should since this is equivalent to the angles at the vertices of a regular n-polygon.

A Mathematica® notebook to do these various calculations is produced below:

```
In[37]:= (*helix_packing_radius.nb - to calculate pore radius of MscL *)
theta = 72. Degree
eta = 36.8 Degree
d = 7.5
angmat = {{Cos[theta] - 1, -Sin[theta]},
          {Sin[theta], Cos[theta] - 1}}
Alfcos = ((Cos[eta]^2) * (1 - Cos[theta]) + Cos[theta] // N
alf = N[(ArcCos[Alfcos]) * (180. / 3.14) , 5]
Alfsin = Sqrt[1. - Alfcos^2]
dx = -(d / Alfsin) * Cos[eta] * Sin[eta] * (1 - Cos[theta])
dy = (d / Alfsin) * Cos[eta] * Sin[eta] * Sin[theta]
slen = (d / Alfsin) * (Sin[eta]^2) * Sin[theta] / Cos[eta]
sx = -slen * Sin[eta] * Sin[theta]
sy = slen * Sin[eta] * Cos[theta]
vec = {(dx + sx), (dy + sy)}
answer = Inverse[angmat].vec
leng = Sqrt[Sum[answer[[i]]^2, {i, 2}]]
bigd = Sqrt[d^2 + slen^2]
radr = (bigd / 2.) / Sin[theta / 2.]
poreradius = (d / 2.) * ((Tan[eta] * Cot[(alf / 2.) Degree]) - 1.)
```

Out[37]= 1.25664

Out[38]= 0.642281

Out[39]= 7.5

Out[40]= {{-0.690983, -0.951057}, {0.951057, -0.690983}}

Out[41]= 0.752055

Out[42]= 41.2522

Out[43]= 0.6591

Out[44]= -3.77145

Out[45]= 5.19095

Out[46]= 4.84973

Out[47]= -2.76291

Out[48]= 0.897725

Out[49]= {-6.53436, 6.08868}

Out[50]= {7.45735, 1.45255}

Out[51]= 7.5975

Out[52]= 8.9314

Out[53]= 7.5975

Out[54]= 3.70322

Finding the Axis that Minimizes Helical Tilt

Let x_i be the direction of the i^{th} helical vector, and a be the direction (to be found) that minimizes the helical tilt, by maximizing the sum of the dot products between x_i and a . The components of a may be found as follows:

$$\text{Maximize } \sum_i \bar{x}_i \cdot \bar{a} \text{ subject to the constraint } \bar{a} \cdot \bar{a} = 1$$

with Lagrange multipliers, this becomes:

$$\Phi = \sum_i \bar{x}_i \cdot \bar{a} + \lambda(\bar{a} \cdot \bar{a} - 1)$$

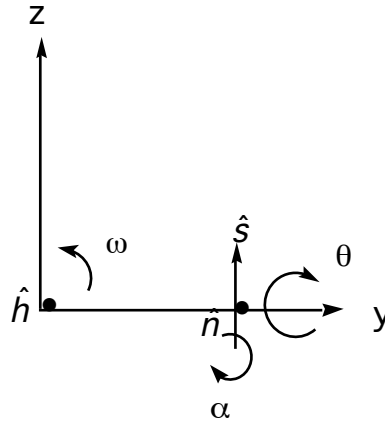
$$\text{Let } \bar{x}_i = \left\{ \begin{matrix} x_i & y_i & z_i \end{matrix} \right\} \text{ and } \bar{a} = \left\{ \begin{matrix} a & b & c \end{matrix} \right\}$$

$$\frac{\partial \Phi}{\partial a} = \sum_i x_i + 2\lambda a = 0, \text{ etc.}$$

From the normalization condition

$$2\lambda = \pm \left(\left(\sum_i x_i \right)^2 + \left(\sum_i y_i \right)^2 + \left(\sum_i z_i \right)^2 \right)^{1/2}$$
$$a = \mp \frac{\sum_i x_i}{2\lambda}, \text{ etc.}$$

Angles between Planar Units in a Helix



Definitions - the helix axis (\hat{h}) is oriented along the x axis. The initial orientation of the planar unit is taken to be in the plane normal to the helix axis, ie, the plane normal, \hat{n} , is parallel to \hat{h} . The tangent, \hat{s} , to the helical path projected into the plane normal to the helix axis, for the first unit under consideration, is defined to be parallel to z. The three angles α , θ and ω correspond to rotations about \hat{s} , y and \hat{h} , respectively, and have the following rotation matrices:

$$\begin{bmatrix} \cos\alpha & -\sin\alpha & 0 \\ \sin\alpha & \cos\alpha & 0 \\ 0 & 0 & 1 \end{bmatrix} \begin{bmatrix} \cos\theta & 0 & \sin\theta \\ 0 & 1 & 0 \\ -\sin\theta & 0 & \cos\theta \end{bmatrix} \begin{bmatrix} 1 & 0 & 0 \\ 0 & \cos\omega & -\sin\omega \\ 0 & \sin\omega & \cos\omega \end{bmatrix}$$

The reference orientation of \hat{n} (along the x axis) is converted into the correct orientation of the planar object by sequential rotations of α and θ to give:

$$\begin{bmatrix} \cos\theta\cos\alpha \\ \sin\alpha \\ -\sin\theta\cos\alpha \end{bmatrix} = \begin{bmatrix} \cos\theta & 0 & \sin\theta \\ 0 & 1 & 0 \\ -\sin\theta & 0 & \cos\theta \end{bmatrix} \begin{bmatrix} \cos\alpha & -\sin\alpha & 0 \\ \sin\alpha & \cos\alpha & 0 \\ 0 & 0 & 1 \end{bmatrix} \begin{bmatrix} 1 \\ 0 \\ 0 \end{bmatrix}$$

The second unit in the helix is generated from the first by a rotation of ω about \hat{h} , so that the plane normal for this unit has the components:

$$\begin{bmatrix} \cos\theta\cos\alpha \\ \sin\alpha\cos\omega + \sin\omega\sin\theta\cos\alpha \\ \sin\alpha\sin\omega - \cos\omega\sin\theta\cos\alpha \end{bmatrix} = \begin{bmatrix} 1 & 0 & 0 \\ 0 & \cos\omega & -\sin\omega \\ 0 & \sin\omega & \cos\omega \end{bmatrix} \begin{bmatrix} \cos\theta\cos\alpha \\ \sin\alpha \\ -\sin\theta\cos\alpha \end{bmatrix}$$

Hence, the dot product between the normals to the planes of these two units in the helix is:

$$\begin{bmatrix} \cos\theta\cos\alpha & \sin\alpha & -\sin\theta\cos\alpha \end{bmatrix} \cdot \begin{bmatrix} \cos\theta\cos\alpha \\ \sin\alpha\cos\omega + \sin\omega\sin\theta\cos\alpha \\ \sin\alpha\sin\omega - \cos\omega\sin\theta\cos\alpha \end{bmatrix}$$

$$= \cos\omega(\cos^2\alpha\sin^2\theta + \sin^2\alpha) + \cos^2\alpha\cos^2\theta$$

which is equivalent to the cosine of the angle between the two plane normals.

Mathematica®:

```
dtor=3.1415926/180.
rtod = 1./dtor
```

```
plane[n_,omega_,theta_,alpha_] :=
  ArcCos[ Cos[n*omega*dtor]*
  ((Sin[alpha*dtor]^2) + (Cos[alpha*dtor]^2)*(Sin[theta*dtor]^2))
  + (Cos[theta*dtor]^2)*(Cos[alpha*dtor]^2) ]*rtod
```

```
err[omega_,theta_,alpha_] :=
  (19.0 - plane[1,omega,theta,alpha])^2 +
  (33.7 - plane[2,omega,theta,alpha])^2 +
  (57.0 - plane[3,omega,theta,alpha])^2 +
  (23.2 - plane[1,omega,theta,alpha])^2 +
  (58.6 - plane[2,omega,theta,alpha])^2 +
  (39.0 - plane[1,omega,theta,alpha])^2
```

```
FindMinimum[err[omega,theta,alpha],
  {omega,45.},{theta,34.},{alpha,1.}]
{536.132, {omega -> 57.3217, theta -> 28.311, alpha -> 0.854799}}
```

```
rms = Sqrt[536./6]
9.45163
```

Useful Properties of Gaussians

1-dimensional Gaussian

$$P_{1D}(x; \mu, \sigma) = \frac{1}{\sqrt{2\pi\sigma^2}} e^{-\frac{(x-\mu)^2}{2\sigma^2}}$$

$$P_{1D}(x) \equiv \frac{1}{\sqrt{2\pi\sigma^2}} e^{-\frac{x^2}{2\sigma^2}}$$

$$\int_{-\infty}^{\infty} P_{1D}(x) dx = 1$$

3-dimensional Gaussian

$$P_{3D}(r) = \frac{1}{\left[\sqrt{2\pi\sigma^2}\right]^3} e^{-\frac{r^2}{2\sigma^2}}$$

$$\int_0^{\infty} P_{3D}(r) 4\pi r^2 dr = 1$$

The Fourier transform of a Gaussian is a Gaussian!

$$F_{1D}(S) = \int_{-\infty}^{\infty} P_{1D}(x) e^{-2\pi i S x} dx = 2 \int_0^{\infty} P_{1D}(x) \cos[2\pi S x] dx = e^{-2\pi^2 S^2 \sigma^2}$$

$$F_{3D}(S) = \int_0^{\infty} P_{3D}(r) \frac{\sin[2\pi S r]}{2\pi S r} 4\pi r^2 dr = e^{-2\pi^2 S^2 \sigma^2}$$

Single Gaussian representation of electron density and the connection to the B-factor

1-Dimensional

$$\rho(x) = Z \sqrt{\frac{4\pi}{B}} e^{-4\pi^2 x^2 / B}$$
$$F(S) = \int_{-\infty}^{\infty} \rho(x) e^{2\pi i S x} dx = Z e^{-BS^2/4}$$

3-Dimensional

$$\rho(r) = Z \left(\frac{4\pi}{B} \right)^{3/2} e^{-4\pi^2 r^2 / B}$$
$$f(S) = Z e^{-B \sin^2 \vartheta / \lambda^2} = Z e^{-BS^2/4}$$

Scattering factor expressions for Gaussian atoms

The variation in atomic scattering factors with scattering angle is often approximated by a sum of Gaussians:

$$f(x) = \sum_{i=1}^N a_i e^{-b_i x^2} + c \quad \text{where } x = \sin \vartheta / \lambda = S / 2$$

The Forsyth-Wells formulation (AC 12, 412 (1959)) uses $N = 2$. It is important to recognize that the fit is only over a defined range of x ; as a consequence of the constant “ c ” term, if this type of expression is used out to the limit $x \rightarrow \infty$ in the absence of an overall temperature factor, the atomic density at the origin goes to infinity (since the FT of a delta function is a constant).

If B is the overall temperature of an atom, then the atomic density corresponding to the FW formulation is given by the following expression

$$\rho(r) = (4\pi)^{3/2} \left[\frac{a_1 e^{-4\pi^2 r^2 / (b_1 + B)}}{(b_1 + B)^{3/2}} + \frac{a_2 e^{-4\pi^2 r^2 / (b_2 + B)}}{(b_2 + B)^{3/2}} + \frac{c e^{-4\pi^2 r^2 / B}}{B^{3/2}} \right]$$

so this is the sum of two Gaussians plus a third term corresponding to the constant “ c ”. By comparison to the single Gaussian density for atomic densities ($f(S) = Z e^{-BS^2/4}$), the pre-exponential a_i terms correspond to an effective number of electrons, and the b_i to the “effective temperature factor” for those electrons.

As a first approximation, atoms may be approximated as a single Gaussian with $B_0 \sim 6-10 \text{ \AA}^2$.

two other useful relationships:

The projection of a Gaussian onto an arbitrary line is a Gaussian (Dunitz, 1.24)

WNL's use of $\langle e^{2\pi i u x} \rangle = 1 - 2\pi^2 u^2 \langle x^2 \rangle + \dots \sim e^{-2\pi^2 u^2 \langle x^2 \rangle}$ in the derivation of the thermal factor (W.N. Lipscomb “X-ray crystallography” in Techniques of Organic Chemistry, A. Weissberger, ed. Vol 1, Part II, 3rd edition, pp. 1641-1738 (1960))

Ellipsoids, B factors and g-Tensors

An ellipsoid can be represented in standard form in terms of the components along the principal axes by the equation:

$$\frac{x^2}{a^2} + \frac{y^2}{b^2} + \frac{z^2}{c^2} = 1$$

the volume of this ellipse = $\frac{4}{3}\pi abc$. In matrix notation, this can be more generally written as

$$\bar{x}^T A \bar{x} = \text{constant}$$

where A is a positive definite matrix (symmetric, determinant > 0). When the coordinate system coincides with the principal axes, A is diagonal (with elements $A_{11} = 1/a^2$, etc.) If A is a non-diagonal matrix, it can be diagonalized by the following transformation:

$$\bar{x}'^T S^{-1} A S \bar{x}' = \text{constant}$$

where S is the matrix that contains the eigenvectors of A as columns, and

$$\bar{x}' = S^{-1} \bar{x}$$

is the transformed version of x in the coordinate system described by the principal axes x', corresponding to the eigenvectors of A.

Two dimensional example (aniso_vibration_ellipsoid.nb)

The equation of a two-dimensional ellipsoid with major and minor axes a and b, respectively, in the principal axes x' frame is given by:

$$\frac{x'^2}{a^2} + \frac{y'^2}{b^2} = 1 \Rightarrow \bar{x}'^T A \bar{x}' = 1 \text{ with } A = \begin{bmatrix} 1/a^2 & 0 \\ 0 & 1/b^2 \end{bmatrix}$$

The area of the ellipse is πab . The rotation matrix R (angle ϕ) that rotates x' to a nonstandard coordinate setting x is given by the following expression (and for an orthogonal matrix $R^T = R^{-1}$)

$$R = \begin{bmatrix} \cos\phi & -\sin\phi \\ \sin\phi & \cos\phi \end{bmatrix}$$

with $\begin{pmatrix} x \\ y \end{pmatrix} = R \begin{pmatrix} x' \\ y' \end{pmatrix}$ or $\bar{x} = R \bar{x}'$ and $R^T \bar{x} = \bar{x}'$

and $\bar{x}'^T A \bar{x}' = \bar{x}^T R A R^T \bar{x} \equiv \bar{x}^T Q \bar{x}$

given the expressions for R and A, Q is equal to

$$Q = \frac{1}{a^2 b^2} \begin{bmatrix} b^2 \cos^2 \varphi + a^2 \sin^2 \varphi & (b^2 - a^2) \cos \varphi \sin \varphi \\ (b^2 - a^2) \cos \varphi \sin \varphi & a^2 \cos^2 \varphi + b^2 \sin^2 \varphi \end{bmatrix}$$

Using Mathematica[®], the eigenvalues and eigenvectors of Q are

$$\frac{1}{a^2}, \begin{bmatrix} \cos \varphi \\ \sin \varphi \end{bmatrix} \text{ and } \frac{1}{b^2}, \begin{bmatrix} -\sin \varphi \\ \cos \varphi \end{bmatrix}$$

The matrix S that diagonalizes Q contains the eigenvectors of Q

$$S = \begin{bmatrix} \cos \varphi & -\sin \varphi \\ \sin \varphi & \cos \varphi \end{bmatrix}$$

$$S^T Q S = A = \begin{bmatrix} 1/a^2 & 0 \\ 0 & 1/b^2 \end{bmatrix}$$

from this, we see $S = R =$ rotation that goes from the principal to the non-standard coordinate system (and the axes of the coordinate system are rotated in the opposite direction (I think!!)).

Plotting 2-D ellipses in Mathematica[®]: (aniso_vibration_ellipsoid.nb)

the basic equation is of the form

$$px^2 + 2qxy + ry^2 = 1$$

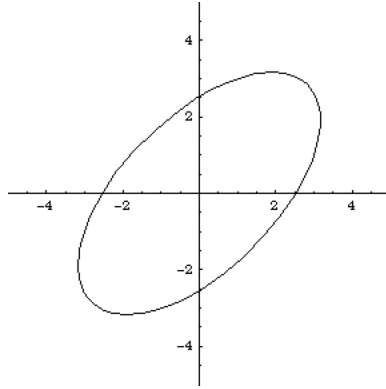
$$x = R \cos \varphi; y = R \sin \varphi$$

$$R = 1 / \sqrt{p \cos^2 \varphi + 2q \cos \varphi \sin \varphi + r \sin^2 \varphi}$$

To plot an ellipse rotated +45° from the standard setting with the major axis along x, the following Mathematica[®] script may be used (in compressed form):

```
a = 4. asq = a^2 b = 2. bsq = b^2
thet = 45. Degree cthet = Cos[thet] sthet = Sin[thet]
p = (bsq*cthet^2 + asq*sthet^2)/(asq*bsq) (= 0.15625)
q = (bsq - asq)*sthet*cthet/(asq*bsq) (= -0.09375)
r = (bsq*sthet^2 + asq*cthet^2)/(asq*bsq) (= 0.15625)
```

```
ParametricPlot[{Cos[ang]/Sqrt[p*Cos[ang]^2 + r*Sin[ang]^2 + 2*q*Cos[ang]*Sin[ang]],
Sin[ang]/ Sqrt[p*Cos[ang]^2 + r*Sin[ang]^2 + 2*q*Cos[ang]*Sin[ang]]}, {ang, 0, 2*Pi},
PlotRange -> {{-5, 5}, {-5, 5}}, AspectRatio -> 1]
```



General equation of an ellipse (see discussion in Wikipedia)

The general equation for an ellipse in the Cartesian plane is

$$Ax^2 + Bxy + Cy^2 + Dx + Ey + F = 0$$

where all the coefficients are real and $B^2 - 4AC < 0$. In the example above

$$B^2 - 4AC = 4q^2 - 4pr = -4a^2b^2 < 0$$

Thermal Ellipsoids

If an atom vibrates around $x = 0$ in a harmonic potential of energy

$$E = \alpha x^2$$

The mean square displacement of the atom $\langle x^2 \rangle$ may be calculated from the Boltzmann distribution:

$$\begin{aligned} \langle x^2 \rangle &= \frac{\int_{-\infty}^{\infty} x^2 e^{-\alpha x^2/RT} dx}{\int_{-\infty}^{\infty} e^{-\alpha x^2/RT} dx} = \frac{RT}{2\alpha} \\ \Rightarrow \alpha &= \frac{RT}{2\langle x^2 \rangle} \end{aligned}$$

and

$$P(x) = \frac{1}{\sqrt{2\pi\langle x^2 \rangle}} e^{-x^2/2\langle x^2 \rangle}$$

with

$$\left[\int_{-\infty}^{\infty} e^{-px^2} dx = \sqrt{\frac{\pi}{p}}, \text{ and } \int_{-\infty}^{\infty} x^2 e^{-px^2} dx = \frac{1}{2p} \sqrt{\frac{\pi}{p}} \right]$$

Now, the observed electron density distribution around an atom is the convolution of the static distribution with the harmonic distribution; consequently, by the convolution theorem, the observed diffraction pattern is the product of the Fourier transforms for the static and harmonic distributions. The Fourier transform of the static distribution is the scattering factor; the Fourier transform of the harmonic distribution is calculated as follows:

$$F_B(S) = FT(P(x)) = \int_{-\infty}^{\infty} \frac{1}{\sqrt{2\pi\langle x^2 \rangle}} e^{-x^2/2\langle x^2 \rangle} \cos(2\pi Sx) dx$$

$$= e^{-2\pi^2 S^2 \langle x^2 \rangle}$$

with $\int_{-\infty}^{\infty} e^{-a^2 x^2} \cos(bx) dx = \frac{\sqrt{\pi}}{a} e^{-b^2/4a^2}$

In diffraction space $S = d^* = 1/d = 2\sin\theta/\lambda$, so that

$$e^{-2\pi^2 S^2 \langle x^2 \rangle} = e^{-8\pi^2 \langle x^2 \rangle \sin^2 \theta / \lambda^2}$$

$$\equiv e^{-B \sin^2 \theta / \lambda^2}$$

$$\Rightarrow B = 8\pi^2 \langle x^2 \rangle$$

and $\langle x^2 \rangle = \frac{B}{8\pi^2} = \frac{RT}{2\alpha}$

in the extension to three dimensions, the probability distribution may be written in terms of the mean squared displacement along the principal axes $\langle x^2 \rangle$, etc, to give:

$$P(xyz) = \frac{1}{\sqrt{8\pi^3 \langle x^2 \rangle \langle y^2 \rangle \langle z^2 \rangle}} e^{-\frac{1}{2} x^T U x}$$

where $U = \begin{bmatrix} 1/\langle x^2 \rangle & 0 & 0 \\ 0 & 1/\langle y^2 \rangle & 0 \\ 0 & 0 & 1/\langle z^2 \rangle \end{bmatrix}$

Following Dunitz (pp 44-49), an anisotropic vibration in three-dimensions in real space (g) and reciprocal space (G) along the principal axes are given by:

$$g(x_1, x_2, x_3) = \frac{(U_1 U_2 U_3)^{-1}}{(2\pi)^{3/2}} \exp\left(-\left[\left(x_1^2/2U_1^2\right) + \left(x_2^2/2U_2^2\right) + \left(x_3^2/2U_3^2\right)\right]\right)$$

$$G(R_1, R_2, R_3) = \exp\left[-2\pi^2\left(U_1^2 R_1^2 + U_2^2 R_2^2 + U_3^2 R_3^2\right)\right] \equiv \exp[-T]$$

In terms of components along the reciprocal axes (b_i), the thermal ellipsoid T may be written:

$$T = 2\pi^2\left(U_{11}h_1^2b_1^2 + \dots + 2U_{12}h_1h_2b_1b_2 + \dots\right) = 2\pi^2\sum_{ij}U_{ij}h_ih_jb_ib_j$$

The isotropic temperature factor is given by

$$G(R) = \exp\left[-2\pi^2U^2R^2\right] = \exp\left[-8\pi^2U^2\sin^2\vartheta/\lambda^2\right] = \exp\left[-B\sin^2\vartheta/\lambda^2\right]$$

and since

$$R^2(=d^{*2}) = h_1^2b_1^2 + \dots + 2h_1h_2b_1 \cdot b_2 + \dots$$

the equivalent anisotropic temperature factors are $U_{ii} = U^2$ and $U_{ij} = U^2 \cos(b_i b_j)$

In this formalism, the mean square amplitude in the direction of a unit vector with components l_1, l_2, l_3 on the same set of reciprocal lattice vectors is given by (Dunitz, Sands pg. 78):

$$U^2(l_1, l_2, l_3) = l^T U l = \sum_i \sum_j U_{ij} l_i l_j$$

In reciprocal space, the general expression in terms of the anisotropic temperature factor tensor is given by (see Dunitz; Stout and Jensen, App. F):

$$\exp\left[-2\pi^2\left(U_{11}h^2a^{*2} + U_{22}k^2b^{*2} + U_{33}l^2c^{*2} + 2U_{12}hka^*b^* + 2U_{13}hla^*c^* + 2U_{23}klb^*c^*\right)\right]$$

or $\exp\left[-\left(\beta_{11}h^2 + \beta_{22}k^2 + \beta_{33}l^2 + 2\beta_{12}hk + 2\beta_{13}hl + 2\beta_{23}kl\right)\right]$

Matrix formulation of the thermal motion probability ellipsoids

ORTEP manual, chapter 6

International Tables, (old) volume IV, pp 314 and following

Let $\phi(\mathbf{X})$ be the probability density function of a trivariate normal (Gaussian) distribution

$$\phi(\vec{X}) = \frac{[\det(M^{-1})]^{1/2}}{(2\pi)^{3/2}} \exp\left[-\frac{1}{2}(\vec{X} - \hat{X})^T M^{-1}(\vec{X} - \hat{X})\right]$$
$$\text{with } M = \begin{bmatrix} \sigma_1^2 & \sigma_1\sigma_2\rho_{12} & \sigma_1\sigma_3\rho_{13} \\ \sigma_1\sigma_2\rho_{12} & \sigma_2^2 & \sigma_2\sigma_3\rho_{23} \\ \sigma_1\sigma_3\rho_{13} & \sigma_2\sigma_3\rho_{23} & \sigma_3^2 \end{bmatrix}$$

and the thermal ellipsoid is given by the quadratic $(\vec{X} - \hat{X})^T M^{-1}(\vec{X} - \hat{X})$

Taking the FT of $\phi(\mathbf{X})$ gives the anisotropic temperature factor coefficient matrix B:

$$\Phi(\vec{T}) = \exp\left[iT^T \hat{X} - \frac{1}{2}T^T M T\right]$$
$$F(\vec{h}) = \sum_j f_j(\vec{h}) \exp[2\pi i \vec{h}^T \hat{X}_j] \exp[-\vec{h}^T B \vec{h}]$$

with $\vec{T} = 2\pi \vec{h}$

$$F(\vec{T}) = \sum_j f_j(T) \exp[2\pi i T^T \hat{X}_j] \exp\left[-\frac{1}{2}T^T \frac{B}{2\pi^2} T\right]$$
$$\Rightarrow M = \frac{B}{2\pi^2} \text{ or } M^{-1} = 2\pi^2 B^{-1}$$

Principal Components of Thermal Ellipsoids (aniso_B_Sands.nb)

Sands, pp 72-78 – note: Sands uses β notation!

Let G = the real space metric tensor, with $G_{ij} = \mathbf{a}_i \cdot \mathbf{a}_j$

and T = the anisotropic temperature factor with $T_{ij} = \beta_{ij}$

The principal components of the thermal ellipsoid are given by the eigenvectors of TG , and the mean square displacement along these directions are the eigenvalues/ $2\pi^2$.

As an illustration, here is the example on pp 73-74 and problem 3-33 of Sands. A monoclinic crystal has unit cell dimensions $a = 8.00 \text{ \AA}$, $b = 10.00 \text{ \AA}$, $c = 9.00 \text{ \AA}$, $\beta = 105.0^\circ$, and values of β_{ij} corresponding to the following G and T matrices:

$$G = \begin{bmatrix} 64. & 0 & -18.63 \\ 0 & 100. & 0 \\ -18.63 & 0 & 81. \end{bmatrix} \quad T = \begin{bmatrix} 0.004 & 0.001 & -0.0005 \\ 0.001 & 0.003 & 0.0007 \\ -0.0005 & 0.0007 & 0.005 \end{bmatrix}$$

$$TG = \begin{bmatrix} 0.265315 & 0.1 & -0.11502 \\ 0.050959 & 0.3 & 0.03807 \\ -0.12515 & 0.07 & 0.414315 \end{bmatrix}$$

The eigenvalues of TG are 0.4817, 0.3499, 0.1481, which correspond to root mean displacements along the principal directions of 0.156 \AA , 0.133 \AA , 0.087 \AA . The eigenvalues, in column form are

$$v_1 = \begin{bmatrix} 0.4460 \\ -0.0620 \\ -0.8929 \end{bmatrix} \quad v_2 = \begin{bmatrix} 0.5697 \\ 0.7799 \\ 0.2592 \end{bmatrix} \quad v_3 = \begin{bmatrix} -0.7924 \\ 0.3844 \\ -0.4736 \end{bmatrix}$$

Note: that these are in fractional coordinates, with lengths of “1”. To reduce to vectors of length 1 \AA , these vectors are divided through by the length (in \AA):

$$\hat{v}_1 = \frac{v_1}{(v_1^T G v_1)^{1/2}} = \begin{bmatrix} 0.0464 \\ -0.0064 \\ -0.0928 \end{bmatrix} \quad \hat{v}_2 = \begin{bmatrix} 0.0631 \\ 0.0864 \\ 0.0287 \end{bmatrix} \quad \hat{v}_3 = \begin{bmatrix} -0.1030 \\ 0.0500 \\ -0.0616 \end{bmatrix}$$

These vectors are normalized (in terms of \AA) and orthogonal, as shown by the following relationship:

$$\hat{v}_i^T G \hat{v}_j = \delta_{ij}$$

Ellipsoid of constant probability

Coppens X-ray charge distribution book, Appendix C

Upper limits for the constant in the ellipsoid equation that encloses a given fraction of the electron density may be evaluated by finding the radius $r = C$ for which the enclosed area/volume inside the probability distribution is equal to the desired fraction

$$\begin{aligned}
 g_1(x) &= (a/\pi)^{1/2} \exp[-ax^2] \\
 g_2(x, y) &= (a/\pi) \exp[-a(x^2 + y^2)] = (a/\pi) \exp[-ar^2] \\
 g_3(x, y, z) &= (a/\pi)^{3/2} \exp[-a(x^2 + y^2 + z^2)] = (a/\pi)^{3/2} \exp[-ar^2] \\
 \int_0^c g(r) dV &= P(C)
 \end{aligned}$$

The bounding ellipsoid is defined by the equation $x^T U x = C^2$, where representative values of C are given below (ellipsoid_prob.nb)

P(C)	1-D probability	2-D probability	3-D probability
0.50	0.67449	1.17741	1.53817
0.90	1.64485	2.14597	2.50028

For the two-dimensional example, the explicit integration of the probability distribution for the ellipsoid in the standard setting may be shown:

$$\begin{aligned}
 \frac{x^2}{a^2} + \frac{y^2}{b^2} &= C^2 \\
 P(C) &= \frac{1}{\sqrt{4\pi^2 a^2 b^2}} \iint \exp\left[-\frac{1}{2}\left(\frac{x^2}{a^2} + \frac{y^2}{b^2}\right)\right] dx dy \\
 &= \frac{4}{\sqrt{4\pi^2 a^2 b^2}} \int_0^{aC} \exp\left[-\frac{1}{2}\left(\frac{x^2}{a^2}\right)\right] \left\{ \int_0^{b\sqrt{C^2 - (x/a)^2}} \exp\left[-\frac{1}{2}\left(\frac{y^2}{b^2}\right)\right] dy \right\} dx
 \end{aligned}$$

The factor of 4 comes from only integrating over one quadrant of the ellipse.

Mathematica®: `(4./(2.*Pi*a*b))*NIntegrate[Exp[-(x^2)/(2.*a^2)]*Exp[-(y^2)/(2.*b^2)], {x, 0, a*c}, {y, 0, b*Sqrt[c^2 - (x/a)^2]}`

g tensors

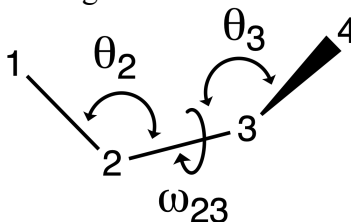
The EPR g tensor is defined in terms of the principal axes as follows:

$$g^2 = x^T G x$$
$$G = \begin{bmatrix} g_x^2 & 0 & 0 \\ 0 & g_y^2 & 0 \\ 0 & 0 & g_z^2 \end{bmatrix}$$

The geometry of 2Fe2S and 4Fe4S clusters

reference: J.D. Dunitz “X-ray Analysis and the Structure of Organic Molecules” Cornell (1979), chapter 9 “Geometric Constraints in Cyclic Molecules”

The consequences of geometric constraints on the conformations of cyclic species like the 2Fe:2S rhomb are beautifully articulated in the Dunitz chapter. For a 4 atom chain, the basic unit of structure consists of 4 points that can be considered to form an irregular tetrahedron. Following Dunitz’ analysis, the separation d_{14} between atoms 1 and 4 will depend on the intervening 3 bond distances, 2 bond angles and 1 torsion angle as follows:



$$d_{14}^2 = d_{12}^2 + d_{23}^2 + d_{34}^2 - 2d_{12}d_{23}\cos\vartheta_2 - 2d_{23}d_{34}\cos\vartheta_3 + 2d_{12}d_{34}(\cos\vartheta_2\cos\vartheta_3 - \sin\vartheta_2\sin\vartheta_3\cos\omega_{23})$$

Bonding between atoms 1 and 4 yields a cyclic molecule that imposes constraints on the geometrical parameters since d_{14} is now equal to the bond distance. For an equilateral four-membered ring (all bond distances equaling d), there are only two independent bond angles and the intervening torsion angle, and the symmetry of the ring must be at least C_{2v} . These parameters must then satisfy the following relationship:

$$d^2 = d^2(3 - 2\cos\vartheta_2 - 2\cos\vartheta_3 + 2\cos\vartheta_2\cos\vartheta_3 - 2\sin\vartheta_2\sin\vartheta_3\cos\omega_{23})$$

$$\cos\omega_{23} = \frac{1 - \cos\vartheta_2 - \cos\vartheta_3 + \cos\vartheta_2\cos\vartheta_3}{\sin\vartheta_2\sin\vartheta_3}$$

With the handy trigonometric identity $\tan\frac{\vartheta}{2} = \frac{1 - \cos\vartheta}{\sin\vartheta}$, this reduces to

$$\cos\omega \equiv \cos\omega_{23} = \frac{(1 - \cos\vartheta_2)(1 - \cos\vartheta_3)}{\sin\vartheta_2\sin\vartheta_3} = \tan\frac{\vartheta_2}{2}\tan\frac{\vartheta_3}{2}$$

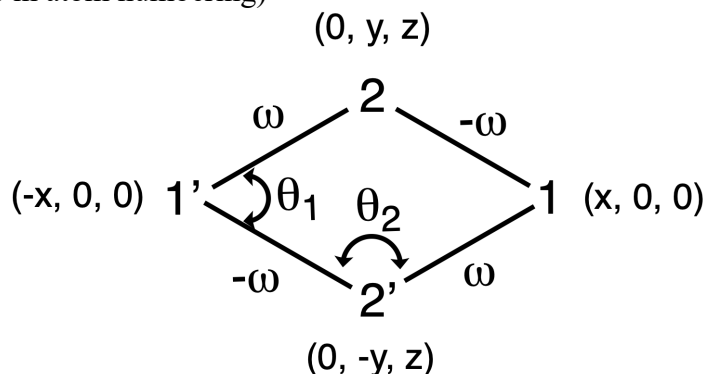
Note that the magnitude of the torsion angle is the same for all bonds when the bond distances are equal. When the bond angles are also equal, the underlying symmetry is at least D_{2d} , and

$$\cos\omega = \tan^2\frac{\vartheta}{2}$$

When $\theta = 90^\circ$, $\omega = 0^\circ$ and the ring is planar (point group D_{4h}). As Dunitz demonstrates, even small deviations from $\theta = 90^\circ$ lead to appreciable non-planarity in the ring, since $\omega \sim 15.1(\delta\vartheta)^{\frac{1}{2}}$ (in degrees), so that a 1° change in θ corresponds to a torsion angle change of $\sim 15^\circ$. For cyclobutene with $\theta = 88^\circ$, $\omega \sim 21.2^\circ$.

The non-planarity of 4-member rings can be expressed not only in terms of the torsion angle, but also the dihedral angle Ψ corresponding to the angle between the normals to planes sharing a

common diagonal – either the 1 – 1' or 2 – 2' diagonals in the following equilateral four-membered ring (note the change in atom numbering)



For simplicity, we'll take the bond distance d as unity. Using the law of cosines, the values of x and y may be derived, and z follows from the bond distance (normalization) constraint:

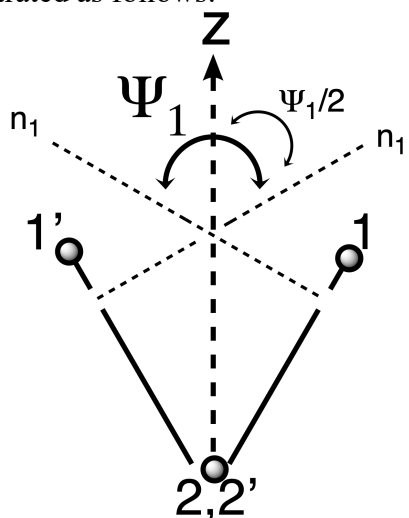
$$x^2 + y^2 + z^2 = 1$$

$$x = \sin(\vartheta_2/2)$$

$$y = \sin(\vartheta_1/2)$$

$$z = \sqrt{1 - \sin^2(\vartheta_1/2) - \sin^2(\vartheta_2/2)}$$

The dihedral angle Ψ_1 between the two planes sharing the 2-2' diagonal (ie – the planes with atoms 1-2-2' and 1'-2-2') may be illustrated as follows:



The normal, n_1 , to the 1-2-2' plane is given by the cross product of the 1-2 and 1-2' bond vectors

$$\begin{aligned}
\{1-2\} &= \begin{Bmatrix} -x & y & z \end{Bmatrix} \\
\{1-2'\} &= \begin{Bmatrix} -x & -y & z \end{Bmatrix} \\
\{1-2\} \times \{1-2'\} &= \begin{Bmatrix} \hat{x} & \hat{y} & \hat{z} \\ -x & y & z \\ -x & -y & z \end{Bmatrix} = \begin{Bmatrix} 2yz & 0 & 2xy \end{Bmatrix} \\
\hat{n}_1 &= \frac{\{1-2\} \times \{1-2'\}}{|\{1-2\} \times \{1-2'\}|} = \frac{1}{\sin \vartheta_1} \begin{Bmatrix} 2yz & 0 & 2xy \end{Bmatrix} \\
\cos \frac{\Psi_1}{2} &= \hat{z} \cdot \hat{n}_1 = \frac{2xy}{\sin \vartheta_1} = \frac{2 \sin(\vartheta_2/2) \sin(\vartheta_1/2)}{\sin \vartheta_1} \\
&\text{equivalently} \\
\cos \frac{\Psi_2}{2} &= \hat{z} \cdot \hat{n}_2 = \frac{2 \sin(\vartheta_2/2) \sin(\vartheta_1/2)}{\sin \vartheta_2} \\
\cos \frac{\Psi_1}{2} \cos \frac{\Psi_2}{2} &= \frac{4 \sin^2(\vartheta_2/2) \sin^2(\vartheta_1/2)}{\sin \vartheta_1 \sin \vartheta_2} = \frac{(1 - \cos_1)(1 - \cos_2)}{\sin \vartheta_1 \sin \vartheta_2} \quad (\text{with } 2 \sin^2 \vartheta = 1 - \cos \vartheta) \\
&= \tan(\vartheta_1/2) \tan(\vartheta_2/2) = \cos \omega \quad \left(\text{with } \tan(\vartheta/2) = \frac{(1 - \cos)}{\sin \vartheta} \right) \\
\text{with } \cos \frac{\Psi_1}{2} &= \frac{\sin \vartheta_1}{\sin \vartheta_2} \cos \frac{\Psi_2}{2} \\
\text{so } \cos^2 \frac{\Psi_1}{2} &= \frac{\sin \vartheta_2}{\sin \vartheta_1} \cos \omega
\end{aligned}$$

For the D_{2d} structures with all bond angles equal, we have

$$\cos^2 \frac{\Psi}{2} = \tan^2 \frac{\vartheta}{2} = \cos \omega$$

Analysis of 2Fe2S and 4Fe4S clusters – based on PDB survey conducted ~2002
FeS_dihedral_calcs_15October2021.nb

parameter	2Fe2S (obs)	(calc)	4Fe4S (obs)	(calc)
Fe-S	2.227 Å		2.286 Å	
S-Fe-S (θ_1)	104.247 °		105.565 °	
Fe-S-Fe (θ_2)	75.511 °		71.677 °	
Fe-Fe (1-1')	2.728 Å	2.727 Å	2.676 Å	2.677 Å
S-S (2-2')	3.516 Å	3.516 Å	3.639 Å	3.641 Å
ω		5.346 °	18.051 °	
ψ_1		6.559 °	21.594 °	
ψ_2		3.516 °	29.082	

Structural parameters for tetrahedrally-symmetric clusters

Reference L.L. Tan, R.H. Holm and S.C. Lee Polyhedron 58, 206-17 (2013) “Structural analysis of cubane-type iron clusters”

As described in Tan, et al., a useful reference geometry for a [4Fe4S] cluster is the T_d symmetric core which for $[M_4Q_4]$ clusters can be described by two independent parameters m and q with

- the M atoms at the vertices $\{(m, m, m), (-m, -m, m), (m, -m, -m), (-m, m, -m)\}$
- the Q atoms at $\{(-q, -q, -q), (q, q, -q), (-q, q, q), (q, -q, q)\}$

With $M = Fe$ and $Q = S$, m and q can be calculated from equations (8) and (9) of Tan et al.

$$\text{Eq. 8 } q = d_{MQ} \sin(\vartheta_M/2) / \sqrt{2}$$

$$\text{Eq. 9 } m = \left[q + d_{MQ} \sqrt{1 + 2 \cos \vartheta_M} \right] / 3$$

where d_{MQ} and $\theta_M =$ the Fe-S distance (2.286 Å) and S-Fe-S angle (105.565 °), respectively. From these relationships, m and q are calculated to be 0.9478 Å and 1.2873 Å, respectively. With these values for m and q , other geometrical parameters can be calculated from Eqs 3-13:

parameter	formula	obs	calc
M-Q distance d_{MQ}	$d_{MQ} = \sqrt{3m^2 - 2mq + 3q^2}$	2.286 Å (input)	
M...M separation	$d_M = 2\sqrt{2}m$	2.676 Å	2.6807
Q...Q separation	$d_Q = 2\sqrt{2}q$	3.639 Å	3.6409
Q-M-Q angle θ_M	$\cos \vartheta_M = (d_{MQ}^2 - 4q^2) / d_{MQ}^2$	105.565 ° (input)	
M-Q-M angle θ_Q	$\cos \vartheta_Q = (d_{MQ}^2 - 4m^2) / d_{MQ}^2$	71.677 °	71.794 °
$V(M_4)$	$8m^3/3$		2.270 Å ³
$V(M_4Q_4)$	$V(M_4) + 4V(MQ_3) = 8qm$		9.250 Å ³

Section VII: Lorentz and Polarization Factors

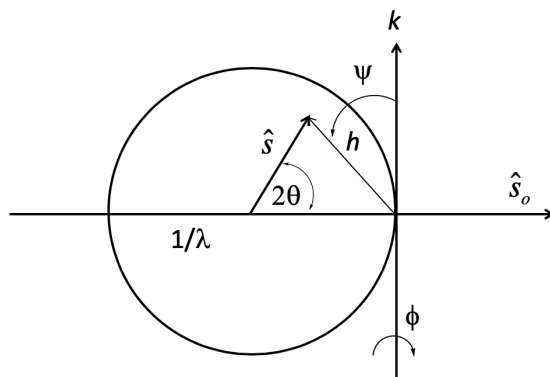
Lorentz Factor

J.D. Dunitz, X-ray Analysis and the Structure of Organic Molecules (1979) Cornell, pp. 281-287
International Tables for X-ray Crystallography, vol II, pp. 266

The time that a reflection spends in the diffracting position depends on various factors such as the mosaic spread, beam divergence and spectral purity, as well as a geometric factor termed the Lorentz factor. The Lorentz factor, L , takes into account the direction that a reflection passes through the Ewald sphere. The more nearly this direction is to the normal of the Ewald sphere, the shorter the diffraction time; conversely, the more obliquely a reflection passes through the Ewald sphere, the longer it takes for the reflection to pass through. The Lorentz factor is defined by angular rotation of the crystal, Ω , divided by the component of the reflection velocity normal to the Ewald sphere, v_n , i.e., $L = \Omega/v_n$. Reflections with relatively low v_n (corresponding to oblique passage through the Ewald sphere), have large L . All other factors being equal, the integrated intensity of a reflection that passes obliquely through the Ewald sphere will be larger, since it is in the diffracting position longer. As a consequence, the measured intensity, I_{obs} , of a reflection needs to be corrected for this effect during data processing before converting to F_{obs} :

$$|F_{obs}|^2 \propto I_{obs}/L$$

To calculate the Lorentz factor, the following representation of the Ewald sphere is used, viewed down the direction normal to both the X-ray beam direction, s_o (coinciding with the x-axis) and the rotation axis (spindle), k , (coinciding with the y-axis). This geometry is the so-called “normal-beam method” in the International Tables, since the rotation axis is perpendicular to the incident X-ray beam. The radius of the Ewald sphere is $1/\lambda$, the angle between the scattered beam, s , and the incident beam is 2θ , the angle between the rotation axis and the diffraction vector h is ψ , the rotation angle about the spindle is ϕ , and the angular rotation rate about the spindle, Ω .



The velocity with which the tip of the reflection vector, h , moves as the spindle rotates is:

$$\frac{d\vec{h}}{dt} = \Omega \frac{d\vec{h}}{d\phi}$$

The matrix for rotation about k is:

$$\begin{bmatrix} \cos\phi & 0 & -\sin\phi \\ 0 & 1 & 0 \\ \sin\phi & 0 & \cos\phi \end{bmatrix}$$

If the starting rotation angle is arbitrarily assigned to 0° , then the change, δh , in h for rotation by an amount $\delta\phi$ is given by:

$$\delta\vec{h} = \left[\begin{pmatrix} \cos\delta\phi & 0 & -\sin\delta\phi \\ 0 & 1 & 0 \\ \sin\delta\phi & 0 & \cos\delta\phi \end{pmatrix} - \begin{pmatrix} 1 & 0 & 0 \\ 0 & 1 & 0 \\ 0 & 0 & 1 \end{pmatrix} \right] \begin{bmatrix} h \\ k \\ l \end{bmatrix}$$

as $\delta\phi \rightarrow 0$, then

$$\begin{aligned} \delta\vec{h} &= \left[\begin{pmatrix} 1 & 0 & -\delta\phi \\ 0 & 1 & 0 \\ \delta\phi & 0 & 1 \end{pmatrix} - \begin{pmatrix} 1 & 0 & 0 \\ 0 & 1 & 0 \\ 0 & 0 & 1 \end{pmatrix} \right] \begin{bmatrix} h \\ k \\ l \end{bmatrix} \\ &= \delta\phi \begin{pmatrix} 0 & 0 & -1 \\ 0 & 0 & 0 \\ 1 & 0 & 0 \end{pmatrix} \begin{bmatrix} h \\ k \\ l \end{bmatrix} \\ &= \delta\phi \begin{bmatrix} -l \\ 0 \\ h \end{bmatrix} = \delta\phi [\vec{h} \times \hat{k}] \end{aligned}$$

where the last step follows from the definition of the cross product:

$$\vec{h} \times \hat{k} = \begin{vmatrix} x & y & z \\ h & k & l \\ 0 & 1 & 0 \end{vmatrix}$$

Hence, the velocity that the h vector moves through the Ewald sphere is given by:

$$\Omega \frac{d\vec{h}}{dt} = \Omega (\vec{h} \times \hat{k})$$

The component, v_n , of the velocity that is normal to the Ewald sphere at h (where the normal is in the direction of the diffracted ray s) is given by the triple product:

$$v_n = \Omega (\vec{h} \times \hat{k}) \cdot \hat{s}$$

The triple product $a \times b \cdot c$ is equivalent to the volume of the parallelepiped defined by the vectors a , b and c , permuted in any fashion so as to keep the same hand, ie

$$a \times b \cdot c = c \cdot a \times b$$

$$c \times a \cdot b = b \cdot c \times a$$

$$b \times c \cdot a = a \cdot b \times c$$

Using these relationships, one can derive the following expression for v_n :

$$\Omega(\vec{h} \times \hat{k}) \cdot \hat{s} = \Omega \hat{k} \cdot (\hat{s} \times \vec{h})$$

$$\begin{aligned} \text{now, } \frac{\hat{s}_o}{\lambda} + \vec{h} &= \frac{\hat{s}}{\lambda} \Rightarrow \hat{s}_o + \lambda \vec{h} = \hat{s} \\ &= \Omega \hat{k} \cdot ((\hat{s}_o + \lambda \vec{h}) \times \vec{h}) \\ &= \Omega \hat{k} \cdot (\hat{s}_o \times \vec{h}) \\ &= \Omega (\hat{k} \times \hat{s}_o) \cdot \vec{h} \end{aligned}$$

$$v_n = \Omega h_z$$

where h_z is the component of \vec{h} along z

Hence, the Lorentz factor, L, is given by:

$$L = \frac{\Omega}{v_n} = 1 / h_z$$

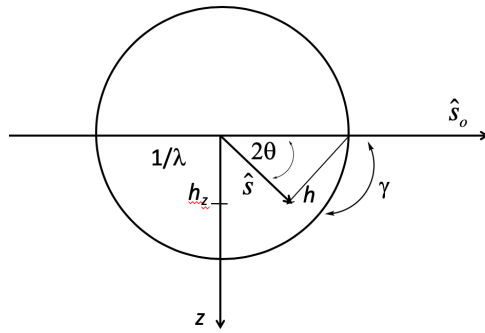
From our definitions of angles in the Ewald sphere, this can be reduced to functions of θ and ψ :

$$\begin{aligned} |h^2| &= h_x^2 + h_y^2 + h_z^2 \\ \left(\frac{2 \sin \theta}{\lambda}\right)^2 &= \left(\frac{2 \sin \theta}{\lambda}\right)^2 [\sin^2 \theta + \cos^2 \psi] + h_z^2 \\ h_z &= \left(\frac{2 \sin \theta}{\lambda}\right) [1 - \sin^2 \theta - \cos^2 \psi]^{1/2} \\ h_z &= \left(\frac{2 \sin \theta}{\lambda}\right) [\cos^2 \theta - \cos^2 \psi]^{1/2} \end{aligned}$$

The Lorentz factor is the reciprocal of this; neglecting λ gives:

$$L = \frac{1}{\sin \theta [\cos^2 \theta - \cos^2 \psi]^{1/2}}$$

Another, equivalent representation can be found as follows, using alternate angular definitions. Let $\pi/2 - \nu$ be the angle between the rotation axis k (perpendicular to the plane of the page/screen in the figure below) and the diffracted ray, s ; and let γ be the projection of 2θ in the xz plane:



Basically, ν and γ are types of spherical polar angles, so that the length of h_z can be expressed (recalling that the length of s is $1/\lambda$):

$$\begin{aligned}
 h_z &= \frac{1}{\lambda} \sin\left(\frac{\pi}{2} - \nu\right) \sin \gamma \\
 &= \frac{1}{\lambda} \cos \nu \sin \gamma \\
 &\text{and} \\
 L &= \frac{1}{\cos \nu \sin \gamma}
 \end{aligned}$$

Polarization Factor

This discussion is based on the analysis of anisotropic anomalous scattering presented elsewhere in this document.

For isotropic scattering in the absence of X-ray absorption, the effective scattering factor for a particular atom is given by (Templetons, 1982; Fanchon & Hendrickson, 1990; Schiltz and Bricogne, 2008)

$$\text{Eq. 1} \quad g = (\hat{p}' \cdot \hat{p}) f_0 \equiv \sqrt{P} f_0$$

where \hat{p} and \hat{p}' are the polarization directions of the incident and scattered wave, respectively, f_0 is the isotropic atomic scattering factor (a function of the scattering angle 2θ) and P is the polarization factor for intensities. Hence for isotropic scattering in the absence of absorption, P is independent of the nature of the scatterer and the polarization correction can be applied during data reduction. (in this analysis, we adopt the convention of Schiltz and Bricogne (2008) for the ordering of the incident and scattered wave in Eq. 1; the order is switched in the earlier studies ((Templetons, 1982; Fanchon & Hendrickson, 1990)).

For calculation of polarization factors, we use the laboratory frame and define the geometry of the diffraction experiment so that \hat{z} and \hat{x} are the directions of the incident beam and the direction of polarization, respectively. In our typical synchrotron experiment, the crystal is rotated around the direction of polarization (\hat{x}); \hat{y} is defined from the directions of the \hat{x} and \hat{z} axis (Figure S1).

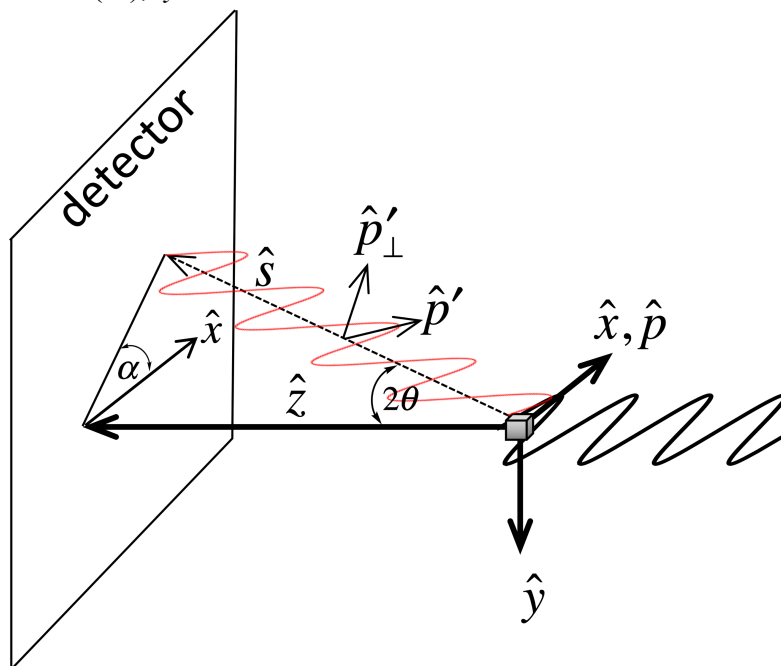


Figure S1. Diffraction geometry used for the polarization analysis

The direction of the scattered wave, \hat{s} , is described according to the XDS convention by two angles (Kabsch, 1977, 2010): the azimuthal angle α and the polar angle β , where $\beta = 2\theta$, such that

Eq. 3 $\hat{s} = \{\cos \alpha \sin 2\vartheta, \sin \alpha \sin 2\vartheta, \cos 2\vartheta\}$

The polarization factor P for intensities is proportional to $\sin^2 \delta$, where δ is the angle between \hat{p} and \hat{s} (Dunitz book)

Eq. 4 $P \propto \sin^2 \delta = 1 - \cos^2 \delta = 1 - (\hat{s} \cdot \hat{p})^2$

It is instructive to evaluate P for the general scattering case, defining the polarization component in the horizontal and vertical planes as follows:

Eq. 5 $\hat{p}_H = \{1, 0, 0\}$
 $\hat{p}_V = \{0, 1, 0\}$

With \hat{s} defined as above, the polarization along the horizontal and vertical directions is given by

Eq. 6 $P_H = 1 - (\hat{s} \cdot \hat{p}_H)^2 = 1 - \cos^2 \alpha \sin^2 2\theta$
 $P_V = 1 - (\hat{s} \cdot \hat{p}_V)^2 = 1 - \sin^2 \alpha \sin^2 2\theta$

For unpolarized radiation, the polarization factor is the average of the components along the horizontal and vertical direction (Dunitz)

Eq. 7 $P = \frac{1}{2}(P_H + P_V) = \frac{1}{2}(1 + \cos^2 2\theta)$

P_H is the polarization factor applicable to synchrotron data when the X-ray beam is 100% linearly polarized along the x-axis.

Section VIII: Anomalous Scattering

Classical Description of Scattering: Anomalous Dispersion

References: Eisenberg & Crothers, pp. 535-546

James "Optical Principles of the Diffraction of X-rays", Chap. IV

The motion of an electron in an atom, in the presence of an electromagnetic field, may be classically described by Newton's second law:

$$m \frac{d^2x}{dt^2} = \sum \text{forces}$$
$$= qE_o e^{i\omega t} - kx - \eta \frac{dx}{dt}$$

where x = position of the electron at time t

m = mass of the electron

q = charge of the electron

E_o = amplitude of the electric field

ω = frequency of electromagnetic radiation

k = force constant between electron and nucleus,
assuming Hooke's law-type behavior

η = damping coefficient. The damping force is due to interactions
between the electron and scattered radiation, and is proportional
to the velocity of the electron.

This equation represents a forced, damped harmonic oscillator, and has the following solution:

$$x(t) = \frac{qE_o}{m} \frac{e^{i\omega t}}{\omega_o^2 - \omega^2 + i \frac{\eta\omega}{m}}$$

where $\omega_o^2 = \frac{k}{m}$ = natural frequency of the electron

The dipole moment of this system is given by:

$$p = qx$$

The amplitude, A , of the scattered wave at unit distance in the equatorial plane is given by

$$A = \frac{\omega^2}{c^2} p = \frac{q^2}{mc^2} \frac{\omega^2 E_o}{\omega_o^2 - \omega^2 + i \frac{\eta\omega}{m}}$$

For a free electron, $\omega_o = \eta = 0$ and $A \equiv A_o = -\frac{q^2 E_o}{mc^2}$. The negative sign means that the scattered wave is 180° out of phase from the incident wave. The scattering of a bound electron, relative to a free electron, is given by the scattering factor, f :

$$f = \frac{A}{A_o} = \frac{\omega^2}{\omega^2 - \omega_o^2 - i \frac{\eta\omega}{m}}$$

- (i) $\omega^2 \gg \omega_o^2, f = +1$, at high energies, the scattered radiation is 180° phase shifted from the incident wave at high frequencies. This is the usual case in an X-ray diffraction experiment.
- (ii) $\omega^2 \ll \omega_o^2, f = -\left(\frac{\omega^2}{\omega_o^2}\right)$, at low frequencies, the oscillator and incident wave are in phase.
- (iii) $\omega^2 = \omega_o^2, f = i\frac{m\omega}{\eta}$, when the incident radiation is at the natural frequency of the oscillator, the scattered wave is 90° phase shifted from the incident wave.

These relationships can be qualitatively established by examining the behavior of simple oscillating systems, such as a pendulum.

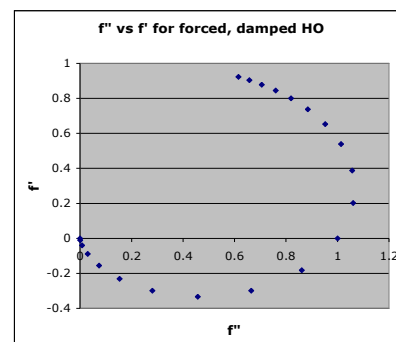
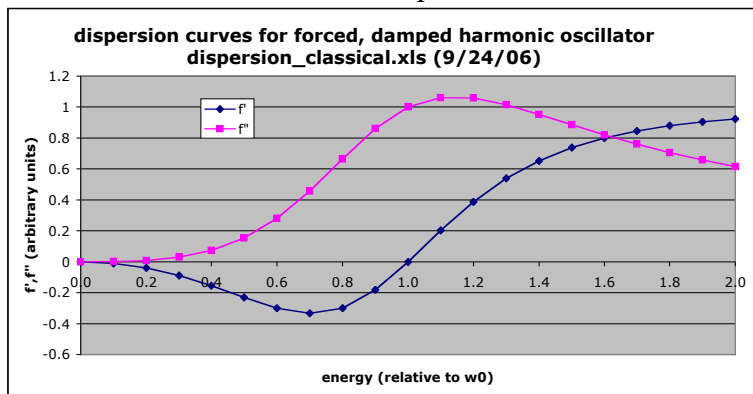
In general, f is a complex number, and may be written as $f = f' + if''$, where:

$$f' = \frac{\omega^2(\omega^2 - \omega_o^2)}{(\omega^2 - \omega_o^2)^2 + \left(\frac{\eta\omega}{m}\right)^2}$$

$$f'' = \frac{\eta\omega^3 / m}{(\omega^2 - \omega_o^2)^2 + \left(\frac{\eta\omega}{m}\right)^2}$$

The f' and f'' terms have important physical significances. f' can be shown to be related to the refractive index, n , and provides the dependence of n on the X-ray wavelength. The dependent of f' (and n) on λ is known as a dispersion relationship. f'' is an absorption term, and can be obtained from measurements of the absorption coefficient, μ , as a function of λ . f' and f'' are not independent, but are related by the Kronig-Kramer's transformation (see below). The description of systems near resonance by these two terms is quite general. In optical spectroscopy, the quantities analogous to f' and f'' are n and ϵ . Similar effects also provide the basis for optical activity measurements using optical rotatory dispersion (ORD, based on Δn) and circular dichroism (CD, based on $\Delta\epsilon$) with polarized light.

Plots of f' and f'' for forced, damped harmonic oscillator with $x = \omega/\omega_0$ and $\eta/m = 1$



Derivation of Kramers-Krönig (KK) Transform

Brian Davies, Integral Transforms and Their Applications, Springer (2002) QA432 .D28

Carrier, Functions of a Complex Variable, pp. 548 and following

D.A.B. Miller 243. Semiconductor Optoelectronic Devices (Winter 2002) web lecture notes

(Beware: there appears to be a fair amount of confusion about signs and the order of $(\omega - \Omega)$)

Bottom line summary of Kramers-Krönig transforms:

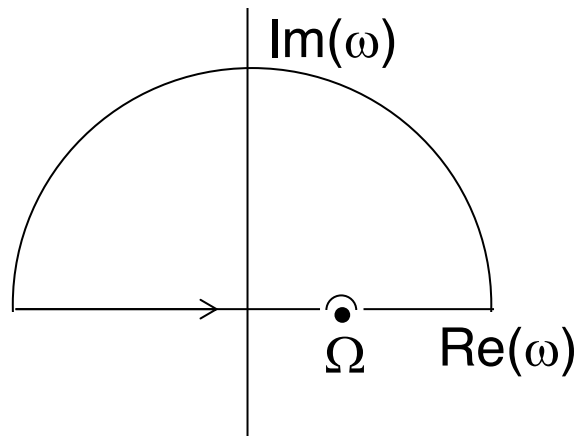
$$f'(\Omega) = \frac{2}{\pi} \int_0^{\infty} \frac{\omega f''(\omega)}{\Omega^2 - \omega^2} d\omega$$

$$f''(\Omega) = -\frac{2\Omega}{\pi} \int_0^{\infty} \frac{f'(\omega)}{\Omega^2 - \omega^2} d\omega$$

Derivation: Assume we have a function $f(\omega)$ (which is complex with real and imaginary parts $f'(\omega)$ and $f''(\omega)$, respectively), where $f(\omega)$ is finite for all ω , there are no singularities (poles) in the half plane $\text{Im}(\omega) > 0$, and $f(\omega) \rightarrow 0$ as $|\omega| \rightarrow \infty$ in the upper half-plane. Then the contour integral equals

$$\oint_C \frac{f(\omega)}{\omega - \Omega} d\omega = 0 = \pi i f(\Omega) + \int_{-\infty}^{\infty} \frac{f(\omega)}{\omega - \Omega} d\omega$$

when evaluated along the contour shown below (since the contour integral = 0 as $f(\omega)$ has no poles inside the contour; $f(\omega)$ vanishes along the outer contour and the last part comes from the residue theorem evaluated as one half the residue at $\omega = \Omega$)



Equating the real and imaginary parts of this relationship gives:

$$f'(\Omega) = -\frac{1}{\pi} \int_{-\infty}^{\infty} \frac{f''(\omega)}{\omega - \Omega} d\omega$$

$$f''(\Omega) = \frac{1}{\pi} \int_{-\infty}^{\infty} \frac{f'(\omega)}{\omega - \Omega} d\omega$$

where the integral denotes the "Cauchy Principal Value" which takes into account the singularity at $\omega = \Omega$. These expressions relate the real and imaginary components of f and represent one form of the Kramers-Krönig relations. This specific form is also known as a "Hilbert Transform".

Since $\rho(r)$ is real, then $f(\omega)$, the Fourier transform of $\rho(r)$, has the property $f(\omega) = f^*(\omega)$ or

$$f(\omega) = f(-\omega) \text{ and } f'(\omega) = -f'(-\omega)$$

These properties can be used to convert this version of the KK relations to a more familiar form as follows.

$$\begin{aligned} f'(\Omega) &= -\frac{1}{\pi} \int_{-\infty}^{\infty} \frac{f''(\omega)}{\omega - \Omega} d\omega = \frac{1}{\pi} \int_{-\infty}^{\infty} \frac{f''(\omega)}{\Omega - \omega} d\omega = \frac{1}{\pi} \int_0^{\infty} \frac{f''(\omega)}{\Omega - \omega} d\omega + \frac{1}{\pi} \int_{-\infty}^0 \frac{f''(\omega)}{\Omega - \omega} d\omega \\ &= \frac{1}{\pi} \int_0^{\infty} \frac{f''(\omega)}{\Omega - \omega} d\omega - \frac{1}{\pi} \int_0^{\infty} \frac{f''(-\omega)}{\Omega + \omega} d\omega \quad (\text{replacing } \omega \text{ by } -\omega) \\ &= \frac{1}{\pi} \int_0^{\infty} \frac{f''(\omega)}{\Omega - \omega} d\omega + \frac{1}{\pi} \int_0^{\infty} \frac{f''(\omega)}{\Omega + \omega} d\omega = \frac{1}{\pi} \int_0^{\infty} \frac{f''(\omega)}{\Omega - \omega} d\omega - \frac{1}{\pi} \int_0^{\infty} \frac{f''(\omega)}{\Omega + \omega} d\omega \\ &= \frac{1}{\pi} \int_0^{\infty} f''(\omega) \left(\frac{1}{\Omega - \omega} - \frac{1}{\Omega + \omega} \right) d\omega = \frac{1}{\pi} \int_0^{\infty} f''(\omega) \left(\frac{(\Omega + \omega) - (\Omega - \omega)}{(\Omega - \omega)(\Omega + \omega)} \right) d\omega \\ &= \frac{2}{\pi} \int_0^{\infty} \frac{\omega f''(\omega)}{\Omega^2 - \omega^2} d\omega \end{aligned}$$

In a similar fashion, the corresponding transform relating f'' and f' may be derived:

$$\begin{aligned} f''(\Omega) &= \frac{1}{\pi} \int_{-\infty}^{\infty} \frac{f'(\omega)}{\omega - \Omega} d\omega \\ &= -\frac{2\Omega}{\pi} \int_0^{\infty} \frac{f'(\omega)}{\Omega^2 - \omega^2} d\omega \end{aligned}$$

Some useful Hilbert transforms from <http://mathworld.wolfram.com/HilbertTransform.html> and "Tables of Integral Transforms" A Erdélyi, editor of "Bateman Integral Project", QA351.B22 (1954), SFL).

$f(x)$	$\frac{1}{\pi} \int_{-\infty}^{\infty} \frac{f(x)}{(x-y)} dy$
$f(x)$	$g(y)$
$g(x)$	$-f(y)$
$f(ax), f(-ax), f(x+a), f'(x)$	$g(ay), -g(-ay), g(y+a), g'(y)$
$xf(x)$	$yg(y) + \frac{1}{\pi} \int_{-\infty}^{\infty} f(x) dx$
$\frac{1}{x^2 + a^2}$	$-\frac{y}{a(y^2 + a^2)}$
$\frac{x}{x^2 + a^2}$	$-\frac{a}{y^2 + a^2}$
e^{ix}	ie^{-iy}
$\frac{\sin x}{x}$	$\frac{\cos y - 1}{y}$
$\delta(x)$	$-(\pi y)^{-1}$
e^{-x^2}	$-\frac{2y}{\sqrt{\pi}} {}_1F_1\left(1; \frac{3}{2}; -y^2\right)$

Idealized form of $\Delta f'$, $\Delta f''$ curves (James, chapter 4, pp 146+)

f'' curves can be derived from the atomic absorption coefficient of different materials, which empirically has been found to vary above the absorption edge (ω_K for the K edge) as ω^{-3} (Eq. 4.32)

$$\begin{aligned} \mu_a(\omega) &= \frac{A}{\omega^n} = \left(\frac{\omega_K^n}{\omega^n}\right) \mu_a(\omega_K) \quad \text{for } \omega \geq \omega_K \\ &= x^{-n} \mu_a(1) \quad \text{with } x \equiv \omega/\omega_K \quad \text{for } x \geq 1 \end{aligned}$$

where $n = 3$. $\Delta f''$ is related to $\mu_a(\omega)$ through equations 4.39 and 4.41 of James (which are referring to the contribution of a particular K edge to the total absorption):

$$\begin{aligned} \Delta f'' &= \frac{mc}{4\pi e^2} \omega \mu_a(\omega) \\ &= \frac{\pi}{2} \frac{n-1}{x^{n-1}} g_K \quad \text{for } x \geq 1 \\ &= \frac{\pi g_K}{x^2} \quad \text{for } n = 3 \end{aligned}$$

where g_K is the oscillator strength and is expected to be 2 (the number of K electrons) but is measured to be ~ 1.3 . This can be seen from the value of $\Delta f' = g_K \pi$ at the absorption edge ($x = 1$) which is ~ 4 electrons at the K edge peak.

For this form of the absorption spectra, $\Delta f'$ may be evaluated from the KK relation:

$$\begin{aligned}
 f'(\omega_i) &= \frac{2}{\pi} \int_0^{\infty} \frac{\omega f''(\omega)}{\omega_i^2 - \omega^2} d\omega \\
 &= \frac{2}{\pi} \int_0^{\infty} \frac{x f''(x)}{x_i^2 - x^2} dx \quad \text{with } x = \omega / \omega_K \\
 &= 2g_K \int_1^{\infty} \frac{dx}{x(x_i^2 - x^2)} \\
 \text{with } \int \frac{dx}{x(a + cx^2)} &= \frac{1}{2a} \ln \left[\frac{x^2}{a + cx^2} \right] \\
 \Delta f'(x_i) &= \frac{g_K}{x_i^2} \ln |x_i^2 - 1| \quad \text{Eqs. (4.37) and (4.45)}
 \end{aligned}$$

The singularity in $\Delta f'$ reflects the infinitely sharp absorption peak; real systems have absorption peaks with finite width, which broadens the dispersion curve. In general, f' is thought to have a large magnitude at energies where the derivative of the f' vs energy curve is greatest (P. Fuoss 1980 Stanford thesis, pg 74, "Since f' is commonly thought to reflect the derivative of f' we would expect the value of f' derived from the dispersion relation to be very sensitive to the broadening induced by the monochromator resolution.").

Evaluation of f' from f'' by the KK transform

JJ Hoyt, D deFontaine, WK Warburton J. Appl. Cryst. 17, 344-351 (1984)

P Dreier, P Rabe, W Malzfeldt, W Niemann J. Phys. C: Solid State Phys. 17, 3123-3136 (1984)

G Evans, RF Pettifer J. Appl. Cryst. 34, 82-86 (2000) program CHOOCH

Evaluation of the KK transform to generate f' curves from measured values of f'' is complicated by the singularity in the denominator. For energies well removed from the absorption edge, values from quantum mechanical calculations can be used, but experimental measurements are required reproduce the chemical environment, oxidation state, EXAFS effects, etc. of the scatterer. In this regime, the KK transform is numerically evaluated; Hoyt et al (incorporated into CHOOCH) fit the experimental data with a polynomial of degree 5 which is then used to evaluate the transform using a Taylor series expansion for f''. Dreier et al use a linear interpolation between successive measured values of f'' at energies $\omega_1, \dots, \omega_n$, to evaluate the integral by dividing the integration regions into n-1 intervals $I_{i,i+1}(\omega_s)$ that gives the contribution of that interval to f'(ω_s)

$$f'(\omega_i) = \frac{2}{\pi} \int_0^{\infty} \frac{\omega f''(\omega)}{\omega_i^2 - \omega^2} d\omega$$

within each interval (ω_i, ω_{i+1}) approximate $f''(\omega)$ by a linear function

$$f''(\omega) = f''(\omega_i) + \frac{f''(\omega_{i+1}) - f''(\omega_i)}{(\omega_{i+1} - \omega_i)} (\omega - \omega_i) \equiv a_i + b_i \omega$$

with the a's and b's, the KK transform can be evaluated analytically for each interval

$$I_{i,i+1}(\omega_s) = \frac{2}{\pi} \int_{\omega_i}^{\omega_{i+1}} \frac{\omega f''(\omega)}{\omega_s^2 - \omega^2} d\omega$$

$$= -\frac{2}{\pi} \left[\frac{a_i}{2} \ln \left| \frac{\omega_s^2 - \omega_{i+1}^2}{\omega_s^2 - \omega_i^2} \right| + b_i \left(\omega_{i+1} - \omega_i - \frac{\omega_s}{2} \ln \left| \frac{\omega_{i+1} + \omega_s}{\omega_{i+1} - \omega_s} \frac{\omega_i - \omega_s}{\omega_i + \omega_s} \right| \right) \right]$$

"The complete dispersion integral is calculated simply by summation of the $I_{i,i+1}$ from $i = 1$ to $i = n-1$. The integrals $I_{s-1,s}$ and $I_{s,s+1}$ which are not defined are substituted by the integral $I_{s-1,s+1}$. " If the experimental data is not extrapolated to higher and lower energies outside of the measured region, the absolute values of the calculated f' are incorrect (by factors of 2 or more), although "in the centre of the integration interval the energy dependence of the fine structure is only weakly influenced."

Bijvoet Difference (Anomalous Difference) Fourier Maps

(J. Kraut *J. Mol. Biol.* **35**, 511-512 (1968))

When the electron density $\rho(x)$ is a real function, Friedel's law is valid, so that $|F(h)| = |F(\bar{h})|$,

$\alpha(h) = -\alpha(\bar{h})$ and $\rho(x)$ is given by:

$$\begin{aligned}\rho(x) &= \frac{1}{V} \sum_h F(h) e^{-2\pi i h \cdot x} = \frac{1}{V} \sum_h |F(h)| e^{+i\alpha - 2\pi i h \cdot x} \\ &= \frac{2}{V} \sum_{h \geq 0} |F(h)| \cos(\alpha - 2\pi h \cdot x) \\ &= \frac{2}{V} \sum_{h \geq 0} (A \cos(2\pi h \cdot x) + B \sin(2\pi h \cdot x))\end{aligned}$$

since $\cos(A-B) = \cos A \cos B + \sin A \sin B$

When Friedel's law breaks down, an imaginary component of $\rho(x)$ is present at positions corresponding to absorbing atoms. This imaginary component can be calculated by a Bijvoet-difference or anomalous Fourier as introduced by Kraut. We first define phases and amplitudes such that the corresponding electron density is identically zero based on the relationships:

$$\alpha_r(h) = \frac{1}{2}(\alpha(h) - \alpha(\bar{h})) \text{ and } |F_r(h)| = \frac{1}{2}(|F(h)| + |F(\bar{h})|).$$

A difference Fourier synthesis of the form

$$\Delta\rho(x) = \frac{1}{V} \sum_h (|F(h)| - |F_r(h)|) e^{+i\alpha_r(h) - 2\pi i h \cdot x}$$

will have a real part that is identically zero and an imaginary component given by:

$$\begin{aligned}\text{Im}(\Delta\rho(x)) &= \frac{1}{V} \sum_{h \geq 0} (|F(h)| - |F(\bar{h})|) \sin(\alpha_r(h) - 2\pi h \cdot x) \\ &= \frac{1}{V} \sum_{h \geq 0} \Delta_{ano}(h) \sin(\alpha_r(h) - 2\pi h \cdot x) \\ &= \frac{1}{V} \sum_{h \geq 0} \Delta_{ano}(h) \cos((\alpha_r(h) - 90^\circ) - 2\pi h \cdot x) \\ &= \frac{1}{V} \sum_{h \geq 0} \Delta_{ano}(h) (\sin \alpha_r(h) \cos 2\pi h \cdot x - \cos \alpha_r(h) \sin 2\pi h \cdot x) \\ &= \frac{1}{V} \left(\sum_{h \geq 0} B_{ano}(h) \cos 2\pi h \cdot x - A_{ano}(h) \sin 2\pi h \cdot x \right)\end{aligned}$$

So, a Bijvoet difference Fourier giving the "imaginary" (ie, absorbing) scatterers can be calculated with a standard Fourier calculation by subtracting 90° from the protein phases, or equivalently by using $A(h) \equiv B_{ano}(h) = \Delta_{ano}(h) \sin \alpha_r(h)$ and $B(h) \equiv -A_{ano}(h) = -\Delta_{ano}(h) \cos \alpha_r(h)$. This map will have positive peaks at the position of the scatterers if the hand (and phases) are correct; if the

wrong hand is used for the phase calculation, this synthesis will have negative peaks at the inverse positions.

Now, $\Delta_{ano}(h) = -2|\delta_h|\sin(\psi - \alpha_r)$, where $|\delta_h|$ and ψ = the amplitude and phase, respectively from the absorbing atoms. (this is an approximate expression that holds when the contribution of the anomalous scattering to the overall scattering is small). Substituting this expression into the equation for the Bijvoet difference Fourier gives:

$$\begin{aligned} \text{Im}(\Delta\rho(x)) &= \frac{1}{V} \sum_{h \geq 0} \Delta_{ano}(h) \sin(\alpha_r(h) - 2\pi h \cdot x) \\ &= -\frac{2}{V} \sum_{h \geq 0} |\delta_h| \sin(\psi - \alpha_r) \sin(\alpha_r(h) - 2\pi h \cdot x) \\ \text{with } \sin A \sin B &= \frac{1}{2} [\cos(A - B) - \cos(A + B)] \\ &= -\frac{1}{V} \sum_{h \geq 0} |\delta_h| [\cos(\psi + 2\pi h \cdot x - 2\alpha_r) - \cos(\psi - 2\pi h \cdot x)] \\ &= -\frac{1}{V} \sum_{h \geq 0} |\delta_h| \cos(\psi + 2\pi h \cdot x - 2\alpha_r) + \frac{1}{V} \sum_{h \geq 0} |\delta_h| \cos(\psi - 2\pi h \cdot x) \\ &= -\frac{1}{V} \sum_{h \geq 0} |\delta_h| \cos(2\alpha_r - \psi - 2\pi h \cdot x) + \frac{1}{V} \sum_{h \geq 0} |\delta_h| \cos(\psi - 2\pi h \cdot x) \end{aligned}$$

The second term is the inverse Fourier transform of the heavy atom scattering (at half-weight); the first term will be Fourier transform with phase $(2\alpha_r - \psi)$ and amplitude $|\delta_h|$, which should give rise to noise.

Equivalent considerations hold for isomorphous difference Fourier maps, which will give the desired term (at half weight) and noise terms. This analysis is detailed in section 11.4 of Blundell and Johnson (page 350); the exact expression for isomorphous difference Fourier has three terms, while the approximate expression $\Delta_{iso}(h) = |f_h| \cos(\psi - \alpha_r)$ only has two terms that correspond to the terms in the Bijvoet difference Fourier analysis just presented.

Anisotropic Anomalous Scattering

The treatment of anisotropic anomalous scattering (AAS) is intimately coupled to the polarization directions of the incident and scattered wave, \hat{p} and \hat{p}' , respectively. For isotropic scattering in the absence of X-ray absorption, the effective scattering factor for a particular atom is given by (Templetons, 1982; Fanchon & Hendrickson, 1990; Schiltz and Bricogne, 2008)

$$\text{Eq. 1} \quad g = (\hat{p}' \cdot \hat{p}) f_0 \equiv \sqrt{P} f_0$$

where f_0 is the isotropic atomic scattering factor (a function of the scattering angle 2θ) and P is the polarization factor for intensities. Hence for isotropic scattering in the absence of absorption, P is independent of the nature of the scatterer and the polarization correction can be applied during data reduction. (in this analysis, we adopt the convention of Schiltz and Bricogne (2008) for the ordering of the incident and scattered wave in Eq. 1; the order is switched in the earlier studies ((Templetons, 1982; Fanchon & Hendrickson, 1990)).

Equation derivations and numerical computations in this section were performed with Mathematica[®].

For anisotropic scattering, the scattering factor must be described by a tensor, Φ

$$\text{Eq. 2} \quad g = \hat{p}' \cdot \Phi \hat{p}$$

Near an X-ray absorption edge, the tensor elements are complex with the absorption described by the imaginary components. The key to the AAS analysis is to evaluate the contribution of this term to each reflection for each absorbing atom. As emphasized by the Templetons (1982), a challenge to this calculation is that “To calculate the total amplitude of scattered radiation one must apply this equation to every combination of each polarization component of the incident ray with each polarization component of the scattering ray, and then combine terms with attention to polarization and phase”.

In this analysis, we make the simplifying assumption that the X-rays are 100% linearly polarized in the plane of the synchrotron ring. We use the laboratory frame and define the geometry of the diffraction experiment so that \hat{z} and \hat{x} are the directions of the incident beam and the direction of polarization, respectively. For the experiments in this paper, the crystal is rotated around the direction of polarization (\hat{x}); \hat{y} is defined from the directions of the \hat{x} and \hat{z} axis (Figure S1). This analysis of the polarization factor also appears in the section with the Lorentz factor.

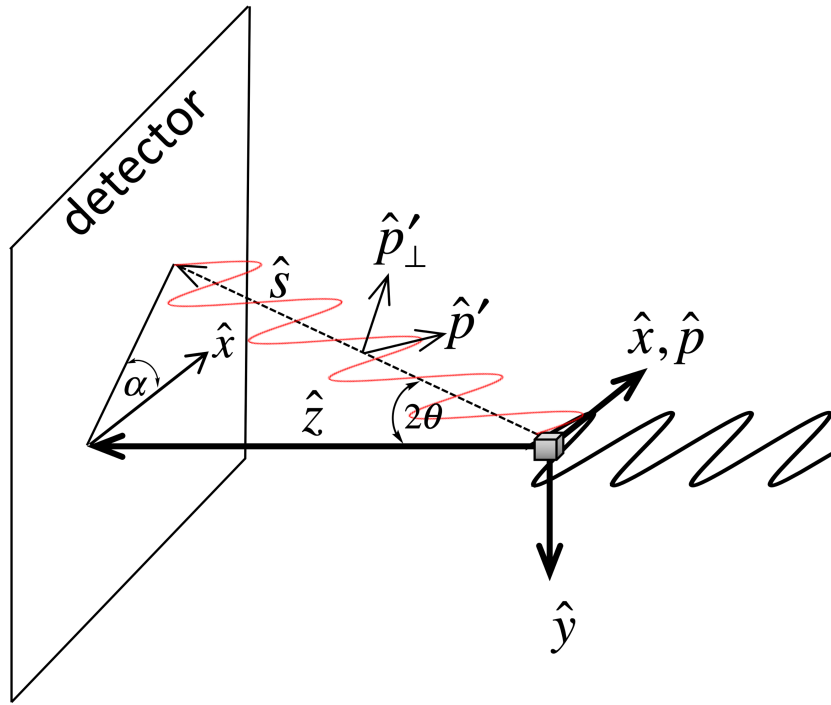


Figure S1. Diffraction geometry used for the AAS analysis

The direction of the scattered wave, \hat{s} , is described according to the XDS convention by two angles (Kabsch, 1977, 2010): the azimuthal angle α and the polar angle β , where $\beta = 2\theta$, such that

$$\text{Eq. 3} \quad \hat{s} = \{\cos \alpha \sin 2\vartheta, \sin \alpha \sin 2\vartheta, \cos 2\vartheta\}$$

The polarization factor P for intensities is proportional to $\sin^2 \delta$, where δ is the angle between \hat{p} and \hat{s} (Dunitz book)

$$\text{Eq. 4} \quad P \propto \sin^2 \delta = 1 - \cos^2 \delta = 1 - (\hat{s} \cdot \hat{p})^2$$

It is instructive to evaluate P for the general scattering case, defining the polarization component in the horizontal and vertical planes as follows:

$$\text{Eq. 5} \quad \begin{aligned} \hat{p}_H &= \{1, 0, 0\} \\ \hat{p}_V &= \{0, 1, 0\} \end{aligned}$$

With \hat{s} defined as above, the polarization along the horizontal and vertical directions is given by

$$\text{Eq. 6} \quad \begin{aligned} P_H &= 1 - (\hat{s} \cdot \hat{p}_H)^2 = 1 - \cos^2 \alpha \sin^2 2\theta \\ P_V &= 1 - (\hat{s} \cdot \hat{p}_V)^2 = 1 - \sin^2 \alpha \sin^2 2\theta \end{aligned}$$

For unpolarized radiation, the polarization factor is the average of the components along the horizontal and vertical direction (Dunitz)

$$\text{Eq. 7} \quad P = \frac{1}{2}(P_H + P_V) = \frac{1}{2}(1 + \cos^2 2\theta)$$

P_H is the polarization factor applicable to synchrotron data when the X-ray beam is 100% linearly polarized along the x-axis. In the following analysis, we will assume that this is the case (ie - $\hat{p} \equiv \hat{p}_H$).

In the absence of AAS, the scattering of linearly polarized radiation by an atom will also be completely linearly polarized, along the direction \hat{p}' . Following Schiltz and Bricogne (2010), the direction of \hat{p}' is obtained by projecting $\hat{p} (\equiv \hat{p}_H)$ onto the plane perpendicular to the scattered beam direction \hat{s} . This can be achieved by subtracting from \hat{p} the component of \hat{p} that is parallel to \hat{s} ; with normalization, yielding:

$$\text{Eq. 8} \quad \hat{p}' = \frac{\hat{p} - (\hat{s} \cdot \hat{p})\hat{s}}{\|\hat{p} - (\hat{s} \cdot \hat{p})\hat{s}\|}$$

$$= \left\{ \sqrt{1 - \cos^2 \alpha \sin^2 2\vartheta}, \frac{-\cos \alpha \sin \alpha \sin^2 2\vartheta}{\sqrt{1 - \cos^2 \alpha \sin^2 2\vartheta}}, \frac{-\cos \alpha \cos 2\vartheta \sin 2\vartheta}{\sqrt{1 - \cos^2 \alpha \sin^2 2\vartheta}} \right\}$$

The polarization component of the scattered wave perpendicular to \hat{p} may then be calculated:

$$\text{Eq. 9} \quad \hat{p}_\perp = \hat{p}' \times \hat{s} = \left\{ 0, -\frac{\cos 2\vartheta}{\sqrt{1 - \cos^2 \alpha \sin^2 2\vartheta}}, \frac{\sin \alpha \sin 2\vartheta}{\sqrt{1 - \cos^2 \alpha \sin^2 2\vartheta}} \right\}$$

These expressions are consistent with the expected properties of \hat{p}' and \hat{p}'_\perp

$$\text{Eq. 10} \quad {}^T \hat{p}' \cdot \hat{p} = {}^T \hat{p}' \cdot \hat{p}_H = \sqrt{1 - \cos^2 \alpha \sin^2 2\vartheta} \equiv \sqrt{P_H}$$

$${}^T \hat{p}'_\perp \cdot \hat{p} = 0$$

Crystal Orientation and Anisotropic Anomalous Scattering

Consider an axial absorber in the molecular frame $\{\hat{x}_m, \hat{y}_m, \hat{z}_m\}$ with \hat{x}_m as the unique axis. The absorption tensor in the molecular frame is then given by

$$\text{Eq. 11} \quad \Phi_m = \begin{bmatrix} f_s & 0 & 0 \\ 0 & f_p & 0 \\ 0 & 0 & f_p \end{bmatrix}$$

where f_p and f_s are the components perpendicular and parallel to the unique axis, respectively.

The transformation of Φ_m to the crystal frame $\{\hat{x}_c, \hat{y}_c, \hat{z}_c\}$ is

$$\text{Eq. 12} \quad \Phi_c = G_m^T \Phi_m G_m$$

where

$$\text{Eq. 13} \quad G_m = \begin{bmatrix} \hat{x}_m \cdot \hat{x}_c & \bar{x}_m \cdot \hat{y}_c & \bar{x}_m \cdot \hat{z}_c \\ \hat{y}_m \cdot \bar{x}_c & \hat{y}_m \cdot \hat{y}_c & \hat{y}_m \cdot \hat{z}_c \\ \hat{z}_m \cdot \bar{x}_c & \hat{z}_m \cdot \hat{y}_c & \hat{z}_m \cdot \hat{z}_c \end{bmatrix} \quad (\text{with } \hat{x}_m = G_m \hat{x}_c \text{ and } \hat{x}_c = G_m^T \hat{x}_m)$$

From the above expressions for \hat{p}' and \hat{p}'_{\perp} , the scattering factor may be calculated from Φ_c

$$\text{Eq. 14} \quad g = {}^T \hat{p}' \cdot \Phi_c \cdot \hat{p}$$

$$g_{\perp} = {}^T \hat{p}'_{\perp} \cdot \Phi_c \cdot \hat{p}$$

These correspond to equations (3) and (4) in Schiltz and Bricogne (2008). From equation (19) of Schiltz and Bricogne, the observed intensity for a given reflection h be may written

$$\text{Eq. 15} \quad I_{obs}(h) = kP_H \left[\left| F(h) + G_{p'p}(h) \right|^2 + \left| G_{p'_{\perp}p}(h) \right|^2 \right]$$

where $F(h)$ is the normal isotropic factor, k is the scale factor, and

$$\text{Eq. 16} \quad G_{p'p}(h) = \sum_j^{N_{atoms}} \frac{g_j}{P_H} O_j T_j(h) \exp[2\pi i h \cdot x_j]$$

$$G_{p'_{\perp}p}(h) = \sum_j^{N_{atoms}} \frac{g_{\perp,j}}{P_H} O_j T_j(h) \exp[2\pi i h \cdot x_j]$$

The sums in Eqs. 16 are over all atoms in the unit cell, and O_j and T_j correspond to the occupancy and thermal factor of the j^{th} atom, respectively. For macromolecular structures, the contribution of the g_{\perp} term is typically neglected for all but the weakest reflections, due to the small number of anomalous scatterers in the unit cell (Schiltz and Bricogne, 2008).

Calculation of g as a function of orientation of the unique axis

For the reference (Figure S2), we start with the unique axis of an axial system aligned along the laboratory x axis (recalling that the x axis coincides with both the polarization direction and the rotation axis for data collection). A rotation around the z axis (beam direction) by κ will then shift the orientation of the unique axis along the direction $\{\cos \kappa, \sin \kappa, 0\}$ in the xy plane.

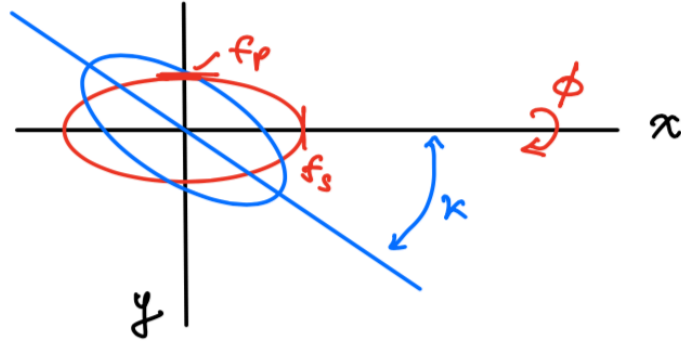


Figure S2. Definition of rotation angles describing the orientation of an axial absorption tensor during data collection.

During data collection, the crystal is rotated around the x axis by ϕ . If the corresponding rotation matrices for these rotations about the z and x axes are defined as $R_z(\kappa)$ and $R_x(\phi)$, respectively, then the scattering factors may be evaluated as

$$\text{Eq. 17} \quad \begin{aligned} g &= {}^T \hat{p}' \cdot (R_x(\phi) R_z(\kappa)) \cdot \Phi_c \cdot (R_x(\phi) R_z(\kappa))^T \cdot \hat{p} \\ g_{\perp} &= {}^T \hat{p}'_{\perp} \cdot (R_x(\phi) R_z(\kappa)) \cdot \Phi_c \cdot (R_x(\phi) R_z(\kappa))^T \cdot \hat{p} \end{aligned}$$

with

$$R_x(\phi) = \begin{Bmatrix} 1 & 0 & 0 \\ 0 & \cos \phi & -\sin \phi \\ 0 & \sin \phi & \cos \phi \end{Bmatrix} \quad \text{and} \quad R_z(\kappa) = \begin{Bmatrix} \cos \kappa & -\sin \kappa & 0 \\ \sin \kappa & \cos \kappa & 0 \\ 0 & 0 & 1 \end{Bmatrix}$$

While these general expressions are complicated, in the limit $2\theta \rightarrow 0$, they reduce to

$$\text{Eq. 18} \quad \begin{aligned} g &\sim f_s \cos^2 \kappa + f_p \sin^2 \kappa \\ g_{\perp} &\sim (f_p - f_s) \cos \phi \cos \kappa \sin \kappa \end{aligned}$$

The important points from this limiting analysis is that the first term corresponds to the orientation averaged scattering factor (and is independent of the rotation angle around x), while the second is non-zero only for anisotropic anomalous scattering (when $f_p \neq f_s$), and depends on both the orientation of the unique axis with respect to x, and the rotation angle around x. The latter effect was used to experimentally extract values of f_p and f_s by rotating around the azimuthal axis (Templetons (AC A42, 478 (1986))).

Calculation of scattering factors as a function of orientation, rotation angle, and scattering direction (Eq. 14)

To assess how the scattering factors defined in Eq. 14 depend on orientation of the unique axis, rotation angle and scattering direction, g and g_{\perp} were numerically evaluated using Eqs. 3, 8, 9, 11 and 12 (Figure S2). In these calculations, g and g_{\perp} were divided by $(P_H)^{1/2}$ to correspond to the appropriate values that would be obtained if the standard polarization correction was applied to

these data during data processing. We note the cautionary remark of Fanchon and Hendrickson (1990) that “a single polarization *factor* cannot be defined and the polarization correction should not be applied when processing data to which this formalism is to be applied”. Nevertheless, the specific values of g and g_{\perp} are distributed about the average values for these parameters as a function of κ captured in the limiting expressions for these parameters (Eq. 18).

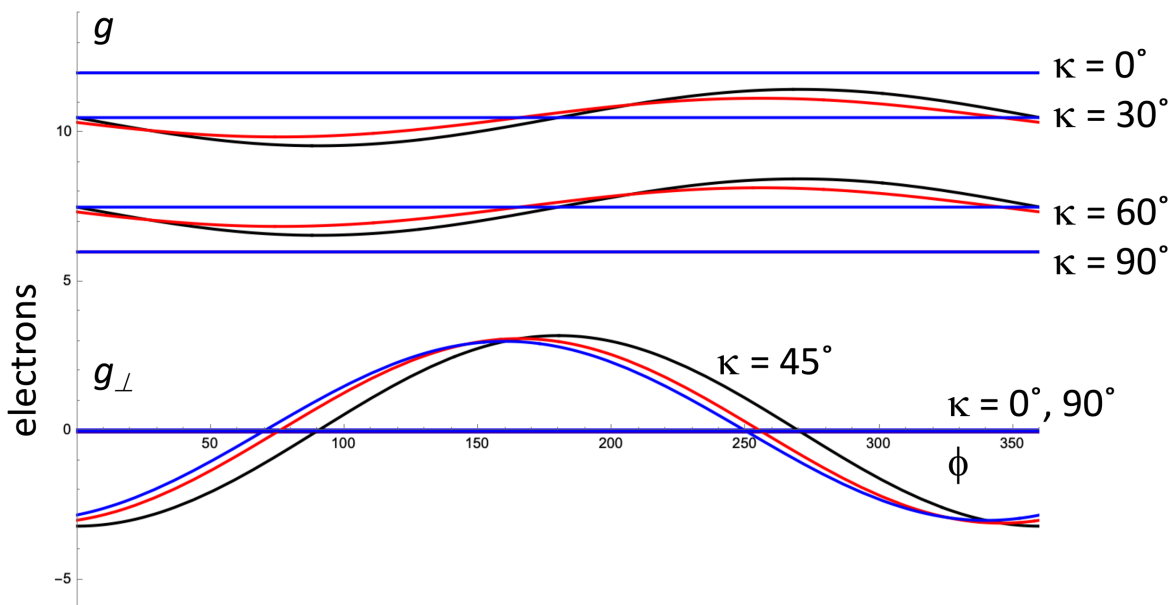


Figure S3. Variation in g and g_{\perp} for different values of κ (the angle between the unique axis and the rotation axis (x)). For these calculations, f_s and f_p were set to $12 e^-$ and $6 e^-$, respectively, with $\theta = 10^\circ$ ($2\theta = 20^\circ$). The black, red and blue curves correspond to $\alpha = 0, 45^\circ$ and 90° , respectively (α is the angle between the projection of the scattered wave on the plane of the detector and the x axis (Figure S1)).

Conclusions from this analysis

Applying the standard polarization factor in XDS approximately corrects for the $\alpha, 2\theta$ dependence of the scattering, as reflected in the distribution of the calculated values for g and g_{\perp} about the average values for these parameters as a function of κ captured in the limiting expressions for these parameters (Eq. 18; Fig. S3).

That said, neglect of the detailed orientation leads to errors of several electrons in the values of g that should be used in structure factor calculations for an individual reflection.

Additionally, neglect of the g_{\perp} term will also likely introduce an error comparable to that of setting g to the average value for a particular orientation of the unique axis with respect to the rotation axis, since g_{\perp} exhibits similar variations about the average value (0 electrons) for this term.

Section IX: Non-crystalline Diffraction Small Angle Scattering

References: A. Guinier, *X-ray Diffraction in Crystals, Imperfect Crystals and Amorphous Bodies*, Chap. 10, Freeman (1963)
C. Cantor & P. Schimmel, *Biophysical Chemistry*, Chap. 14, Freeman (1980)
D.A. Jacques and J. Trewhella, *Protein Science* **19**, 642 (2010)

For problems with spherical symmetry, the basic diffraction equation

$$F(\vec{S}) = \int \rho(\vec{x}) e^{2\pi i \vec{S} \cdot \vec{x}} d\vec{x}$$

is most appropriately expressed in terms of the spherical polar coordinates r , ϕ and θ , where θ is the angle between the S vector (taken as along the y axis) and the radial vector to the point x , r is the length of the vector, and ϕ defines the projected angle of the radial vector in the xz plane.

NOTE: it is not uncommon for the scattering variable to be defined as $\frac{4\pi \sin \vartheta}{\lambda} = 2\pi S = \frac{2\pi}{d}$!!!

With this angular convention, the diffraction expression becomes:

$$\begin{aligned} F(\vec{S}) &= \int \rho(\vec{r}) e^{2\pi i \vec{S} \cdot \vec{r}} r^2 \sin \theta d\phi d\theta dr \\ &= \int_0^{2\pi} d\phi \int_0^{\infty} r^2 \rho(r) dr \int_0^{\pi} \sin \theta e^{2\pi i S r \cos \theta} d\theta \end{aligned}$$

With the substitution $x = \cos \theta$, the θ integral can be evaluated (Cantor & Schimmel, pg. 701):

$$\begin{aligned} &= 4\pi \int_0^{\infty} r^2 \rho(r) \frac{\sin(2\pi S r)}{2\pi S r} dr \\ &= \frac{2}{S} \int_0^{\infty} r \rho(r) \sin(2\pi S r) dr \end{aligned}$$

From any of these expressions, the scattering from a sample of completely uniform density over all space, is zero, except in the forward scattering direction ($S=0$). This means that only problems with non-uniform density (on the scale of the radiation wavelength) can be probed by diffraction methods.

The inverse Fourier transform for a spherically symmetric system is given by

$$\rho(r) = \frac{2}{r} \int_0^{\infty} S F(S) \sin(2\pi S r) dS$$

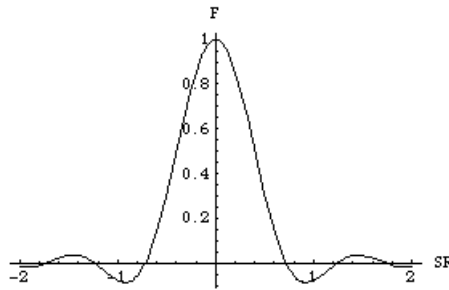
(Note: there is some confusion whether the inverse FT is for a 1-D or a 3-D system (as above for a spherically symmetric system. This again introduces confusion (more factors of 2π , etc.))

As an example, the scattering pattern of a uniform sphere may be found by imposing the conditions $\rho(r) = 1, 0 \leq r \leq R; \rho(r) = 0, r > R$, and evaluating the above integral to obtain:

$$F(S) = \left(\frac{4\pi}{3} R^3 \right) \left[\frac{3(\sin(2\pi SR) - 2\pi SR \cos(2\pi SR))}{(2\pi SR)^3} \right] = \frac{\sin(2\pi SR) - (2\pi SR) \cos(2\pi SR)}{2\pi^2 S^2}$$

The intensity of the scattered radiation is given by $F^2(S)$. The dependence of a normalized $F(S)$ on the product RS of the sphere radius (R) and the reciprocal space vector (S) is shown below:

```
In[2]:= F[SR_] := 3. * (Sin[2. * Pi * SR] - 2. * Pi * SR * Cos[2. * Pi * SR]) / (2. * Pi * SR)^3
Plot[F[SR], {SR, -2, 2}, PlotRange -> All, AxesLabel -> {"SR", "F"}]
```



Out[3]= - Graphics -

The zeroes of this function occur at $RS = 0.72, 1.23, 1.73, \dots$. Information about the size of a spherical object can be obtained from the S values where the diffracted intensity is zero.

While the above expression is correct only for uniform, spherical objects, the very low resolution diffraction from non-spherical objects can be modeled by a similar expression. The low resolution dependence of the scattering expression may be determined by expanding the expression for the intensity $= F^2(S)$ in a power series of S , and truncating to second order (this can be easily done by Mathematica®):

$$I(S) = \left(\frac{4\pi}{3} R^3 \right)^2 \left[1 - \frac{4\pi^2 R^2}{5} S^2 + \dots \right]$$

The normalized ratio $I(S)/I(0)$ is then given by:

$$\frac{I(S)}{I(S=0)} = 1 - \frac{4\pi^2 R^2}{5} S^2 + \dots$$

For non-spherical objects, the relevant radius in this expression is the radius of gyration, R_G . For a sphere, $R_G^2 = (3/5)R^2$. Making this substitution yields:

$$\frac{I(S)}{I(S=0)} = 1 - \frac{4\pi^2 R_G^2}{3} S^2 + \dots$$

Since $S = 2 \sin \theta / \lambda$

$$\frac{I(S)}{I(S=0)} = 1 - \frac{16\pi^2 R_G^2}{3\lambda^2} \sin^2 \theta + \dots$$

Recalling that $\ln(1-x) \sim -x$, then the small-angle scattering can be represented as:

$$\ln \left[\frac{I(S)}{I(S=0)} \right] \cong -\frac{16\pi^2 R_G^2}{3\lambda^2} \sin^2 \theta$$

which is called a Guinier plot. From Guinier plots, the radius of gyration of an object can be determined without knowledge of the molecular weight.

It is sometimes useful to be able to calculate the expected small angle scattering curve from atomic coordinates, which can be achieved as follows. The general diffraction expression for one molecule can be written:

$$F(\vec{S}) = \sum_{n=1}^N f_n(S) e^{2\pi i \vec{S} \cdot \vec{r}_n}$$

$$I(\vec{S}) = F(\vec{S}) F^*(\vec{S}) = \sum_{n=1}^N f_n(S) e^{2\pi i \vec{S} \cdot \vec{r}_n} \sum_{m=1}^N f_m(S) e^{-2\pi i \vec{S} \cdot \vec{r}_m}$$

$$I(\vec{S}) = \sum_{n=1}^N \sum_{m=1}^N f_n(S) f_m(S) e^{2\pi i \vec{S} \cdot \vec{r}_n} e^{-2\pi i \vec{S} \cdot \vec{r}_m}$$

To calculate the spherically averaged intensity, in the absence of intermolecular interactions (achieved experimentally by working at sufficiently high dilution), it is necessary to average over all orientations, as follows:

$$\langle I(\vec{S}) \rangle = \sum_{n=1}^N \sum_{m=1}^N f_n(S) f_m(S) \langle e^{2\pi i \vec{S} \cdot \vec{r}_n} e^{-2\pi i \vec{S} \cdot \vec{r}_m} \rangle$$

$$\langle I(\vec{S}) \rangle = \sum_{n=1}^N \sum_{m=1}^N f_n(S) f_m(S) \langle e^{2\pi i \vec{S} \cdot (\vec{r}_n - \vec{r}_m)} \rangle$$

$$\langle I(\vec{S}) \rangle = \sum_{n=1}^N \sum_{m=1}^N f_n(S) f_m(S) \langle e^{2\pi i \vec{S} \cdot \vec{r}_{nm}} \rangle$$

The average value of the exponential term can be calculated using methods introduced at the beginning of this section, yielding the Debye formula for the small angle scattering intensity:

$$\langle e^{2\pi i \vec{S} \cdot \vec{r}_{nm}} \rangle = \int_0^{2\pi} d\phi \int_0^{\pi} \sin \theta e^{2\pi i S r_{nm} \cos \theta} d\theta$$

$$= 4\pi \frac{\sin(2\pi S r_{nm})}{2\pi S r_{nm}}$$

giving, $\langle I(S) \rangle = 4\pi \sum_{n=1}^N \sum_{m=1}^N f_n(S) f_m(S) \frac{\sin(2\pi S r_{nm})}{2\pi S r_{nm}}$

A useful relationship that can be derived from further analysis of these scattering expressions (following the earlier derivation of the Guinier expression) relates R_G to the interatomic vectors:

$$R_G^2 = \frac{1}{N^2} \sum_{n < m} r_{nm}^2 = \frac{1}{2N^2} \sum_n \sum_m r_{nm}^2$$

The overall shapes of molecules can be assessed by calculating the small angle scattering for various models, and comparing them to the observed distribution. Alternatively, if some estimate of the phases are available (by assuming, for example as in the case of a true sphere, that the sign of $F(S)$ alternates +-+ for each peak), it is possible to calculate spherically averaged Fourier/Patterson maps, or the related radial distribution function:

inverse Fourier transform:

$$\rho(r) = \frac{2}{r} \int_0^{\infty} SF(S) \sin(2\pi Sr) dS$$

radial distribution function

$$4\pi r^2 \rho(r) = 8\pi r \int_0^{\infty} SF(S) \sin(2\pi Sr) dS$$

Volume $\overline{V(r)}$ common to a particle both before and after a translation r , averaged over all orientations

$$\overline{V(r)} = \frac{2}{r} \int_0^{\infty} SI(S) \sin(2\pi Sr) dS$$

characteristic function $\gamma(r) = \overline{V(r)} / V$

$$\gamma(r) = \frac{2}{rV} \int_0^{\infty} SI(S) \sin(2\pi Sr) dS$$

radial Patterson function

$$4\pi r^2 P(r) = 8\pi r \int_0^{\infty} SI(S) \sin(2\pi Sr) dS$$

(Note: the equations given in Cantor and Schimmel differ from these by a factor of $1/2\pi$ since they are using a 1-D inverse FT, and not the 3-D form with spherical symmetry)

The maximum length of a Patterson function vector (beyond which $P(r) = 0$) can provide a useful parameter for evaluating different models. For a sphere of radius R , the following relationships may be derived

$$\overline{V(r)} = \frac{\pi}{12} (r - 2R)^2 (r + 4R)$$

$$\gamma(r) = \frac{(r - 2R)^2 (r + 4R)}{16R^3} = 1 + \frac{r^3}{16R^3} - \frac{3r}{4R}$$

$$4\pi r^2 P(r) = \frac{\pi^2 r^2}{3} (r - 2R)^2 (r + 4R) = \frac{\pi^2 r^5}{3} - 4\pi^2 r^3 R^2 + \frac{16}{3} \pi^2 r^2 R^3$$

For further information, see the old International Tables, Vol. III (not Vol II - fixed 4/8/13) section 5.3.4 (5.3), P.B. Moore, J. Appl. Cryst. 13, 168 (1980); Guinier and Fournet, Small-Angle Scattering of X-rays (1955), sections 2.1.2.2 - 2.1.2.4.

Example: Small Angle X-ray Scattering (SAXS) Studies of the Nitrogenase Cofactors
Eliezer, et al., *J. Biol. Chem.* **268**, 20953-20957 (1993)

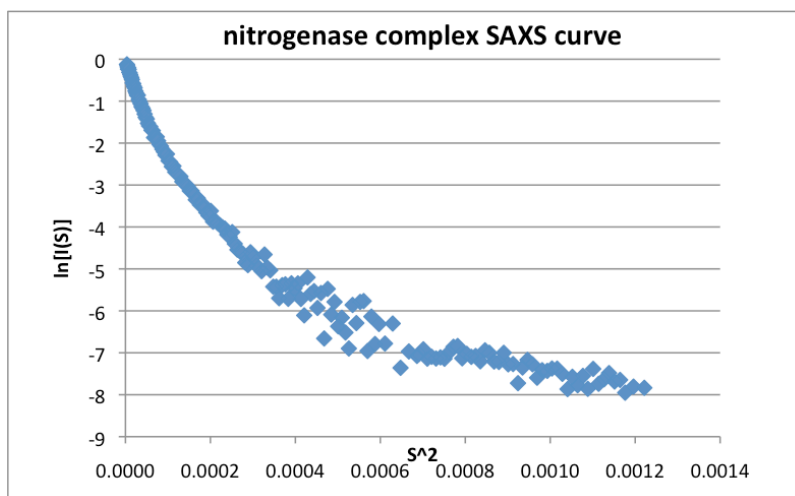
Small angle scattering studies can provide a sensitive method for obtaining R_G values, and the changes in these parameters as a function of environmental conditions. A beautiful example of the power of small angle scattering is provided by the study of the oligomeric state of the extracted FeMo-cofactor in solution (where it turns out to be at least dimeric; (Eliezer, et al., *J. Biol. Chem.* **268**, 20953-20957 (1993))) and to study the AIF stabilized complex. This type of information can be difficult to obtain by other methods, and provides important constraints for the development of more detailed structural models.

In Figure 1 of Eliezer analysis, the R_G of FeMoco(ox) is reported as 6.51 ± 0.18 at 1.93 mM. From the slope of that data, with $S = 2\sin\theta/\lambda$, and $\text{Log} = \text{Ln}$ (I think),

$$\frac{d \ln I}{dS^2} = -\frac{4\pi^2 R_G^2}{3} \sim \frac{(-7.1 + 6.8)}{(.001 - .0004)} = -500$$

$$R_G = \sqrt{(3 \times 500)/4\pi^2} = 6.2 \text{ \AA}$$

Example: Small Angle Scattering Analysis of the Nitrogenase Complex
Grossmann *et al. Acta Cryst.* **D55**, 727 (1999)



Analysis of the very low angle region ($S^2 < 0.00002 \text{ \AA}^{-2}$ or $S < 0.0045 \text{ \AA}^{-1}$) gives $R_G \sim 50 \text{ \AA}$ or $R_{\text{sphere}} \sim 64 \text{ \AA}$. A better fit is given assuming an ellipsoid of rotation with semi-axes $(a, b, c) \equiv (a, a, va)$, with the equivalent radius of gyration to the sphere:

$$R_G^2 = \frac{3}{5} R_{\text{sphere}}^2 = \frac{1}{5} (a^2 + b^2 + c^2) = \frac{a^2}{5} (2 + v^2)$$

$$a = \sqrt{\frac{3}{(2 + v^2)}} R_{\text{sphere}}$$

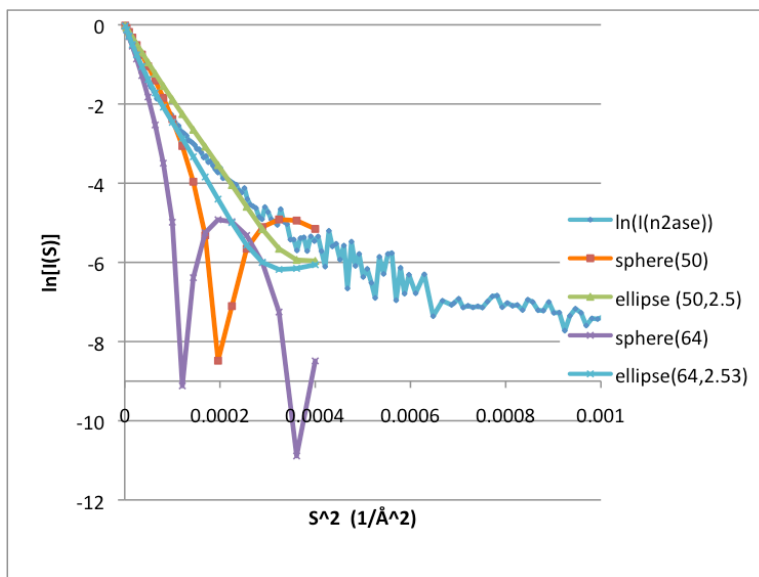
The scattering of an ellipsoid of revolution is given by Eq. 10.9 of Guinier

$$I(S) = \int_0^{\pi/2} \Phi^2 \left(\frac{2\pi S a v}{\sqrt{\sin^2 \alpha + v^2 \cos^2 \alpha}} \right) \cos \vartheta d\vartheta \text{ with } \alpha = \tan^{-1}(v \tan \vartheta)$$

where Φ is the Fourier transform of a uniform sphere. A similar, but simpler, expression is found in the International Tables, Vol II section 5.3.4.2 - these should be equivalent, but I haven't tested them.

$$I(S) = \int_0^{\pi/2} \Phi^2 \left(2\pi S a \sqrt{\sin^2 \vartheta + v^2 \cos^2 \vartheta} \right) \cos \vartheta d\vartheta$$

Using the Guinier expression, the best fit was obtained for $v \sim 2.5$ (see following), which seems to be a reasonable fit out to about $S^2 < 0.0002 \text{ \AA}^{-2}$.



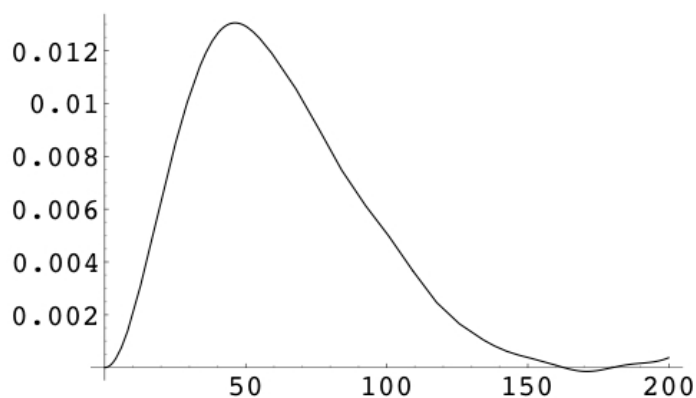
For comparison to the actual structure, the gyration tensor was calculated from the Ca positions of PDB entry 1N2C; for this calculation, the coordinates are taken relative to the center of mass of the structure.

$$\frac{1}{N} \begin{bmatrix} \sum_{k=1}^N x_k^2 & \sum_{k=1}^N x_k y_k & \sum_{k=1}^N x_k z_k \\ & \sum_{k=1}^N y_k^2 & \sum_{k=1}^N y_k z_k \\ & & \sum_{k=1}^N z_k^2 \end{bmatrix}$$

The trace of this matrix equals R_G^2 , and the eigenvectors and eigenvalues give the directions of the principal axes and the squared distance along each axis. For 1N2C, $R_G = 51.4 \text{ \AA}$, while the lengths of the principal axes (square root of eigenvalues) are 45.3 \AA , 17.7 \AA and 16.6 \AA , which gives an axial ratio of $\sim 45/17 = 2.65$, close to the values from the SAXS analysis. A direct calculation of R_G from the coordinates using the equation

$$R_G^2 = \frac{1}{N^2} \sum_{n < m} r_{nm}^2$$

gives $R_G \sim 51.3 \text{ \AA}$, with a maximum distance of 187 \AA . A crude numerical integration of the n2ase saxs data gives a radial Patterson with a maximum distance $\sim 170 \text{ \AA}$.



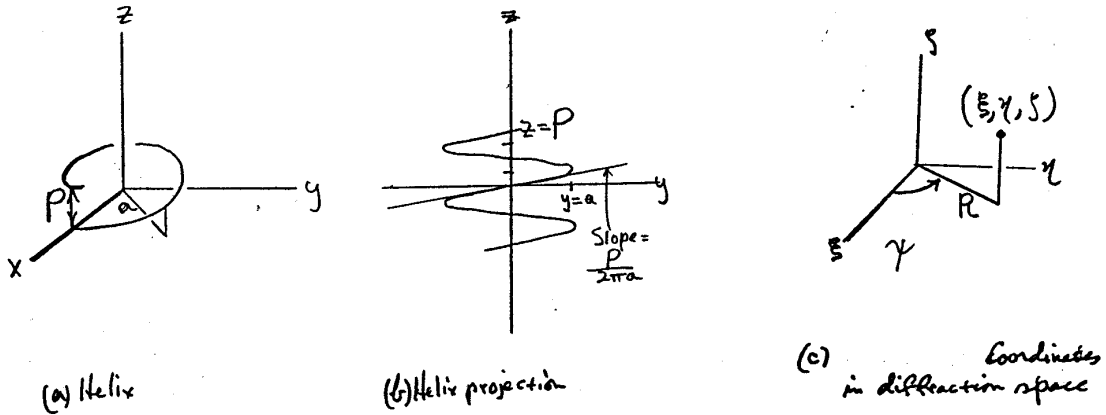
Diffraction Pattern of Helical Structures

- References: W. Cochran, F.H.C. Crick, V. Vand, *Acta Cryst.* **5**, 581-586 (1952)
 W.N. Lipscomb, Lecture Notes (1975)
 C. Cantor & P. Schimmel, *Biophysical Chemistry*, Chap. 14, Freeman (1980)
 S. Arnott, *Trans. Am. Cryst. Assoc.* **9**, 31-56 (1973)
 A. Klug, F.H.C. Crick, H.W. Wyckoff, *Acta Cryst.* **11**, 199-213 (1958)
 R. Langridge *et al*, *J. Mol. Biol.* **2**, 19—36 and 38-64 (1960)
 Appendix pp 63-64 “Calculation of Fourier Transform of a Helical Molecule”
 C. Kittel, *Am. J. Physics* **36**, 610 (1968)

A continuous wire helix of infinite length, radius a and axial repeat (pitch) P is defined by the equations:

$$\begin{aligned} x &= a \cos(2\pi z/P) \\ y &= a \sin(2\pi z/P) \\ z &= z \end{aligned}$$

The helix repeats when $z = \dots, -2P, -P, 0, P, 2P, \dots$. Below are illustrated figures showing the helix in three dimensions and in a two-dimensional projection. The latter emphasizes the two sets of prominent average planes of approximate slope $\pm P/2\pi a$, which give rise to two prominent lines of diffraction intensities in reciprocal space. These latter lines have slopes $\mp 2\pi a/P$, since they are perpendicular to the sets of planes in the helix projection. Qualitatively, the slopes of these lines in the diffraction pattern of a helix provides the ratio of the helix pitch to radius. ((Figure from W.N. Lipscomb, lecture notes, ca. 1975))



In terms of a reciprocal space coordinate system defined by three orthogonal coordinates ξ, η, ζ , the fundamental diffraction equation becomes:

$$F(\xi\eta\zeta) = \int e^{2\pi i(\xi x + \eta y + \zeta z)} dx dy dz$$

where the integral is taken over the helical path. Converting to the parametric expression for the helix, this may be written ("apart from unimportant constants of proportionality"):

$$F(\xi\eta\zeta) = \int_0^P e^{2\pi i(\xi a \cos(2\pi z/P) + \eta a \sin(2\pi z/P) + \zeta z)} dz$$

Converting to the cylindrical coordinates R, ψ, ζ in reciprocal space, with $R^2 = \xi^2 + \eta^2$, $\cos \psi = \xi/R$, and $\sin \psi = \eta/R$, this expression may be rewritten as:

$$F(R\psi\zeta) = \int_0^P e^{2\pi i \left(Ra \cos\left(\frac{2\pi z}{P} - \psi\right) + \zeta z \right)} dz$$

Since the helix repeats after a distance P along z , the diffraction pattern in reciprocal space will be non-zero only for those planes where $\zeta = n/P$:

$$F\left(R\psi \frac{n}{P}\right) = \int_0^P e^{2\pi i \left(Ra \cos\left(\frac{2\pi z}{P} - \psi\right) + \frac{nz}{P}\right)} dz$$

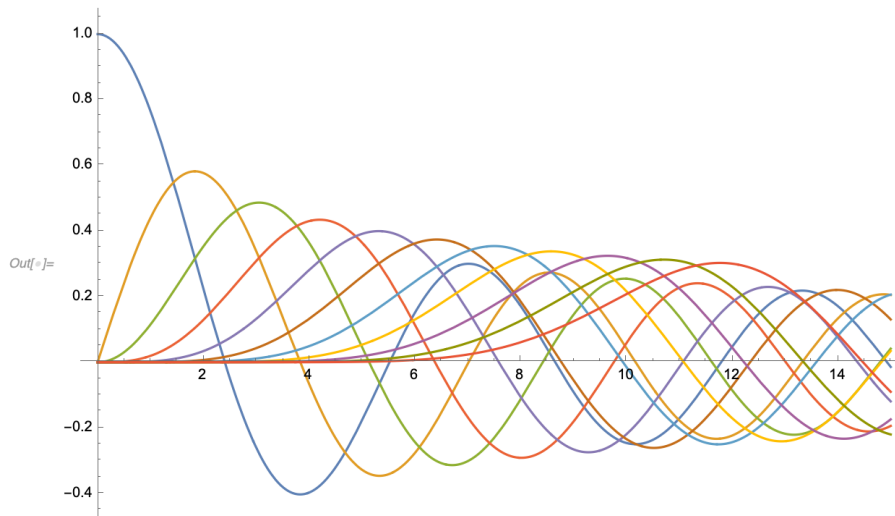
This integral may be evaluated from the identity:

$$J_n(X) = \frac{1}{2\pi i^n} \int_0^{2\pi} e^{iX \cos \phi} e^{in\phi} d\phi$$

by taking $X = 2\pi Ra$ and $\phi = 2\pi z/P$. $J_n(X)$ is the n th-order Bessel function of the first kind, or *the* Bessel function. Bessel functions typically arise in problems with cylindrical symmetry. Values of $J_n(X)$ for $0 \leq n \leq 10$ and $0 \leq x \leq 15$ are illustrated below (generated with Mathematica®):

In[]:= (*plot out helical diffraction patterns *)

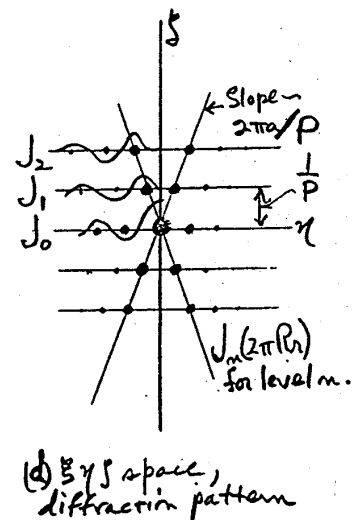
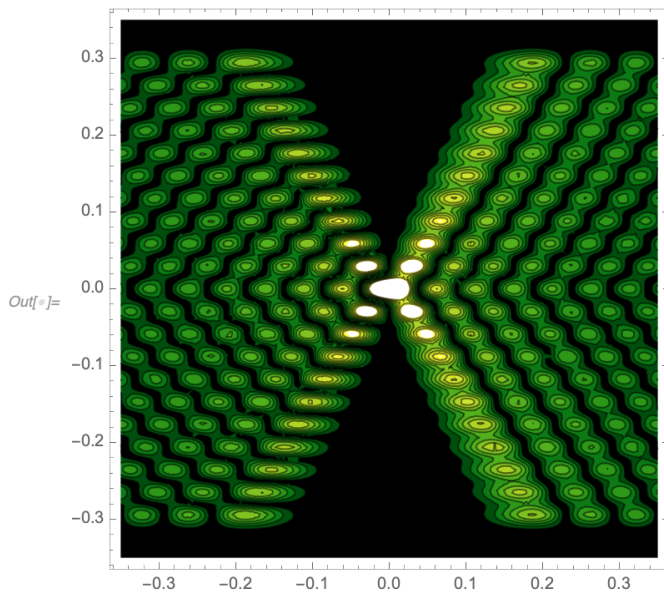
```
Plot[{BesselJ[0, x], BesselJ[1, x], BesselJ[2, x], BesselJ[3, x], BesselJ[4, x],
      BesselJ[5, x], BesselJ[6, x], BesselJ[7, x], BesselJ[8, x], BesselJ[9, x], BesselJ[10, x]},
     {x, 0, 15}, PlotRange -> All]
```



With this identity, it can be shown that $F\left(R, \psi, \frac{n}{P}\right) = 2\pi e^{in(\psi+\pi/2)} J_n(2\pi Ra)$

This expression gives the amplitude and phase of the X-ray scattering on the n th layer line. The amplitude ($J_n(2\pi Ra)$) is independent of ψ , and hence the diffraction pattern has cylindrical symmetry. The positions of the first (and largest) maxima of J_n satisfy the approximate expression $2\pi Ra = n$, so that for a particular n , the Bessel function maximum occurs at $R \sim n/2\pi a$. The slope of the line defined by these maxima then has the value $(n/P)/R = 2\pi a/P$, consistent with the simple analysis presented above. Hence, the transform of a continuous helix consists of a series of layer lines, with the maxima forming the characteristic "X". No reflections exist along the meridian, except for the origin, since $J_n(0) = 0$, except when $n = 0$. (Figure from W.N. Lipscomb, lecture notes, ca. 1975). A Mathematica® script for generating the diffraction pattern of a continuous helix follows (displaying the amplitude of the diffraction pattern, rather than the amplitude squared):

```
In[ ]:= r = 10.;
P = 34.;
F0[R_, Z_] := Sum[BesselJ[n, 2*Pi*R*r] * Exp[-(Abs[Z] - n/P)^2 / (2 / (3*P)^2)], {n, 0, 10}]
ContourPlot[Abs[F0[R, Z]], {R, -0.35, .35}, {Z, -0.35, 0.35}, ColorFunction -> "AvocadoColors",
PlotLegends -> Automatic]
```



For the purposes of this calculation, the n^{th} layer lines are specified using a narrow Gaussian defined as $\exp\left[-\left(|Z| - \frac{n}{P}\right)^2 / \left(\frac{2}{(3P)^2}\right)\right]$, where the breadth is given by $1/(3P)$.

The next simplest type of helix, the rational discontinuous helix, is defined as a set of points separated by a vertical spacing p on a continuous helix, that have an exact repeat after an integral number of turns, t . Let u = the number of units in t turns, and $c = up = tP$ be the repeat distance along z . The periodicity of the structure along the z direction gives a set of regularly spaced units separated by intervals of p , and hence gives rise to a non-zero diffraction planes with ζ values = m/p , where m can have any integer values. Hence, this structure can be thought of as the product of the helix times a function that is zero, except when z is an integer multiple of p . The diffraction pattern of this collection can be obtained by application of the Fourier convolution theorem, that states the Fourier transform of the product of two functions is the convolution of the transforms of the two functions. Hence, in this case, the overall diffraction pattern reflects the convolution of the helical transform with the transform of the function that is zero, except for $z=mp$. This means that the diffraction pattern is generated by putting down images of the transform of a continuous helix, $F\left(R, \psi, \frac{n}{P}\right)$, separated by intervals of m/p along ζ . This behavior is then responsible for the characteristic double X pattern that is observed for helical polymers such as DNA. As a result of the convolution, diffraction is only observed on layer lines defined by the expression:

$$\zeta = \frac{n}{P} + \frac{m}{p}$$

When these conditions are satisfied, the transform of the rational, discontinuous helix becomes:

$$2\pi e^{in(\psi+\pi/2)} J_n(2\pi Ra)$$

Now, if P/p cannot be expressed as a ratio of whole numbers (the so-called irrational, discontinuous helix), then these planes will fill the whole of reciprocal space. In the rational case, however, P/p can be expressed as the ratio of whole numbers, and the transform is confined to a series of planes that satisfy the following relationship, where l is any integer:

$$\zeta = \frac{n}{P} + \frac{m}{p} = \frac{l}{c}$$

To calculate the Fourier transform from the j atoms in a helical molecule of real space coordinates R_j, ϕ_j, Z_j , the following equation is used (R. Landgridge, et al, in the Appendix of *J. Mol. Biol.* **2**, 63-64 (1960)):

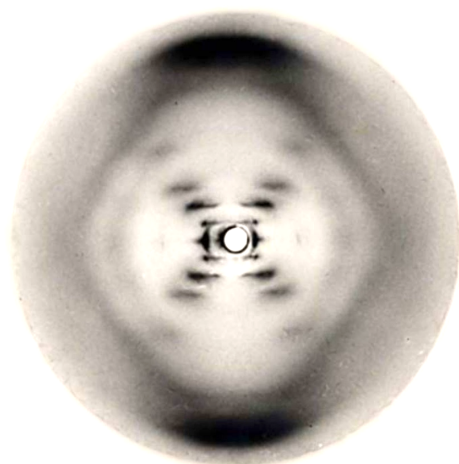
$$F(l, \psi, \xi) = \sum_n \sum_j f_j J_n(2\pi R_j \xi) e^{i\left\{n\left(\psi - \phi_j + \frac{\pi}{2}\right) + \frac{2\pi l z_j}{c}\right\}}$$

where n is defined as the integral solution:

$$\frac{n}{P} = \frac{l}{c} - \frac{m}{p} = \zeta - \frac{m}{p}$$

An illuminating representation of helical (and other) diffraction patterns may be found in Harburn, Taylor and Wells, *Atlas of Optical Transforms*, Cornell (1975).

The DNA double helix provides a qualitatively straightforward case of extracting information of the helical geometry from a fiber pattern. In this case, $p = 3.4 \text{ \AA}$, $P = 34 \text{ \AA} = c$, $u = 1$ helix turn/repeat, and $t = 1$ helix turn/repeat. Hence, layer lines occur at spacings that satisfy the integer relationship $n + 10m = l$. For $l = 0$, this corresponds to n values = ..., -10, 0, 10, ...; for $l = 1$, $n = \dots -9, 1, 11, \dots$, etc. The difference between successive values of n will always be 10. A meridional reflection will occur at $1/3.4 \text{ \AA}^{-1}$, which is the tenth layer line. Hence, from qualitative inspection of the fiber diffraction pattern, one can deduce that the helix repeat is $P = 34 \text{ \AA}$ formed by 10 units separated by $p = 3.4 \text{ \AA}$, with a radius of $\sim 7.3 \text{ \AA}$ derived from the helical slope of ~ 1.35 . Photograph 51 of B-form DNA recorded by Franklin and Gosling (Nature 171, 740 (1953)) is depicted below showing these features (as near as I can tell, this photo is not subject to copyright). Note that no significant reflections are present on the 4th layer line, which is indicative of the double helix as discussed in the next section.



Diffraction patterns from other helical polymers, such as the α -helix formed by poly L-methyl glutamate, can be more complex. In the α -helix case, since the helix repeats after 5 helical turns formed by 18 residues, $P = 5.4 \text{ \AA}$, $p = 1.5 \text{ \AA}$, $P/p = 18/5$ and the layer lines occur when $l = 5n + 18m$. Hence, when $l = 0$, $n = -18, 0, 18, \dots$; $l = 1$, $n = -7, 11, \dots$ etc. Since J_n tends to be small for large n and large arguments, 'layer lines to which only high-order Bessel functions contribute will be weak or absent, and those to which low-orders contribute will be strong', so that, at least for simple helical polymers, one typically observes only those layer lines for which $n < \sim 5$.

Often, the fiber needs to be tilted so that the meridional reflection can contact the Ewald sphere and hence be visible in the diffraction pattern. For example, an α -helix fiber needs to be rotated in the X-ray beam to see the meridional reflection at $1/p = (1.5 \text{ \AA})^{-1}$; a fascinating account of this is provided by Perutz in his book "I Wish I'd Made You Angry Earlier" – this particular reflection was critical to establishing the rise per residue in the α -helix, but was experimentally missed until he rotated the fiber by 31° ($= \sin^{-1}(\lambda/(2 \times 1.5))$), for $\lambda = 1.54 \text{ \AA}$ (Cu K α)

An informative discussion of fiber diffraction applied to biopolymers may be found in Saenger *Principles of Nucleic Acid Structure*, Springer (1984).

Computational Background to Fourier Transforms and Helical Diffraction

J.W. Goodman *Introduction to Fourier Optics* McGraw Hill (1968) (later editions available)

J.W. Goodman *Fourier Transforms Using Mathematica* SPIE (2020) ISBN: 9781510638556
(the version of this informative book that I use is a Mathematica® notebook)

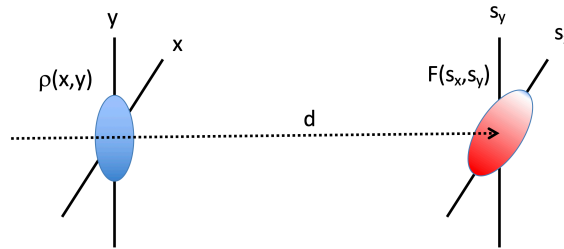
Lucas et al. “Revealing the backbone structure of B-DNA from laser optical simulations of Its X-ray diffraction pattern” *J. Chem. Ed.* 76, 378 (1999)

Thompson et al. “Rosalind Franklin’s X-ray photo of DNA as an undergraduate optical diffraction experiment” *Am. J. Phys.* 86, 95 (2018)

Preliminaries

Calculations are in the Mathematica® notebooks slit.nb and DNA_helix.nb. The Fraunhofer approximation can be used to calculate the diffraction pattern ($F(s_x, s_y)$) of an object ($\rho(x, y)$) at a sufficiently long distance from that object when illuminated with plane waves.

$$F(s_x, s_y) = \int \rho(x, y) \exp\left[\frac{-2\pi i}{\lambda d}(s_x x + s_y y)\right] dx dy$$



If a is the dimension of the scattering object, then the Fraunhofer condition is that $a^2/(\lambda d) \ll 1$. For an X-ray scattering experiment with $a \sim 100 \text{ \AA}$, $d \sim 10 \text{ cm} = 10^9 \text{ \AA}$, $\lambda \sim 1 \text{ \AA}$, this ratio $\sim 10^{-5}$. (As a working hypothesis, I think this is equivalent to assuming that the Ewald sphere is flat, and that the diffraction pattern is equivalent to the Fourier transform of the projection perpendicular to the beam.)

The normalized Fourier transform of a two-dimensional slit may be calculated (with $\lambda d \equiv 1$)

$$F(s_x, s_y) = \frac{1}{4ab} \int_{-b-a}^{+b+a} \int \rho(x, y) \exp[2\pi i(s_x x + s_y y)] dx dy = \frac{\sin[2\pi a s_x] \sin[2\pi b s_y]}{4\pi^2 a b s_x s_y}$$

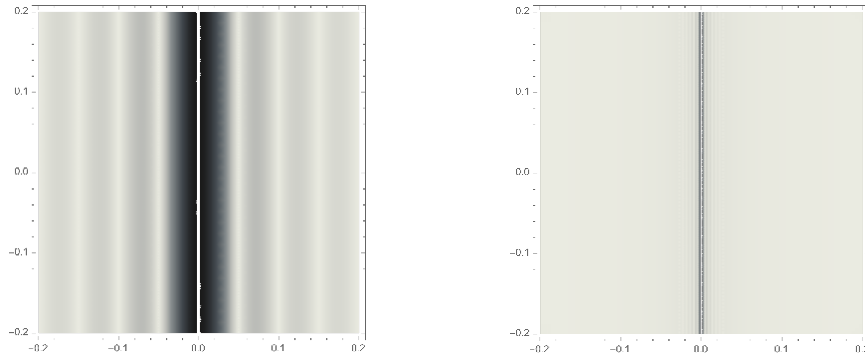
in the limit $b \rightarrow 0$ (ie – generating a line segment along the x axis)

$$F(s_x, s_y) = \frac{\sin[2\pi a s_x]}{2\pi a s_x}$$

In the limit $a \rightarrow \infty$, this expression goes to 0, except in the limit $s_x \rightarrow 0$, when this expression goes to 1, so that

$$F(s_x, s_y) = \int_{-a}^{+a} \exp[2\pi i s_x x] dx = 0, \quad s_x \neq 0; \quad = 1, \quad s_x = 0$$

The Fourier transforms of line segments between ± 10 and ± 1000 along x may be calculated:



The Fourier Transform of a line through the origin described by the equation $y = mx$ is given by (normalizing the contributions of s_x and s_y in the exponential):

$$F(s_x, s_y) = \int_{-a}^{+a} \rho(x, y) \exp \left[-2\pi i \left(\frac{s_x x + s_y (mx)}{\sqrt{1+m^2}} \right) \right] dx = \frac{\sin \left[2\pi a \left(\frac{s_x + ms_y}{\sqrt{1+m^2}} \right) \right]}{2\pi a \left(\frac{s_x + ms_y}{\sqrt{1+m^2}} \right)}$$

which in the limit $a \rightarrow \infty$ is non-zero along the perpendicular to the line $y = mx$.

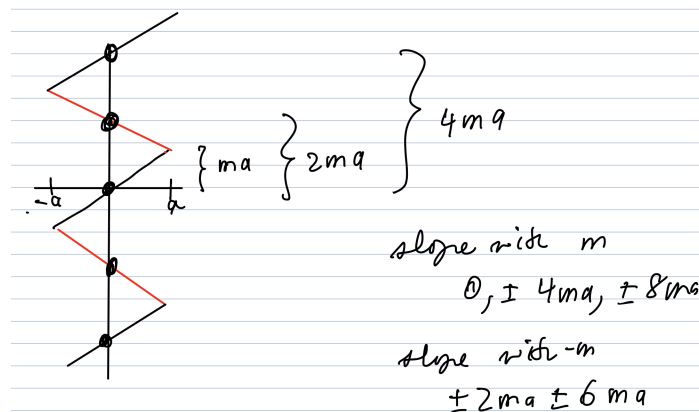
The normalized interference function corresponding to the translations of an object at regular spacings along the y axis given by: $-nb, -(n-1)b, \dots, -b, 0, +b, \dots, +(n-1)b, +nb$, is

$$\Phi(n, b, s_y) = \frac{1 + 2 \sum_{k=-n}^{k=+n} \cos(2\pi k b s_y)}{2n+1}$$

Helical diffraction approximations

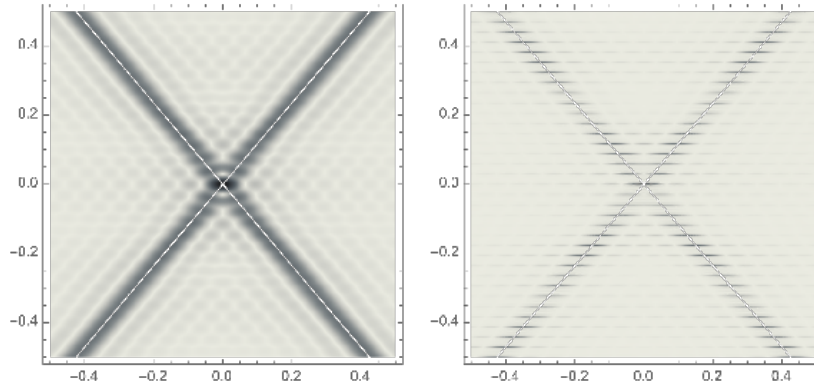
For these calculations, dimensions approximately appropriate to B-form DNA are utilized, with radius R = projection half-length $a = 10 \text{ \AA}$, pitch = 34 \AA , rise per residue = 3.4 \AA , slope = $(P/2)/(2a) = P/(4a) = 0.85$

“zig-zag”



The Fourier transforms with 1 and 11 repeating units (left and right figures, below), respectively, illustrate the characteristic “X” shaped where the slope of the arms is related to the slopes of the

zig-zag (equal to $-1/m$). When multiple helical units are present, the continuous transform is sampled along discrete lines spaced by $1/P \sim 0.0294$



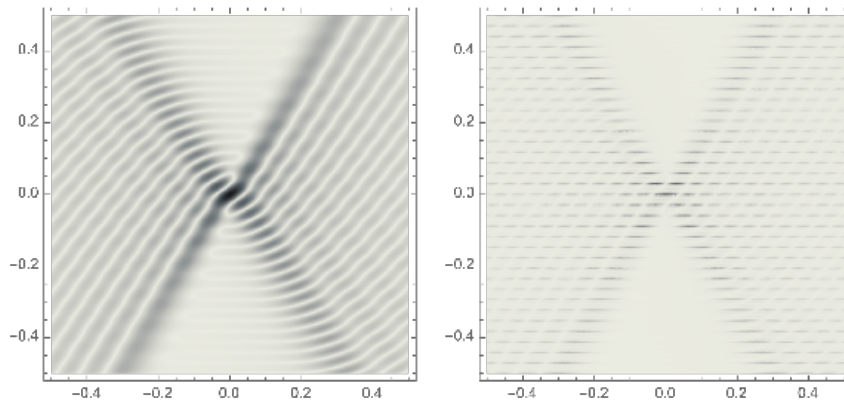
Transform of a continuous helix

When the helical axis is in the plane of the page (oriented vertically along y), the x coordinate is given by $R \sin(2\pi y/P)$, so that the Fraunhofer diffraction pattern from one helical turn is:

$$F(s_x, s_y) = \int_0^P \exp \left[-2\pi i \left(s_x \cdot R \sin \frac{2\pi y}{P} + s_y y \right) \right] dy$$

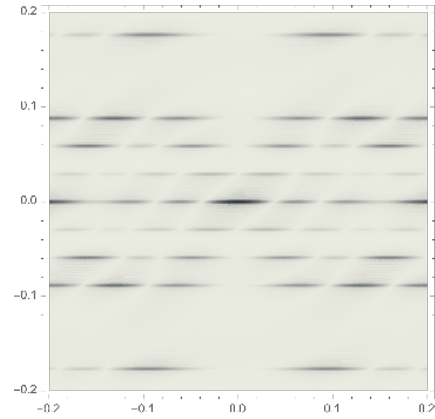
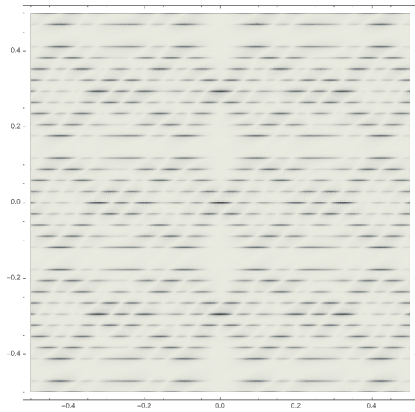
The convention adopted here is that $x = 0$ when $y = 0$ in an attempt to put an inversion center at the origin. This expression is equivalent to the general scattering expression for a continuous helix derived in the previous section from Lipscomb's notes (except that the axes are defined differently)

The calculated patterns for 1 and 11 helical turns (left and right, respectively) are illustrated below:



Transform of a discontinuous helix

In this case, the integral for a continuous helix is replaced by a summation over discrete points spaced by 3.4 \AA ($P/\text{residues per turn} = 34 \text{ \AA}/10$) along the helix axis (y). As show below (left; calculated for a helix extending from -5 to $+5$ turns from the reference orientation), this yields the characteristic meridional reflection at 3.4 \AA (at $\sim 0.29 \text{ \AA}^{-1}$) resolution dominating the 10^{th} layer line. For the B-form DNA double helix, a second strand is present, displaced by $\sim 3P/8$ or 12.8 \AA along the helix axis (and of opposite polarity, which is irrelevant to this example). Inclusion of this term leads to disappearance of the 4^{th} layer line (right).



Reading images into Mathematica

Mathematica[®] is great not only for calculating Fourier transforms of functions, but also of input images. Basic commands are detailed in the Goodman book; a summary follows

```
img = ColorConvert[Import["~/Dropbox/FourierTransform_images/duck_text.tiff"], "Grayscale"]
Information[%]
ImageHistogram[img]
```

(* extract out the color part (3rd element, #1 = b/w *)

```
data = ImageData[img];
d = data[[All, All, 1]];
Image[d] (* displays figure *)
Dimensions[d]
```

color scale	white	black
gray scale	1	0
byte	255	0

dimensions of data array = (ncol,nrow) \equiv (x,y)

